Physik-Department
Technische Universität München
Institut für Theoretische Physik
Lehrstuhl Univ.-Prof. A. J. Buras

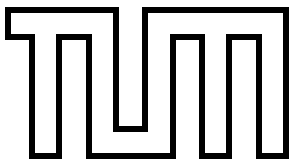

Indirect CP–Violation in the Neutral Kaon System Beyond Leading Logarithms

and related topics

Ulrich Nierste

Vollständiger Abdruck der von der Fakultät für Physik der Technischen Universität München zur Erlangung des akademischen Grades eines

Doktors der Naturwissenschaften (Dr. rer. nat.)

genehmigten Dissertation.

Vorsitzender:		Univ.-Prof. Dr. F. v. Feilitzsch
Prüfer der Dissertation:	1.	Univ.-Prof. A. J. Buras
	2.	Univ.-Prof. Dr. W. Weise
3. Gutachter der Dissertation:		Univ.-Prof. Dr. W. Buchmüller (Univ. Hamburg)

Die Dissertation wurde am 25.1.1995 bei der Technischen Universität München eingereicht und durch die Fakultät für Physik am 23.2.1995 angenommen.

Abstract

One of the least accurate tested sectors of the Standard Model of elementary particles is the quark mixing mechanism. It encodes the transitions between different quark families in weak charged–current decays in terms of the Cabibbo–Kobayashi–Maskawa–matrix V_{CKM}. A complex phase δ in this matrix is the only possible source of the violation of the CP–symmetry in the Standard Model. This fact makes the study of V_{CKM} mandatory: As soon as the measurements of CP–violation cannot be fitted with the single parameter δ, evidence of new laws of physics will be found. Today the only unambiguously measured CP–violating phenomenon is the indirect CP–violation present in the $|\Delta \mathrm{S}|=2$ transitions inducing the mixing of the neutral Kaon states K^0 and $\overline{K^0}$. It is characterized by the well determined parameter ε_K. Even from this single experiment on CP–violation one can test the Standard Model, because together with the unitarity of V_{CKM} it constrains some parameters of the Standard Model such as the mass of the top–quark.
On the theoretical side the study of V_{CKM} is challenged by the presence of the strong interaction, which may screen or enhance the weak transition amplitudes of quarks and which binds the quarks into hadrons. The short distance QCD effects are comprised in the parameters η_1, η_2 and η_3 of the effective $|\Delta \mathrm{S}|=2$ –hamiltonian:

$$H^{|\Delta S|=2}(\mu) = \frac{G_F^2}{16\pi^2} M_W^2 \left[\lambda_c^2 \eta_1 S(\frac{m_c^2}{M_W^2}) + \lambda_t^2 \eta_2 S(\frac{m_t^2}{M_W^2}) + 2\lambda_c \lambda_t \eta_3 S(\frac{m_c^2}{M_W^2}, \frac{m_t^2}{M_W^2}) \right] b(\mu) \widetilde{Q}_{S2}(\mu) + \text{h.c.}.$$

For the following outline we only have to explain that $\lambda_j = V_{jd} V_{js}^*$ encodes the relevant elements of V_{CKM} and that $\eta_j b(\mu) = 1$ in the absence of QCD corrections.
Now for the investigation of ε_K the coefficient η_2 is most important, but a precise determination of the subdominant term involving η_3 is also required for a reliable analysis. The mass difference between the two physical neutral K–mesons $\mathrm{K_L}$ and $\mathrm{K_S}$, however, is dominated by η_1. When this work was begun, only the coefficient η_2 was known beyond the leading log approximation [15]. This approximation is unsatisfactory, as it involves large errors due to renormalization scale ambiguities and as it does not allow for the use of the fundamental QCD scale parameter $\Lambda_{\overline{\mathrm{MS}}}$.
The results of this thesis include the following:

i) The calculation of η_1 and η_3 in the next–to–leading order (NLO) is presented in detail.

ii) An improved determination of $\mathrm{Im}\,\lambda_t$, which is the key quantity for CP–violation, using the measurement of ε_K and the NLO values for η_1, η_2 and η_3 is given. Results

are tabulated as functions of the CKM–parameters V_{cb} and V_{ub}/V_{cb}, the mass of the top–quark and of B_K, which parametrizes the size of the hadronic matrix element.

iii) The bounds on the Standard Model parameters resulting from the unitarity of V_{CKM} are studied. We have found that with the new values for η_1 and η_3 a wider range of the parameters mentioned in ii) are allowed. In this sense the calculation has vindicated the Standard Model.

iv) The NLO value of η_1 leads to an enhancement of the short distance contribution to the $\mathrm{K_L}-\mathrm{K_S}$–mass difference. Now the short distance QCD contributions explain the dominant part of the measured mass difference. The old leading order result has suggested a long–distance dominance. This has been a puzzle, because long–distance effects are expected to be suppressed by a factor of $\Lambda^2_{\mathrm{QCD}}/m_c^2$ with respect to the short distance contributions.

A new feature of the NLO calculation of η_1 and η_3 is the presence of Green's functions with two insertions of operators (bilocal structures) both of which have a non–zero anomalous dimension. These Green's functions have required a subtle analysis of the renormalization of effective field theories. The discussion includes the following points:

v) The RG of bilocal structures is analyzed in detail. Different methods for the solution are presented. These include the framework of an inhomogeneous RG equation, which is best suited for formal proofs like those mentioned in vii). For the practical calculation a matrix formulation is given which in the case of η_3 only involves one 8×8–matrix instead of four of them as in the old LO calculation in [45].

vi) The structure of the reduced effective $|\Delta \mathrm{S}|=1$ lagrangian is discussed. In matrix elements with single operator insertions those operators which vanish by the field equation of motion or which are BRS–exact do not contribute to the matrix elements. But one faces non–trivial contact terms, if the Green's function contains two operator insertions. It is well–known [52,54,58] that these terms can be absorbed into $|\Delta \mathrm{S}|=2$ operators. In our case the contact terms have been identified to correspond to operators describing subleading effects in m_s/m_c.

vii) Likewise $|\Delta \mathrm{S}|=1$ evanescent operators appear in the effective lagrangian. Here we had to develop the correct prescription to deal with evanescent operators in bilocal structures. Just as in the case of the operators mentioned in vi) non–vanishing terms appear, which are also equivalent to the matrix elements of $|\Delta \mathrm{S}|=2$ operators. But now they can be absorbed into a finite renormalization of the $|\Delta \mathrm{S}|=2$ operators.

viii) The analysis of vii) has stimulated a related investigation: The definition of evanescent operators is not unique, because one can add $(D-4)$ times any physical operator to them. We show that any definition of them leads to an effective lagrangian, in which the physical sector is unaffected by the presence of properly renormalized evanescent operators. Hence one can drop the latter from the reduced lagrangian.

Yet the arbitariness in the definition leads to a renormalization scheme dependence in the *physical* sector. This result is important for practical NLO calculations, because the Wilson coefficients and the anomalous dimension matrix depend on the definition of the evanescents. Formulae to transform between the schemes are presented.

ix) Last but not least there are about 40 two–loop tensor integrals up to rank six involved in the calculations. The calculation of η_1 has required to calculate their finite part. Here we present a compact formula for the most general integral which can appear in two–loop calculations of light hadron systems. This is the two–loop vacuum bubble diagram with arbitrary tensor structure, small infrared regulating masses on the lines flown through by one loop momentum and arbitrary heavy masses on the other lines. The formula holds in D dimensions and is therefore a good investment into the future of higher order QCD corrections.

Contents

List of Figures

1. Introduction

The aim of elementary particle physics is the discovery of new fundamental laws of nature and their classification within a theoretical framework which arranges the observed elementary particles into simple patterns and describes their interactions in a unified way. The stage for this theoretical description is the Relativistic Quantum Field Theory incorporating both Einstein's theory of Special Relativity and Heisenberg's, Pauli's and Schrödinger's Quantum Mechanics. Its story of success started in 1947, when the experiment of Lamb and Retherford [1] gave unambigous evidence for the splitting of the $2s_{1/2}$ and the $2p_{1/2}$ energy levels of the hydrogen atom by $4\,\mu$eV. At the same time Dirac, Feynman, Tomonaga, Schwinger and others [2] developed the theory of Quantum Electrodynamics, which explains the Lamb shift by quantum fluctuations of the photon field. Since then many more actors have joined the electron and the photon field on the stage: Starting with the works of Gell-Mann and Zweig the partonic constituents of hadrons were successfully described by quark fields, whose strong interaction is mediated by gluons as encoded in the Lagrangian of Quantum Chromodynamics [3]. And with the unification of the electromagnetic and weak interaction by Glashow, Salam and Weinberg [4] the scene was entered by three more vector bosons, which are massive owing to their interaction with the Higgs particle [5]. These elements form what is now called the Standard Model of elementary particle physics. It is the most successful theory of physics: It covers energy scales between those of the Lamb shift and the center of mass energy of today's particle colliders such as LEP at CERN, which are separated by 17 orders of magnitude! No experiment has yet contradicted its quantitative predictions, although many of them have been tested to an extraordinary precision (e.g. an accuracy of 10^{-10} for the anomalous magnetic moment of the electron on both the experimental and the theoretical side).

On the other hand some sectors of the standard model are poorly verified at present. One of them is the quark mixing sector, which describes the coupling of quark fields to the charged electroweak vector bosons in terms of the Cabibbo–Kobayashi–Maskawa (CKM) matrix [6]. Here the non–perturbative nature of the long–distance strong interaction prevents an easy extraction of the CKM parameters.

Further we know that the Standard Model cannot be true for another 17 orders of magnitude in energy, as we then would reach the Planck scale, where gravitation becomes important requiring a new theoretical concept. Yet we know from other considerations such as vacuum stability that there must be new physics much below the Planck scale. How can we detect new physics apart from building accelerators with higher and higher energy?

First one can look at rare processes which are forbidden in the tree level approximation.

Since they are suppressed in the standard model new physics can contribute sizeably to their transition rates. Moreover, even low–energy rare hadronic processes are sensitive to the masses of heavy particles appearing in intermediate states. This allows to derive bounds on the mass of the recently discovered top–quark [7] from these processes [8, 9]. When the experimental determination of the top mass improves, these bounds provide a consistency check of the Standard Model quark sector over more than two orders of magnitude in energy.

Second one can look for violations of symmetries which are respected or weakly broken by the Standard Model. Here the CP symmetry is of utmost importance, because the only possible source of its violation in the Standard Model is a single parameter, the phase δ in the CKM matrix.[1] The CP transformation exchanges particles and antiparticles and reflects the spacial coordinates. If in the future we cannot fit all CP violating observables with this single phase, we will have discovered new physics. Further in the calculation of these observables the difficulties with the long–distance strong interaction are sometimes reduced, as the strong (as well as the electromagnetic) interaction respects CP symmetry indicated by the smallness of the neutron electric dipole moment.

All these aspects make the study of hadronic physics mandatory. Here a key object is the K–meson system, to which we owe a significant part of our present day knowledge about the Standard Model quark sector: In 1964 Christenson, Cronin, Fitch and Turlay have found the first evidence for CP violation by observing decays of the long–lived neutral K–meson K_L into the CP even two–pion state [10]. There are two potential sources for this phenomenon: The K_L state is not a pure CP odd state but has admixtures of the CP even neutral Kaon state or the weak interaction triggering this decay violates the CP symmetry thereby allowing transitions from the CP odd neutral Kaon state to CP even final states. In the first case we speak of *indirect CP violation* in contrast to *direct CP violation* in the second case. The CKM mechanism of the Standard Model predicts both types, if the phase δ is not equal to 0 or π. While precise measurements are available for the parameter ε_K [11] characterizing the size of the indirect CP violation in the neutral Kaon system, there is still a controversy about the direct CP violation [11]. Then in 1970 the suppression of flavour–changing neutral current (FCNC) decays of K–mesons lead Glashow, Iliopoulos and Maiani (GIM) to postulate the existence of the charm quark [12]. We finally mention the prediction of the charm–quark mass from the observed $K_L - K_S$–mass difference by Gaillard and Lee in 1974 [13]. On the other hand the theoretist's work to relate the measured quantities to the Standard model parameters is made difficult by the presence of the strong interaction: Its long range interaction confines the quarks into K–mesons and it modifies the weak CP violating amplitudes of interest. Since these transitions take place on short distance scales of the order of the inverse W–boson mass M_W, the QCD corrections can be reliably calculated perturbatively. The long–range effects, however, must be treated by other methods such as $1/N_c$–expansion, sum rule techniques or lattice gauge theory.

The Technical University of Munich has already largely contributed to the theoretical understanding of short distance QCD corrections to various rare hadronic processes [8, 15,

[1] We do not consider a possible θ–term in the QCD lagrangian here.

17, 41, 43, 44, 46, 49, 61, 62, 66].
In this work we will focus on short distance QCD calculations to the mixing of the flavour eigenstates K^0 and $\overline{K^0}$ of the neutral K–meson. Since the mass eigenstates K_L and K_S are linear combinations of them, $K^0-\overline{K^0}$–mixing encodes the information on the indirect CP violation.
The hamiltonian describing this mixing reads:

$$H^{|\Delta S|=2}(\mu) = \frac{G_F^2}{16\pi^2}M_W^2\left[\lambda_c^2\eta_1 S(\frac{m_c^2}{M_W^2})+\lambda_t^2\eta_2 S(\frac{m_t^2}{M_W^2})+2\lambda_c\lambda_t\eta_3 S(\frac{m_c^2}{M_W^2},\frac{m_t^2}{M_W^2})\right]b(\mu)\widetilde{Q}_{S2}(\mu) + \text{h.c.}. \quad (1.1)$$

Here $|\Delta S| = 2$ denotes the change in the strangeness quantum number in the transition between K^0 and $\overline{K^0}$, G_F is the Fermi constant, $\lambda_j = V_{jd}V_{js}^*$ comprises the CKM–factors, and $\widetilde{Q}_{S2}$ is the local four quark operator (see fig. 5.3 on p. 64)

$$\widetilde{Q}_{S2} \;=\; (\overline{s}_j\gamma_\mu(1-\gamma_5)d_j)(\overline{s}_k\gamma^\mu(1-\gamma_5)d_k) \;=\; (\overline{s}d)_{V-A}(\overline{s}d)_{V-A} \quad (1.2)$$

with j and k being colour indices. The Inami–Lim functions $S(x)$ and $S(x,y)$ [14] depend on the masses of the charm– and top–quark and describe the $|\Delta S| = 2$–transition amplitude in the absence of strong interaction. They are obtained by calculating the lowest order box diagrams depicted in fig. 5.1 on p. 61. The short distance part is included in the coefficients η_1, η_2 and η_3 with a common factor $b(\mu)$ split off.
Here η_2 and η_3 are most important for the size of ε_K, while η_1 gives the dominant contribution to the short distance part of the K_L-K_S–mass difference. When this work was begun, a next–to–leading order (NLO) calculation for η_2 had been performed [15], but no QCD corrections beyond leading logarithms had been known for η_1 and η_3. The leading log (LL) approximation is very unsatisfactory, because it is plagued with huge renormalization scale uncertainties and no use of the QCD scale parameter $\Lambda_{\overline{\text{MS}}}$ can be made. In this thesis the complete $|\Delta S| = 2$–hamiltonian in the NLO will be presented [67].
As the importance of ε_K has been stressed already, let us now discuss the K_L-K_S–mass difference: Its measured value is $3.5\,\mu$eV, which, by the way, is of the same order of magnitude as the Lamb shift mentioned in the beginning of this chapter. The prediction of the charm–quark mass, $m_c \approx 1.5\,\text{GeV}$, from the K_L-K_S–mass difference in [13] was surprisingly good for an analysis which neglected strong interaction effects. The inclusion of the latter, however, made the theoretical prediction worse, as estimates of the hadronic matrix element $\langle\widetilde{Q}_{S2}\rangle$ by various nonperturbative methods resulted in a significant reduction of the naive vacuum insertion value used in [13]. Further the leading–log calculation of the short distance QCD corrections gave an additional suppression of the predicted K_L-K_S–mass difference due to $\eta_1 < 1$, so that the calculation reproduced less than half of the measured K_L-K_S–mass difference. On the other hand one also expects additive long–distance contributions corresponding to light meson poles which are not contained in (1.1). These contributions are poorly calculable, but should be suppressed with respect to the short distance part by power counting arguments. Therefore the low result of the short distance

calculation is somewhat surprising and in fact triggered some speculation to assign the deficit to new physics. Our NLO calculation for η_1 [17], however, together with present day values for the input parameters such as $\Lambda_{\overline{\rm MS}}$ has established $\eta_1 > 1$ implying a sizeable increase of the short distance contribution to the $\rm K_L - K_S$–mass difference, which is now roughly of the order of 70% of the observed value. This fits much better with the expectation, especially when contrasted with an earlier incorrect NLO calculation [18] finding a drastical decrease of the short distance part.
In the following chapter we will summarize some field theoretic basics needed for the subsequent chapters. Chapter 3 will discuss the operator product expansion and renormalization group techniques. Here we will also develop the renormalization group formalism for Green's functions with two operator insertions. Chapter 4 contains new results about evanescent operators [19]. They comprise the correct treatment of bilocal structures involving evanescent operators, which had to be developed for the calculation of η_3. Further a new scheme dependence associated with the definition of the evanescents is discussed. In chapter 5 the operator basis involved in the NLO $|\Delta {\rm S}| = 2$ lagrangian will be analyzed. In chapter 6 the NLO calculation of η_1 and η_3 will be described in detail, and chapter 7 is devoted to the phenomenological analyses. Here we will analyze the consequences of the new NLO prediction for $\varepsilon_{\rm K}$ on the Standard Model parameters. We will also look at the new prediction of the short distance contribution to the $\rm K_L - K_S$–mass difference.

2. Quantum Field Theory and the Standard Model

Our today's knowledge about the rich field of elementary particle physics is the result of many decades of research probing the laws of nature at small distances. The experimental effort has been paralleled by a similarly successful development of the theoretical framework to understand the guiding principles of the observed phenomena.
Clearly we cannot summarize all results of this development here, so that we instead focus on those aspects of modern quantum field theory which are relevant for the actual calculations concerning the $\mathrm{K}^0-\overline{\mathrm{K}^0}$–mixing performed for this thesis.

2.1. Lagrangian Field Theory

A classical field theory like electrodynamics contains a set of functions $\{\phi_j(x)\}$ of the space–time variable $x = (t, \vec{x})$[1] as its basic building blocks. The dynamics of these fields $\phi_j(x)$ is encoded in a scalar functional, the lagrangian (density) $\mathcal{L}\left[\phi_j(x), \partial_\mu\phi_j(x), x\right]$, from which the field equations of motions can be obtained. Here we have collectively summarized indices related to intrinsic properties like spin or charge quantum numbers and those distinguishing different physical fields into the single multi–index j.
When passing from classical to quantum field theory the functions $\phi_j(x)$ are replaced by field operators $\widehat{\phi}_j(x)$. Hence one has to deal with a quantum mechanical system with an uncountable infinity of degrees of freedom labeled by the space–time coordinate x. Its hamiltonian density $\mathcal{H}(x)$ is a polynomial in the elementary fields $\widehat{\phi}_j(x)$. For non–interacting fields the field theory can be solved, i.e. one can construct a Hilbert space (the Fock space) whose elements are eigenfunctions of the Fourier–transformed hamiltonian density $\widehat{\mathcal{H}}(\vec{k})$. A short glimpse on the simple structure of the lagrangian and on the variety of particle phenomenology shows that it is hopeless to try to solve the interacting quantum field theory exactly.

2.2. Symmetries

Before discussing the dynamics of field theory it is useful to look for underlying patterns which may possibly restrict the particle spectrum and the interactions. This is indeed the

[1] Throughout this thesis we use natural units $\mathrm{c} = \hbar = 1$.

case, if the total action

$$S\left[\phi_j\right] \;=\; \int d^4x \mathcal{L}\left[\phi_j(x), \partial_\mu \phi_j(x), x\right] \tag{2.1}$$

is invariant under some group of transformations of the arguments of $\mathcal{L}$.
Consider first some group G of linear transformations of the space–time variable:

$$x^\mu \to x'^\mu := \omega^\mu_\nu x^\nu \qquad \text{with } \; \omega \in G \tag{2.2}$$

If we can find a (possibly multivalued) representation $\mathcal{D}(G)$ of G such that with

$$\begin{aligned} \omega^\mu_\nu \;&\to\; \left[d\left(\omega\right)\right]_{jk} \in \mathcal{D}(G) \\ \phi_j(x) \;&\to\; \phi'_j(x') \;=\; \phi'_j(\omega \cdot x) \;:=\; \left[d\left(\omega\right)\right]_{jk} \phi_k(x) \end{aligned} \tag{2.3}$$

the action (2.1) satisfies $S[\phi'_j] = S[\phi_j]$, we speak of an *external* symmetry.
A symmetry group which only transforms the fields according to (2.3) but leaves the space–time coordinate unchanged is likewise generating an *internal* symmetry.
The key importance of symmetries for a classical field theory is due to Noether's theorem: If a symmetry Lie group leaves S invariant, one can construct a conserved current from the fields and find a globally conserved charge. These charges can be used to label different solutions of the equations of motion. A quantized theory may or may not enjoy a certain symmetry of the corresponding classical theory. In the second case one terms the symmetry to be broken. Otherwise the operator corresponding to the conserved charge commutes with the hamiltonian so that we can find a common eigenbasis of both operators. We can use the quantum numbers of the conserved charge to label the eigenstates of the hamiltonian and transitions between states with different quantum numbers are forbidden. In fact this property also applies to discrete symmetries.

2.2.1. External Symmetries

Poincaré–Invariance

When probing the laws of nature at distance scales at which gravitation is unimportant they turn out to be invariant with respect to

- translations in space and time,
- rotations

  and
- boosts into uniformly moving coordinate systems.

The last two types of transformations generate the proper Lorentz group $L^\uparrow$, all of them generate the Poincaré–group. We can test the abovementioned symmetries in a twofold

way: First we can repeat the experiments in different transformed coordinate frames[2] and second we can check the associated conservation laws predicted by Noether's theorem. They include the conservation of energy, momentum and angular momentum.
The fact that nature is invariant under (2.2) with $G = L^{\uparrow}$ greatly simpifies the theorist's work to guess the correct lagrangian describing the non–gravitational interactions: $\mathcal{L}$ must not explicitly depend on x and all fields must transform as in (2.3) according to some (possibly multivalued) representation of the proper Lorentz group. Since with (2.2) $d^4x = d^4x'$, these fields must combine to $L^{\uparrow}$–singlets in $\mathcal{L}$.
The proper Lorentz transformations leave the Minkowskian scalar product $x_\mu x^\mu = x_0^2 - \vec{x}^2$ invariant. Yet there are more transformations which have this property: We may extend $L^{\uparrow}$ by

the *parity* transformation $\mathbf{P}$: $\vec{x} \to -\vec{x}$

and

the *time reversal* transformation $\mathbf{T}$: $x_0 \to -x_0$.

$L := \{L^{\uparrow}, \mathbf{P}L^{\uparrow}, \mathbf{T}L^{\uparrow}, \mathbf{PT}L^{\uparrow}\}$ is the full Lorentz group. Unlike the transformations of $L^{\uparrow}$ we cannot carry out the *discrete* symmetries $\mathbf{P}$ and $\mathbf{T}$ by any active transformation of our experimental device, but still we can test them via the conservation or nonconservation of the associated charges. Since $\{\mathbf{1}, \mathbf{P}\}$ and $\{\mathbf{1}, \mathbf{T}\}$ are two–element groups, the associated charges P and T can only assume two different values. We may choose P and T as multiplicative quantum numbers being $+1$ or -1.
There is no reason why nature should respect these discrete symmetries. Nevertheless it was not before 1956 that Lee and Yang discovered the nonconservation of parity [20]. In the following we will need the transformation property of Dirac fields under $\mathbf{P}$ and $\mathbf{T}$. They transform as

$$\mathbf{P}: \quad \psi(x) \;\to\; \psi'(x') \;=\; \eta_P \gamma^0 \psi(x) \tag{2.4}$$

with an arbitrary phase η_P in any representation of the Dirac algebra. The current $j^\mu(x) = \overline{\psi}(x)\gamma^\mu\psi(x)$ is easily found to transform as a vector field, i.e. like x^μ, under $\mathbf{P}$. With $\gamma_5 := i\gamma_0\gamma_1\gamma_2\gamma_3$ the axial current $j^{A\,\mu}(x) = \overline{\psi}(x)\gamma^\mu\gamma_5\psi(x)$ likewise transforms with an extra factor of (-1) compared to $j^\mu(x)$. In the standard representation of the Dirac algebra one further finds:

$$\mathbf{T}: \quad \psi(x) \;\to\; \psi'(x') \;=\; \eta_T i\gamma^1\gamma^3\psi^*(x) \tag{2.5}$$

with η_T also being an arbitrary phase factor.

Scale Transformations

In the early 1950's Stückelberg and Peterman as well as Gell-Mann and Low for the first time studied the behaviour of a quantum field theory under dilatations of the space–time

[2]Theorists are allowed to neglect the technical problems, if this is tried for the boosts.

variable:

$$x \;\rightarrow\; x' = \lambda^{-1} x \tag{2.6}$$

or equivalently in momentum space

$$p \;\rightarrow\; p' = \lambda p. \tag{2.7}$$

One might expect that for large λ masses in $\mathcal{L}$ become negligible and any physical quantity scales according to its naive dimension determined by power counting. But this is not the case for a quantized theory due to the subtleties of renormalization to be discussed in sect. 2.4.3. Here we find the powerlike scaling behaviour modified by so called anomalous dimensions. In the context of renormalization the symmetry under scale transformations becomes a powerful calculational tool which will be looked at in detail in chapter 3.

2.2.2. Internal Symmetries

Gauge Symmetries

In view of the discussion of Quantum Chromodynamics (QCD) we first look at an SU(N)–symmetric theory containing Dirac fermions, which are chosen to transform according to the defining representation of SU(N):

$$\psi \;\rightarrow\; \psi_i' = U_{ij}(\theta^a)\psi_j, \quad U = e^{-iT^a\theta^a}. \tag{2.8}$$

Here the T^a's span the Lie algebra su(N). They satisfy

$$\left[T^a, T^b\right] = i f^{abc} T^c \tag{2.9}$$

with the structure constants f^{abc}. Continous internal symmetries are called gauge symmetries. If the gauge parameters θ^a in (2.8) are independent of x, one speaks of a *global* symmetry. *Local* gauge symmetries, where the θ^a's are allowed to depend on x, play a key role in field theory: They incorporate a natural description of interactions between the fermions mediated by a vector field $A^a_\mu(x)$. The lagrangian

$$\mathcal{L} \;=\; \overline{\psi}_i \left(i \not{D}_{ij} - m\delta_{ij}\right) \psi_j - \frac{1}{4} F^a_{\mu\nu} F^{a\,\mu\nu} \tag{2.10}$$

with

$$\begin{aligned} \not{D}_{ij} &= \not{\partial}\delta_{ij} - i g T^a_{ij} \not{A}^a \\ F^a_{\mu\nu} &= \partial_\mu A^a_\nu - \partial_\nu A^a_\mu + g f^{abc} A^b_\mu A^c_\nu \end{aligned}$$

is invariant under local SU(N) transformations, if the vector field $A^a_\mu(x)$ transforms as

$$T^a A'^a_\mu \;=\; U\left(\theta(x)\right) \left[T^a A^a_\mu - \frac{i}{g} U^{-1}\left(\theta(x)\right) \partial_\mu U\left(\theta(x)\right)\right] U^{-1}\left(\theta(x)\right). \tag{2.11}$$

Charge Conjugation

Charge conjugation is a discrete global internal transformation. The **C** operation exchanges particles and antiparticles. In the standard representation of the Dirac algebra a Dirac field transforms as

$$\mathbf{C}: \quad \psi(x) \;\rightarrow\; \psi'(x') \;=\; \eta_C i\gamma^0\gamma^2\overline{\psi}^T(x) \tag{2.12}$$

with the usual arbitrary phase η_C.
Soon after the discovery of parity non–conservation the charged weak lepton current was proposed to be of the type $\overline{e}(x)\gamma^\mu(1-\gamma_5)\nu_e(x)$. This interaction also violates charge conjugation symmetry, but it is invariant under the combined transformation **CP**. Finally in 1964 it became clear that the weak charged hadronic current violates **CP** invariance [10].

2.2.3. CPT Theorem

After quantizing a theory one wishes to find a representation of the symmetry transformations of interest in the space of state vectors on which the field operators $\widehat{\phi}(x)$ act. A theorem of Wigner states that one can always find such a transformation, the corresponding operator is either unitary or anti–unitary and commutes with the hamiltonian. We have already alluded to this theorem in the discussion before sect. 2.2.1. In the case of **C** and **P** this operator is unitary, while it is anti–unitary for **T**.
According to our present knowledge the electromagnetic and the strong interaction respect **C**, **P** and **T** separately, while the weak interaction violates all of them. Nevertheless Lüders and Pauli [21] have proven that any Poincaré–invariant field theory must respect the combined anti–unitary transformation **CPT**. This has the consequences that particles and antiparticles have the same mass and spin and that particles with zero quantum numbers are identical to their antiparticles. The implications of the **CPT** theorem are experimentally confirmed.

2.3. Standard Model

In the Standard Model the electromagnetic and the weak interaction are unified in a $\mathrm{SU(2)_L \times U(1)_Y}$ gauge invariant lagrangian $\mathcal{L}_{\mathrm{ew}}$ [4]. The strong interaction is comprised in the SU(3) invariant lagrangian of Quantum Chromodynamics, $\mathcal{L}_{\mathrm{QCD}}$ [3]. Both combine to the Standard Model lagrangian $\mathcal{L}_{\mathrm{SM}}$.
The weak sector is the richest field of the Standard Model. First the electroweak gauge group $\mathrm{SU(2)_L \times U(1)_Y}$ is chiral, because left–handed fermion fields transform differently from the right–handed ones implying parity violating couplings. Second the $\mathrm{SU(2)_L \times U(1)_Y}$ gauge symmetry is spontaneously broken to the electromagnetic gauge group $\mathrm{U(1)_{em}}$. This means that the physical vacuum state does not have the $\mathrm{SU(2)_L \times U(1)_Y}$–symmetry of the lagrangian. In the Standard Model the symmetry breaking is provided by the Higgs–Kibble mechanism [22] introducing a scalar potential in $\mathcal{L}$ with degenerate minima which transform into each other under $\mathrm{SU(2)_L \times U(1)_Y}$ transformations instead of being individually

invariant. As a consequence three gauge bosons become massive due to their interaction with the Higgs field. The chiral structure of the Standard Model forbids explicit mass terms for the fermions. Fermion masses are therefore generated through Yukawa interactions with the Higgs field. After diagonalizing the resulting quark mass matrix the coupling between the mass eigenstates of the quarks and the weak charged vector bosons $W_\mu^\pm$ is found to be of the form:

$$\mathcal{L}_{wc} = -\frac{g_w}{2\sqrt{2}} J_{cc}^\mu(x) W_\mu^+(x) + \text{h.c.} \tag{2.13}$$

Here g_w is the weak coupling constant and $J_{cc}(x)$ is the weak charged current:

$$J_{cc}^\mu(x) = \overline{u}_j(x)\gamma^\mu(1-\gamma_5)V_{jk}d_k(x) \tag{2.14}$$

where u_j denotes the up–type quarks of the three families, u,c,t, and d_k stands for the down–type quarks d,s,b. The Yukawa interactions in $\mathcal{L}_{\text{SM}}$ do not only induce fermion masses, but also allow for family–changing couplings in (2.14) described by the unitary Cabibbo–Kobayashi–Maskawa (CKM) matrix (V_{jk}) [6]. A unitary 3×3–matrix can be parametrized by nine parameters, five of which are redundant in (2.14), as they correspond to physically irrelevant redefinition of the quark fields by U(1) phase transformations. The other four correspond to a complex phase δ and three rotation angles, i.e. V is real for $\delta = 0$. If V is real the charged current interaction $\mathcal{L}_{wc}$ in (2.13) is **CP**–conserving. A non–zero δ corresponds to **CP** violation. This can easily be seen by recalling from sect. 2.2.3 that the latter is equivalent to **T** violation which is an antiunitary transformation involving a complex conjugation. Hence since $\mathcal{L}_{wc}$ is **T** invariant for real V, it must in general transform under **T** into an expression with complex conjugate V. Since further $J_{cc} \neq J_{cc}^\dagger$ this is different from the untransformed $\mathcal{L}_{wc}$. Yet only a non–zero δ is not sufficient for **CP** violation, we must also ensure that it cannot be absorbed into a redefinition of the quark fields. This means that the three up–type quarks as well as the three down–type quarks must have different masses. In the lepton sector any mixing matrix can likewise be absorbed into a redefinition of the neutrino fields, if the neutrinos are massless.
For the weak neutral current such flavour–changing vertices do not occur as a consequence of the unitarity of V. This phenomenon is called GIM mechanism [12] implying the suppression of flavour changing neutral current (FCNC) processes.
The QCD lagrangian enjoys an unbroken SU(3) gauge symmetry. It is obtained by adding a flavour label k to the fermion field in (2.10):

$$\mathcal{L}_{\text{QCD}} = \overline{\psi}_k \left(i\not{D} - m_k\right) \psi_k - \frac{1}{4} F_{\mu\nu}^a F^{a\,\mu\nu} \tag{2.15}$$

with the colour indices now being suppressed. In (2.15) the fermion fields $\psi_k(x)$ correspond to quarks with mass m_k and the vector fields $A_\mu^a(x)$ correspond to gluons.

2.4. Perturbation Theory

When quantizing a theory we want to preserve the symmetries of the classical theory. I.e. we wish to have the vectors of the Hilbert space on which our field operators act transform

according to a representation of the symmetry group. E.g. for some internal symmetry Lie group with generators T^a and structure constants f^{abc} one seeks to find a set of operators $\widehat{Q}^a$ satisfying

$$\left[\widehat{Q}^a, \widehat{Q}^b\right] = if^{abc}\widehat{Q}^c \tag{2.16}$$

and

$$e^{-i\epsilon_a\widehat{Q}^a}\widehat{\phi}_k e^{i\epsilon_a\widehat{Q}^a} = \left[e^{-i\epsilon_a T^a}\right]_{kj}\widehat{\phi}_j. \tag{2.17}$$

Here the second condition implies the consistency between the symmetry transformation in the Hilbert space (LHS) with the corresponding transformation of the fields (RHS). In (2.17) an additional unphysical phase factor is allowed, too. Further microcausality requires that the operators corresponding to the Noether currents commute, if the distance of their arguments is spacelike. All these conditions are fulfilled, if one postulates canonical commutation relations for boson field operators and canonical anticommutation relations for fermion field operators:

$$\left[\widehat{\phi}_j(x), \frac{\delta\mathcal{L}}{\delta\left(\partial_0\widehat{\phi}_k\right)}(y)\right]_{\pm} = i\delta^{(3)}(\vec{x}-\vec{y}) \quad \text{for } x^0 = y^0. \tag{2.18}$$

The operators $\widehat{Q}^a$ are then obtained by simply replacing the classical fields ϕ_j by $\widehat{\phi}_j$ in the expressions for the classical Noether charges Q^a. Finally for an unbroken symmetry the vaccuum state $|0\rangle$ is chosen to be invariant with respect to the symmetry transformations.

2.4.1. Green's Functions, S–Matrix

In this section we consider for simplicity a theory with a single real scalar field $\widehat{\phi}(x)$. The vacuum–to–vacuum amplitude of a product of n field operators is called n–point Green's function:

$$G_n(x_1, \ldots x_n) = \langle 0|\,\mathbf{T}\,\widehat{\phi}(x_1)\cdot\ldots\widehat{\phi}(x_n)|0\rangle. \tag{2.19}$$

Here $\mathbf{T}$ means time ordering of the fields such that the time coordinates increase from right to left. For a noninteracting theory all Green's functions can be easily expressed in terms of the simplest nonvanishing Green's function

$$G_2(x_1, x_2) = \frac{1}{(2\pi)^4}\int d^4x e^{ik\cdot(x_1-x_2)}\widetilde{G}_2(k) \tag{2.20}$$

with the Stückelberg–Feynman propagator

$$\widetilde{G}(k) = \frac{i}{k^2 - m^2 + i\varepsilon}. \tag{2.21}$$

(2.18) implies that the Fourier components of a free field $\widehat{\phi}(x)$ satisfy the commutation relations of annihilation and creation operators. Hence one can use them to create n–particle states from the vacuum state $|0\rangle$. These n–particle states form the canonical basis of the Fock space $\mathcal{F}$.
For an interacting field theory we neither know the form of $\widetilde{G}(k)$ in (2.20) nor can we relate the n–point function in (2.19) to the two–point function (2.20). On the other hand we empirically know that largely separated particles essentially behave as free particles. Further in a scattering experiment the relevant distances $|\vec{x}_j - \vec{x}_k|$ and $|x_j^0 - x_k^0|$ are large. The Riemann–Lebesgue lemma states that for $|x_j^\mu - x_k^\mu| \to \infty$ only non–integrable singularities of $\widetilde{G}(k)$ can give a contribution to the integral in (2.20). Hence one assumes that also for an interacting theory $\widetilde{G}(k)$ develops a pole as in (2.21):

$$\widetilde{G}_2(k) \;=\; \frac{R}{k^2 - m^2_{\text{pole}}} + \text{less singular terms} \,. \tag{2.22}$$

This makes the concept of asymptotic states and fields plausible: One assumes that the Hilbert space of the interacting field theory contains some subset of state vectors which for $t \to -\infty$ develop into states which correspond to n–particle momentum eigenstates of the free hamiltonian. I.e. for $t \to -\infty$ any of these *in–states* tends to an element of the canonical basis of a Fock space $\mathcal{F}$. These states describe the incoming particles in scattering experiments. The in–states are created and annihilated by the Fourier components of a free field operator $\widehat{\phi}_{\text{in}}$. On the subspace spanned by the in–states one has

$$\widehat{\phi}(x) \quad \underset{t\to-\infty}{\simeq} \quad R^{1/2}\widehat{\phi}_{\text{in}}(x) \tag{2.23}$$

in the weak sense. Here one has to allow for a real constant factor R, because (2.18) fixes an overall normalization of $\widehat{\phi}_{\text{in}}$. Next one postulates a field $\widehat{\phi}_{\text{out}}(x)$ and a set of *out–states* which have the described property for $t \to \infty$ corresponding to the outgoing particles in the particle collider. It is reasonable to assume that every particle species which can be used to prepare the incoming beam can possibly be observed in the final state and vice versa, thus the out–states span the same Fock space $\mathcal{F}$ as the in–states. Lorentz invariance implies the invariance of the vaccuum, $|0\rangle_{\text{interacting}} = |0\rangle_{\text{in}} = |0\rangle_{\text{out}}$, and of one–particle states, $|\vec{p}\rangle_{\text{interacting}} = |\vec{p}\rangle_{\text{in}} = |\vec{p}\rangle_{\text{out}}$. Hence with (2.23) one finally obtains an interacting two–point function which behaves asymptotically for $|x_1^0 - x_2^0| \to \infty$ in accordance with (2.22).
The scattering experiment is described by the transition amplitude or S–matrix element

$$S_{\alpha\beta} \;=\; \langle \alpha,\, \text{out}\,|\beta,\, \text{in}\,\rangle = \langle \alpha,\, \text{in}\,|S|\beta,\, \text{in}\,\rangle. \tag{2.24}$$

With the concept of asymptotic fields and states it is now possible to relate the S–matrix elements to the Green's functions. This relationship is given by the reduction formula of Lehmann, Symanzik and Zimmermann (LSZ) [23]. It is particularly simple in terms of the Fourier transformed $(n+l)$–point Green's function $(2\pi)^4\delta(\sum_{i=1}^{n+l} k_i) \cdot \widetilde{G}_{n+l}(k_1, \ldots, k_{n+l-1})$:

$$\langle p_1, \ldots p_n,\, \text{out}|q_1, \ldots q_l\,\text{in}\rangle \;=$$

$$R^{\frac{n+l}{2}}(2\pi)^4\delta(\sum_{i=1}^{n}p_i-\sum_{i=1}^{l}q_i)\cdot\widetilde{G}^t_{n+l}\left(-p_1,\ldots,-p_n,q_1,\ldots q_{l-1}\right), \tag{2.25}$$

where we have for simplicity assumed that $p_i \neq q_j$ for all (i,j). In (2.25) the *truncated* Green's function G^t is defined by

$$\widetilde{G}^t_r(k_1,\ldots,k_{r-1}) \;=\; \lim_{k_1^2\to m^2}\cdots\lim_{k_r^2\to m^2}\left.\frac{\widetilde{G}_r(k_1,\ldots,k_{r-1})}{\prod_{i=1}^{r}\widetilde{G}_2(k_1)}\right|_{k_r=-\sum_{i=1}^{r-1}k_i} \tag{2.26}$$

If vector bosons or fermions are scattered the fields in (2.25) carry indices which are contracted with spinors or polarization vectors of the external particles.
From (2.25) and (2.26) one realizes that Green's functions carry a lot of redundant information, only their on–shell values are related to physical observables.
Finally one is left with the evaluation of the Green's functions $G_n(x_1,\ldots x_n)$. They can be most conveniently expressed in terms of the path integral:

$$G_n(x_1,\ldots x_n) \;=\; \frac{\int[d\phi]\,\phi(x_1)\cdots\phi(x_n)e^{iS[\phi]}}{\int[d\phi]\,e^{iS[\phi]}} \tag{2.27}$$

In perturbation theory one expresses $\widetilde{G}_n$ by a power series in the coupling constants of the lagrangian. In (2.27) this is done by expanding the kernel

$$e^{iS[\phi]} \;=\; e^{iS_{\rm free}[\phi]}\sum_n\frac{i^n}{n!}\left[\int d^4x\mathcal{L}_{\rm int}\left[\phi(x),\partial_\mu\phi(x)\right]\right]^n \tag{2.28}$$

with $\mathcal{L}_{\rm int}$ being the interaction lagrangian. The individual terms of this perturbation series are usually depicted in a collection of *Feynman diagrams*. With (2.28) and (2.27) one realizes that one can formally write for the S–matrix in (2.24):

$$S \;=\; \mathbf{T}\,e^{i\int d^4x\mathcal{L}_{\rm int}[\phi(x),\partial_\mu\phi(x)]}. \tag{2.29}$$

Within perturbation theory the assumption (2.22) is indeed verified: In any finite order of perturbation theory the interacting two–point function is of the form given in (2.22). $m_{\rm pole}$ and the residue R of the single particle pole are also power series in the couplings.
In gauge theories the path integral (2.27) includes the integration over field configurations which are related to each other by gauge transformations. Further even the free propagator (2.20) of a gauge boson when derived from (2.10) does not exist. A remedy is the addition of a gauge fixing term $\mathcal{L}_{\rm gf}=-\left(\partial^\mu A^a_\mu\right)^2/(2\xi)$ with gauge parameter ξ and the introduction of Faddeev–Popov ghost fields η^a via $\mathcal{L}_{\rm FP}=(\partial^\mu\overline{\eta}^a)\,D^{ab}_\mu\eta^b$ [24]. The graphs with FP ghosts correct for the unphysical polarizations of the gauge fields corresponding to gauge degrees of freedom. FP ghosts are scalar Grassmann fields meaning that they anticommute.
Hence the QCD lagrangian suitable for perturbative calculations reads:

$$\mathcal{L}_{\rm pQCD} \;=\; \overline{\psi}_k\left(i\not{D}-m_k\right)\psi_k-\frac{1}{4}F^a_{\mu\nu}F^{a\,\mu\nu}-\frac{1}{2\xi}\left(\partial^\mu A^a_\mu\right)^2+(\partial^\mu\overline{\eta}^a)\,D^{ab}_\mu\eta^b \tag{2.30}$$

One terms quantities which do not depend on the arbitrary gauge parameter ξ *gauge independent*. S–matrix elements and physical observables are gauge–independent. In contrast a field polynomial or Green's function is called *gauge invariant*, if it is invariant with respect to the gauge transformation (2.8) and (2.11).
After all in the case of QCD the standard reduction procedure sketched above does not seem very useful, because in the very beginning the assumption (2.22) is in contradiction with the observed confinement property. The poles in the Green's functions are not related to the particles described by the elementary fields in the lagrangian as suggested by (2.25), but rather by bound states, hadrons, formed by them. The asymptotic states are hadron states which we cannot simply relate to quark and gluon fields. We may then ask how to make use of perturbative QCD at all. To answer this questions one has to mention a further property of perturbative quantum field theory discovered by Wilson [25]: It is possible to expand a Green's function in terms of some ratio of mass parameters and each term of this expansion is the product of a Green's function involving a composite operator and a coefficient being independent of the external states. This *Wilson coefficient* comprises the short distance physics whose scale is set by the inverse heavy mass parameter. Further QCD enjoys the feature of asymptotic freedom ensuring that the QCD coupling is small when probed at small distances. Hence for the calculation of the Wilson coefficients one can use perturbation theory and can further take external quark states rather than hadron states.
Sometimes people try to describe hadron properties in terms of off–shell quark Green's functions. They, however, are unphysical, as mentioned in the discussion after (2.25), e.g. they are gauge dependent. This point will be relevant in the discussion of the use of the field equation of motion in sect. 3.10.1.

2.4.2. BRS Invariance

The lagrangian (2.30) is no more gauge invariant due to the gauge–fixing term and the Faddeev–Popov term. It seems as if we have lost all the nice features of local gauge symmetry. This is not so, because (2.30) is still invariant under *Becchi–Rouet–Stora* (BRS) transformations [26]. They are constructed by factorizing the gauge parameter in (2.8) and (2.11) into the product of the FP field and a Grassmann parameter $\delta\lambda$:

$$\delta\theta^a(x) = \eta^a(x)\delta\lambda.$$

The infinitesimal transformations of the various fields read:

$$\begin{aligned}
\delta_{\mathrm{BRS}}\psi &= -ig(\eta^a\delta\lambda)T^a\psi \;=\; igT^a\eta^a\psi\delta\lambda, \\
\delta_{\mathrm{BRS}}\overline{\psi} &= ig\overline{\psi}T^a\eta^a\delta\lambda, \\
\delta_{\mathrm{BRS}}A^a_\mu &= \left(\partial_\mu\eta^a + gf^{abc}\eta^b A^c_\mu\right)\delta\lambda \\
\delta_{\mathrm{BRS}}\eta^a &= -\frac{1}{2}gf^{abc}\eta^b\eta^c\delta\lambda \\
\delta_{\mathrm{BRS}}\overline{\eta}^a &= \frac{1}{\xi}\partial^\mu A^a_\mu\delta\lambda.
\end{aligned} \tag{2.31}$$

The basic QCD lagrangian (2.15) is clearly BRS invariant, because for the quark and gluon fields the BRS transformation is just a gauge transformation. The ghost fields transform such that $\mathcal{L}_{\rm gf} + \mathcal{L}_{\rm FP}$ is invariant. The BRS symmetry is a global supersymmetry, because it involves an x–independent anticommuting parameter $\delta\lambda$. Its magic is that it encodes the original local gauge symmetry which had to be destroyed by adding $\mathcal{L}_{\rm gf} + \mathcal{L}_{\rm FP}$ to $\mathcal{L}_{\rm QCD}$.
A global symmetry of $\mathcal{L}$ induces relations between Green's functions called *Ward–Takahashi identities* [28]. The Ward–Takahashi identities implied by BRS invariance are *Slavnov–Taylor* identities [29]. We will need them in the form

$$\delta_{\rm BRS}\langle 0|\,\mathbf{T}\,XY|0\rangle \;=\; \langle 0|\,\mathbf{T}\,(\delta_{\rm BRS}X)\,Y|0\rangle + \langle 0|\,\mathbf{T}\,X\,(\delta_{\rm BRS}Y)\,|0\rangle \;=\; 0, \qquad (2.32)$$

where X and Y are product of fields whose arguments may coincide. When making use of (2.32) one has to anticommute $\delta\lambda$ to the right (or to the left) thereby picking up a relative "–"–sign between the terms involving $\delta_{\rm BRS}X$ and $\delta_{\rm BRS}Y$, if they contain an odd number of Dirac fields.

2.4.3. Renormalization

The perturbative evaluation of Green's functions involves integrations over loop momenta. Some of these integrals diverge when the loop momenta get large, they are *UV divergent*. To give a meaning to these divergent expressions one first has to regularize the divergence: An additional parameter D is introduced in the lagrangian such that the latter coincides for $D = D_0$ with the original lagrangian. The loop integrals are finite in some range for D and analytic functions in D. For $D \to D_0$ one rediscovers the divergence in the form of some singularity. Throughout this paper we use dimensional regularization which conserves most of the interesting symmetries. Here D is the space–time dimension and $D_0 = 4$. The appearance of UV divergences originates in the fact that quantum field operators are singular distributions, see (2.18). In general their product is ill-defined when their arguments coincide. The renormalization process gives a meaning to the field products in the interaction lagrangian.
The renormalization process is carried out recursively in the power of the coupling constant g or equivalently in the number of loops. It is encoded in *Zimmermann's forest formula* [27]. Starting from the one–loop order one finds that one can absorb all divergences into a multiplicative redefinition of the parameters of the lagrangian such as masses, couplings and the normalization of the fields which is connected to the quantity R in (2.23). These multiplicative renormalization constants are Laurent series in $D-4$ in dimensional regularization. In the n–th order all divergences of 1– to (n–1)–loop subdiagrams are already remedied by the earlier renormalization steps. The remaining overall divergence can then be absorbed into new n–th order terms in the renormalization constants. For this to work it is crucial that after the subtraction of subdivergences the divergences are local, i.e. polynomial in the external momenta of the Green's function under consideration. Further the renormalization constants must be universal meaning they must remove the divergence of some subloop in whatever diagram it occurs.

Yet for a predicative theory we must also ensure that the renormalization process does not induce new couplings in any new order of perturbation theory, because then we would end up with a theory with infinitely many undetermined parameters. This can be ensured, if the lagrangian contains only couplings with non–negative dimension. In this case we term the theory to be *renormalizable by power counting*. This criterion applies to the Standard Model.
In the following we will also be confronted with *effective* field theories which contain couplings with negative dimension. The parameters of such effective field theories, however, will be fixed by a *matching* procedure in which the effective theory Green's functions are related to Standard Model Green's functions, so that the theory is predicative.
Since we will always work to lowest nonvanishing order in the weak coupling constant, we will only have to discuss renormalization of the QCD lagrangian. First we define

$$\varepsilon \;=\; \frac{4-D}{2}.$$

The QCD Lagrangian now reads in terms of the unrenormalized (*bare*) parameters:

$$\begin{aligned}\mathcal{L}_{\mathrm{pQCD}} \;=\;& -\frac{1}{4}\left(\partial_\rho A^{(0),a}_\nu - \partial_\nu A^{(0),a}_\rho\right)\left(\partial^\rho A^{(0),\nu\,a} - \partial^\nu A^{(0),\rho\,a}\right)\\ & -\frac{1}{2\xi^{(0)}}\left(\partial^\rho A^{(0),a}_\rho\right)^2 + \overline{\psi}^{(0)}_k\left(i\partial\!\!\!/ + g^{(0)}T^a A\!\!\!/^{(0),a} - m^{(0)}_k\right)\psi^{(0)}_k\\ & +\left(\partial^\rho\overline{\eta}^{(0),a}\right)\left(\partial_\rho\delta^{ab} - g^{(0)}f^{abc}A^c_\rho\right)\eta^{(0),b}\end{aligned} \tag{2.33}$$

The bare fields and parameters are related to the renormalized ones by

$$\begin{aligned}&A^{(0),a}_\rho = Z_A^{1/2}A^a_\rho, \qquad \psi^{(0)} = Z_\psi^{1/2}\psi, \qquad \eta^a = Z_\eta^{1/2}\eta^a,\\ &g^{(0)} = Z_g g\mu^\varepsilon, \qquad \xi^{(0)} = Z_A\xi, \qquad m^{(0)} = Z_m m.\end{aligned} \tag{2.34}$$

Here an arbitrary dimension–1 parameter, the *renormalization scale* μ has been introduced to keep the renormalized coupling constant g dimensionless. In dimensional regularization the n–loop diagrams involve poles in ε up to order n. Hence the renormalization constants are of the form:

$$Z \;=\; 1+\sum_j\left(\frac{g^2}{16\pi^2}\right)^j Z^{(j)}, \qquad Z^{(j)} \;=\; \sum_{k=0}^{j}\frac{1}{\varepsilon^k}Z^{(j)}_k. \tag{2.35}$$

Now the renormalized lagrangian reads:

$$\begin{aligned}\mathcal{L}_{\mathrm{pQCD}} \;=\;& -\frac{1}{4}Z_A\left(\partial_\rho A^a_\nu - \partial_\nu A^a_\rho\right)\left(\partial^\rho A^{\nu\,a} - \partial^\nu A^{\rho\,a}\right) - \frac{1}{2\xi}\left(\partial^\rho A^a_\rho\right)^2\\ & +Z_\psi\overline{\psi}_k i\partial\!\!\!/\psi_k - Z_\psi Z_m m_k\overline{\psi}_k\psi_k + Z_\eta\partial^\rho\overline{\eta}^a\partial_\rho\eta^a\\ & -Z_g Z_A^{3/2}\frac{g}{2}\mu^\varepsilon f^{abc}\left(\partial_\rho A^a_\nu - \partial_\nu A^a_\rho\right)A^{b\,\rho}A^{c\,\nu} + Z_g Z_\psi Z_A^{1/2}g\mu^\varepsilon\overline{\psi}A\!\!\!/^a T^a\psi\\ & -Z_g^2 Z_A^2\frac{g^2}{4}\mu^{2\varepsilon}f^{abe}f^{cde}A^a_\rho A^b_\nu A^{c\rho}A^{d\nu} - Z_g Z_\eta Z_A^{1/2}g\mu^\varepsilon f^{abc}\left(\partial^\rho\overline{\eta}^a\right)A^c_\rho\eta^b\end{aligned} \tag{2.36}$$

Sometimes it is useful to decompose $\mathcal{L}_{\mathrm{pQCD}}$ in (2.36) into a sum $\mathcal{L}_0 + \mathcal{L}_{\mathrm{ct}}$, where $\mathcal{L}_0$ has the form of (2.33) with the bare quantities replaced by renormalized ones. $\mathcal{L}_{\mathrm{ct}}$ is called *counterterm lagrangian*.
Gauge invariance has implied that all interaction terms in $\mathcal{L}_{\mathrm{pQCD}}$ involve the same coupling constant g. Dimensional regularization has the advantage that it manifestly preserves gauge invariance in the unrenormalized Green's functions. As shown by 't Hooft the subsequent renormalization procedure does not spoil gauge invariance, so that Z_g is the same in all these interaction terms [30]. Finally also renormalized Green's functions obey the Slavnov–Taylor identities, but with a renormalized parameter

$$\delta\lambda_r \quad = \quad Z_A^{-1/2} Z_\eta^{-1/2} \delta\lambda. \tag{2.37}$$

3. Renormalization Group and Operator Product Expansion

3.1. Renormalization Schemes

When determining the renormalization constants in (2.36) one calculates Green's functions obtained from $\mathcal{L}_0 + \mathcal{L}_{\rm ct}$ and adjusts the renormalization constants such that the result is finite. The Green's function to some fixed order in g involves n–loop diagrams with interaction vertices only from $\mathcal{L}_0$ and subloop counterterm diagrams with fewer loops and with vertices also from $\mathcal{L}_{\rm ct}$. The individual contributions contain divergent terms which depend non–polynomial on the external momenta p_i, but they cancel in the sum of every n–loop diagram and its sub–loop counterterm diagrams [27]. Since these *non–local poles* cancel, one can absorb the remaining divergences into n–loop counterterms.
Now one is free to subtract any momentum–independent constant $Z_0^{(n)}$ together with the divergences order by order in perturbation theory. Any such choice of the $Z_0^{(n)}$'s in (2.35) corresponds to a different renormalization scheme. In the *minimal subtraction* scheme (MS) [31] one picks $Z_0^{(n)} = 0$. All schemes in which the $Z_0^{(n)}$'s do not depend on the masses are called *mass independent*. Due to *Weinberg's theorem* [32] they enjoy the property that also the divergent parts of the $Z^{(n)}$'s are independent of the masses (see e.g. [33]). In other words in mass independent schemes the divergences are not only polynomial in the momenta but also in the masses. The main advantage of these schemes, however, is that they allow for the solution of the renormalization group equations to be discussed in sect. 3.2.
Since in every renormalization scheme the divergences are removed, any two schemes can at most differ by a finite renormalization, for example an arbitrary scheme is related to the MS scheme via

$$Z \;=\; Z^{\rm MS}\left[1 + Z_0^{(1)}\frac{g^2}{16\pi^2} + Z_0^{(2)}\frac{g^4}{(16\pi^2)^2}\ldots\right]. \tag{3.1}$$

From this one sees that the $Z_n^{(n)}$'s are scheme–independent while the other Laurent coefficients in (2.35) depend on the lower order $Z_0^{(k)}$'s. In fact the $Z_n^{(n)}$'s are simply related to the one–loop $Z_1^{(1)}$'s. The finite renormalization $\left[1 + Z_0^{(1)}g^2/(16\pi^2) + Z_0^{(2)}g^4/(16\pi^2)^2\ldots\right]$ in (3.1) may be viewed as a perturbative redefinition of the fields, masses and coupling constants in $\mathcal{L}$ in (2.36).
In dimensional regularization all loop integrals involve an additive term $\gamma_{\rm E} - \ln(4\pi)$ with $\gamma_{\rm E}$ being Euler's constant. It is reasonable to subtract this term in every order of perturbation

theory. The resulting scheme is called $\overline{\text{MS}}$ scheme [34]. There is a simple way to relate the $\overline{\text{MS}}$ scheme to the MS scheme: One first replaces the renormalization scale μ in (2.34) by

$$\overline{\mu} \;=\; \mu \left(\frac{e^{\gamma_{\text{E}}}}{4\pi}\right)^{1/2}. \tag{3.2}$$

Recalling that μ resp. $\overline{\mu}$ has been introduced into (2.36) to maintain integer dimensions for the renormalized parameters one realizes that each loop integral $\int d^D q$ comes with a factor of $\overline{\mu}^{2\varepsilon}$. Then one expands (3.2) to the desired order in ε and multiplies this power series with the Laurent series in ε of the unrenormalized diagrams. In this way one modifies the pole part of the unrenormalized Green's functions such that γ_E and $\ln(4\pi)$ vanishes. Finally one simply applies minimal subtraction to the remaining expression. This method, which will be used in this thesis, has the advantage that one can avoid Euler's constant and $\ln(4\pi)$ in intermediate steps of the calculation. Further one can easily translate relations proven in the MS scheme into the $\overline{\text{MS}}$ scheme.
Yet there is another aspect of (3.2): When inserted into (2.36) one may view (3.2) as a redefinition of g by a g–independent power series in ε, $1 + \sum_{k=1} a_k \varepsilon^k$, or alternatively as a redefinition of the field monomials multiplied by g. Here in (3.2) this series reads

$$\left(\frac{e^{\gamma_{\text{E}}}}{4\pi}\right)^{\varepsilon/2} \;=\; 1 + \frac{1}{2}\varepsilon\left(\gamma_{\text{E}} - \ln(4\pi)\right) + \ldots. \tag{3.3}$$

Clearly multiplying with such a power series does not commute with the renormalization process, so that it corresponds to a change of the renormalization scheme. Let us call this procedure *evanescent redefinition* of the coupling or of the field monomial. Such evanescent redefinitions appear naturally in the context of effective four–fermion couplings. We will investigate them in chapter 4 [19]. One task will be to translate an evanescent redefinition into a finite renormalization (3.1). We finally remark that the change from the MS to the $\overline{\text{MS}}$ scheme is equivalent to a change of the scale μ as evidenced from (3.2).
Any S–matrix element and any physical observable is independent of the chosen renormalization scheme to the calculated order. This means, if one calculates some observable in scheme I to order g_{I}^m and afterwards expresses g_{I} and the other parameters such as masses in terms of the coupling g_{II} and the parameters of some other scheme II, the result differs at most by terms of order g_{II}^{m+1} from the calculation of the observable in scheme II.

3.2. Renormalization Group, Λ_{QCD}

The invariance of the S–matrix with respect to the change of the renormalization prescription implies a continous symmetry of the quantized theory as noticed first by Stückelberg and Petermann [35]. The group associated to this symmetry is the *renormalization group* (RG). Its power roots in the fact that it links different orders of the perturbative series: By applying a renormalization group transformation to some n–th order Green's function we can add some logarithmic term of all uncalculated higher orders to the result. When

the RG is applied properly, these logarithms are the dominant contribution of the higher orders and they are summed to all orders by the RG transformation.
In mass independent schemes renormalized Green's functions depend on the renormalization scale μ. Changing μ corresponds to a very simple way of modifying the renormalization prescription as discussed after (3.2). The S–matrix is independent of μ, if the bare quantities in (2.33) are chosen μ–independent. Hence the renormalization scale invariance is a special case of the renormalization scheme invariance.

3.2.1. Renormalization Group Functions in QCD

In this section we will collect the important RG functions of QCD in the $\overline{\rm MS}$ scheme (see e.g. [36]). From the μ–independence of the unrenormalized parameters in (2.34) one easily finds:

$$\mu\frac{dg}{d\mu} \;=\; \beta(g(\mu)), \qquad \mu\frac{dm}{d\mu} \;=\; -m\gamma_m(g(\mu)) \tag{3.4}$$

with the *beta–function*

$$\beta(g(\mu)) \;=\; -\varepsilon g - \frac{\mu}{Z_g}\frac{dZ_g}{d\mu}g \tag{3.5}$$

and the *anomalous dimensions* of quark mass and quark field

$$\gamma_m(g(\mu)) \;=\; \frac{\mu}{Z_m}\frac{dZ_m}{d\mu}, \quad \gamma_\psi(g(\mu)) \;=\; \frac{\mu}{Z_\psi^{1/2}}\frac{dZ_\psi^{1/2}}{d\mu}. \tag{3.6}$$

m in (3.4) is the *current mass* appearing in the lagrangian (2.36). It is also called *running* mass, because it depends on μ. The renormalization group functions in mass independent schemes depend on μ only through $g(\mu)$ as indicated in (3.4). This feature allows to solve the renormalization group equation, which reads for a renormalized truncated connected n–quark Green's function:

$$\mu\frac{d}{d\mu}\left[Z_\psi^{-n/2}\left(g(\mu)\right)\widetilde{G}_n^{tc}\left(p_i, g(\mu), m(g(\mu)), \mu\right)\right] \;=\; 0. \tag{3.7}$$

Here $\mu\frac{d}{d\mu}$ means

$$\mu\frac{d}{d\mu} \;=\; \mu\frac{\partial}{\partial\mu} + \beta\frac{\partial}{\partial g} - \gamma_m m\frac{\partial}{\partial m} - n\gamma_\psi, \tag{3.8}$$

where the partial derivatives are performed with the bare quantities kept fixed.
Let us briefly sketch the relation of (3.7) to the scale transformations alluded to in sect. 2.2.1: Recalling that μ has been introduced to maintain an integer dimension d for $\widetilde{G}_n^{tc}$ one easily finds (see e.g [36, p. 199]):

$$\left(\mu\frac{\partial}{\partial\mu} + m\frac{\partial}{\partial m} + \lambda\frac{\partial}{\partial\lambda} + d\right)\widetilde{G}_n^{tc}\left(\lambda p_i, g(\mu), m(g(\mu)), \mu\right) \;=\; 0,$$

which may be used to eliminate $\mu\frac{\partial}{\partial\mu}$ in (3.7) in favour of the scaling factor λ of the external momenta.
Now μ enters Green's functions only in powers of ε, thus after expanding in ε only in powers of logarithms. Since $\beta(g) = O(g^3)$, $\gamma_\psi = O(g^2)$, $\gamma_m = O(g^2)$ and $\mu\frac{\partial}{\partial\mu} = \frac{\partial}{\partial \ln\mu}$, (3.7) connects the $\ln\mu$'s of different orders in g of G_n^{tc} to each other.
We will need the renormalization group functions up to the next–to leading order (NLO) [36]. The beta–function reads:

$$\beta(g) \;=\; -\beta_0^{(f)}\frac{g^3}{16\pi^2} - \beta_1^{(f)}\frac{g^5}{(16\pi^2)^2} + O(g^7) \tag{3.9}$$

with

$$\beta_0^{(f)} \;=\; \frac{11N-2f}{3}, \qquad \beta_1^{(f)} \;=\; \frac{34}{3}N^2 - \frac{10}{3}Nf - 2C_F f. \tag{3.10}$$

Here N is the number of colours, $C_F = (N^2-1)/(2N)$ and f is the number of quark flavours. For the anomalous mass dimension one finds:

$$\gamma_m(g) \;=\; \gamma_m^{(0)}\frac{g^2}{16\pi^2} + \gamma_m^{(1)(f)}\left(\frac{g^2}{16\pi^2}\right)^2 + O\left(g^6\right)$$

with

$$\gamma_m^{(0)} \;=\; 6C_F, \qquad \gamma_m^{(1)(f)} \;=\; C_F\left(3C_F + \frac{97}{3}N - \frac{10}{3}f\right). \tag{3.11}$$

Whenever we discuss leading order (LO) expressions, only the first term is kept in (3.9) and (3.11). The anomalous dimension of the quark field will only be needed in the leading order:

$$\gamma_\psi \;=\; \gamma_\psi^{(0)}\frac{g^2}{16\pi^2} + O(g^4) \tag{3.12}$$

with

$$\gamma_\psi^{(0)} \;=\; C_F\xi. \tag{3.13}$$

With these definitions it is easy to write down the solutions of the RG equations (3.4) for $\alpha(\mu) = g^2(\mu)/(4\pi)$:

$$\frac{\alpha(\mu)}{4\pi} \;=\; \frac{1}{\beta_0^{(f)}\log(\mu^2/\Lambda_f^2)} - \frac{\beta_1^{(f)}\log\left[\log(\mu^2/\Lambda_f^2)\right]}{\left(\beta_0^{(f)}\right)^3\log^2(\mu^2/\Lambda_f^2)} + O\left(\frac{\log^2[\ldots]}{\log^3(\ldots)}\right). \tag{3.14}$$

The mass parameter Λ_f has entered (3.14) as a constant of integration. Hence the massless coupling g of the classical lagrangian has become a function of the dimension–one parameter Λ_f in the quantized theory. (3.14) also exhibits the property of asymptotic freedom, $\alpha(\mu) \rightarrow$

0 for $\mu \to \infty$. By inverting (3.14) one can define Λ_f. For α defined in the $\overline{\text{MS}}$ scheme one has

$$\Lambda_{\overline{\text{MS}}} = \mu \left(\beta_0^{(4)} \frac{\alpha(\mu)}{4\pi}\right)^{\frac{-\beta_1^{(4)}}{2\left(\beta_0^{(4)}\right)^2}} \left[e^{-\frac{2\pi}{\beta_0^{(4)}\alpha(\mu)}} + O\left(\alpha(\mu)\right)\right]. \tag{3.15}$$

In the limit $\mu \to \infty$ this is a precise definition of $\Lambda_{\overline{\text{MS}}}$. Since the NLO coefficient β_1 appears in an overall factor rather than in a radiative correction, one realizes that it is mandatory to go to the NLO to define $\Lambda_{\overline{\text{MS}}}$. Conversely only in NLO expressions for some physical observable of interest one can make use of $\Lambda_{\overline{\text{MS}}}$. This is an important reason to perform perturbative calculations beyond the leading order. Λ_f has been defined in the MS scheme by Buras, Floratos, Ross and Sachrajda [37] and the $\overline{\text{MS}}$ scheme has been introduced by Bardeen, Buras, Duke and Muta [34].
Solving the RG equation (3.4) for the running quark mass yields for the mass at some scale μ expressed in terms of $m(\mu = m)$:

$$m(\mu) = m(m) \left(\frac{\alpha(\mu)}{\alpha(m)}\right)^{d_m^{(f)}} \left(1 + \frac{\alpha(m) - \alpha(\mu)}{4\pi} J_m^{(f)}\right). \tag{3.16}$$

In (3.16) $d_m^{(f)}$ and $J_m^{(f)}$ are defined by

$$d_m^{(f)} = \frac{\gamma_m^{(0)}}{2\beta_0^{(f)}} \quad \text{and} \quad J_m^{(f)} = \frac{-\gamma_m^{(1)(f)} + 2\beta_1^{(f)} d_m^{(f)}}{2\beta_0^{(f)}}$$

If $\widetilde{G}_n^{tc}$ only contains a single mass parameter apart from μ, for example some spacelike external momentum $\sqrt{-q^2}$, $\ln \mu^2$ must necessarily appear in the form $\ln(-q^2/\mu^2)$ To make sense of a perturbative calculation we must choose $\mu^2 \approx -q^2$ in order to avoid a large logarithm multiplying the expansion parameter $\alpha(\mu)$. One may solve (3.7) to obtain $\widetilde{G}_n^{tc}$ at any other scale μ. This RG improved expression differs from a standard perturbative result such that it includes the terms involving $\alpha(\mu)\ln(-q^2/\mu^2)$ to all orders in perturbation theory. The LO RG improved perturbation theory is therefore called *leading log* (LL) approximation.

3.3. A First Look at $K^0-\overline{K^0}$–Mixing

Yet in most physical processes more than one mass scale is involved. To make use of RG improved perturbation theory more field theoretic tools are needed. To motivate the following sections let us have a first look at the main subject of this thesis, the $|\Delta S|=2$ transition inducing $K^0-\overline{K^0}$–mixing.
Fig. 5.1 on p. 61 shows the lowest order $\Delta S=-2$ transition amplitude in the Standard Model. One–gluon radiative corrections are depicted in fig. 5.2 on p. 64. Now this amplitude is not useful to describe physical $|\Delta S|=2$ processes for the following reasons:

i) The diagrams of fig. 5.2 incorporate QCD corrections perturbatively. While this is appropriate for short distance effects, the long distance QCD interaction is non–perturbative and cannot be described by the exchange of gluons.

ii) There are largely separated mass scales involved: The radiative corrections of fig. 5.2 contain large logarithms such as $\alpha \ln(m_c/M_W) = O(1)$, so that the radiative corrections have the same order of magnitude as the leading term. One would like to sum this logarithm to all orders in perturbation theory. RG techniques applied to the Standard Model amplitude, however, will not achieve this, because with them only logarithms of μ can be summed to all orders.

iii) For the same reason it is not clear at which scale the running coupling should be evaluated. Between $\mu = m_c$ and $\mu = M_W$ the coupling $\alpha(\mu)$ changes roughly by a factor of three.

iv) The real external states are mesons rather than on–shell quarks. Off–shell quarks are an even worse description of mesons, because off–shell amplitudes are unphysical as mentioned in the end of sect. 2.4.1.

Hence to tackle the problem one wishes to separate short distance effects from the long distance physics. This separation is provided by Wilson's operator product expansion [25] discussed in the following section.

3.4. Operator Product Expansion

In weak processes involving hadrons one is confronted with two couplings: While ordinary perturbation theory in the weak coupling g_w works well, we have already seen in sect. 3.3 that we need a framework to include all–order effects in the strong coupling g and possibly non–perturbative features of QCD.
For this we expand the kernel of the path integral $\exp[i \int \mathcal{L}_{\rm SM}]$ in terms of the electroweak (and Higgs) interaction lagrangian, but keep the QCD interaction in the exponential. I.e. we expand as in (2.28), but with the QCD action added to $S_{\rm free}$ instead of being kept in $\mathcal{L}_{\rm int}$. Hence with (2.13) a four–quark Green's function corresponding to a weak charged current tree level process is found as

$$\begin{aligned} G_4^{(2)\,tc}(x_1,x_2,x_3,x_4) \;=\; & \frac{g_w^2}{8}\,\langle 0|\,\mathbf{T}\,\overline{\psi}_1(x_1)\overline{\psi}_2(x_2)\psi_3(x_3)\psi_4(x_4) \\ & \left[-\frac{1}{2!}\int d^Dy \int d^Dz J_{cc}^{\dagger\,\mu}(y) W_\mu^+(y) J_{cc}^\nu(z) W_\nu^-(z) + h.c.\right] |0\rangle^{tc}. \end{aligned} \tag{3.17}$$

Here the quark fields are free fields with respect to the electroweak interaction, but interacting fields with respect to QCD. (3.17) represents all diagrams with one W–boson exchange and an arbitrary number of gluons. The index 2 in $G_4^{(2)\,tc}$ means second order in the weak coupling constant. The weak current J_{cc}^ν is the first example of a *composite operator*, as it contains interacting fields at the same space–time point.

Now Wilson has shown that one can expand a product of field operators in a series of composite operators with increasing dimension. For the product of the two currents in (3.17) this reads[1]:

$$J^{\dagger\,\mu}_{cc}(y)J^{\nu}_{cc}(z) \;=\; \widehat{C}^{\mu\nu}_{j}(y-z)\widehat{Q}_j\left(\frac{y+z}{2}\right), \tag{3.18}$$

with the $\widehat{Q}_j$'s being local four–quark operators as depicted in fig. 5.7 on p. 69. The Green's functions on the RHS of the *operator product expansion* (OPE) (3.18) are the *matrix elements* of $\widehat{Q}_j$. The *Wilson coefficients* $\widehat{C}^{\mu\nu}_j$ are functions which are singular at $y = z$. The coefficient multiplying the operator with the lowest dimension is the most singular one by power counting. They comprise the short distance behaviour of the current product in (3.18) when y approaches z. After inserting (3.18) into (3.17) one performs the path integration over the W–boson fields. By this the open Lorentz indices in (3.18) are contracted with a W propagator $i\mathcal{D}^{(W)}_{\mu\nu}(y-z, M_W, \mu)$. With

$$C_j(M_W,\mu) \;=\; -\frac{g_W^2}{8}\int d^D\zeta \widehat{C}^{\mu\nu}_j(\zeta)\mathcal{D}^{(W)}_{\mu\nu}(\zeta, M_W, \mu) \tag{3.19}$$

one realizes that (3.18) turns into an expansion in the (inverse) W mass M_W. With (3.19) one finally obtains for (3.17):

$$\begin{aligned} &G_4^{(2)\,tc}(x_1,x_2,x_3,x_4) \;= \\ &\quad C_j(M_W,\mu)\langle 0|\,\mathbf{T}\,\overline{\psi}_1(x_1)\overline{\psi}_2(x_2)\psi_3(x_3)\psi_4(x_4)\,i\!\int\! d^Dy\widehat{Q}_j(y)|0\rangle^{\,tc}. \end{aligned} \tag{3.20}$$

Here we have absorbed the weak coupling constant into C_j. When we pass to the operator basis for $\mathrm{K}^0-\overline{\mathrm{K}^0}$–mixing in chapter 5 we will extract a factor of

$$-\frac{G_F}{\sqrt{2}} \;=\; -\frac{g_W^2}{8M_W^2} \tag{3.21}$$

out of C_j to show that the operator product expansion in weak decays replaces the Standard Model weak interaction by a four–fermion interaction with the Fermi constant G_F as the coupling constant. We will also sometimes leave out the integral over the space–time coordinate y of the composite operator in (3.20). This merely leaves out an overall momentum conserving δ–function when (3.20) is Fourier transformed into momentum space.
In momentum space (3.20) corresponds to an expansion in $m^2_{\mathrm{light}}/M^2_W$, where m_{light} stands collectively for the light[2] quark masses and the small external momenta and Mandelstam variables. The local operators in (3.18) may be obtained by expanding the momentum space W propagator[3]:

$$\frac{-1}{M_W^2-p^2} \;=\; \frac{-1}{M_W^2}+\frac{-p^2}{M_W^4}+\ldots. \tag{3.22}$$

[1] sum on repeated indices
[2] lighter than M_W
[3] We use the Feynman rules of [36].

While it is trivial from (3.22) that (3.20) works for tree level diagrams with $C_j^{(0)} = g_W^2/8$, it is not obvious that (3.20) can be extended to diagrams with gluon loops, in which p in (3.22) is a loop momentum. From Wilson's work we know that (3.18) holds to any order in perturbation theory. Clearly for small loop momenta (3.22) is a good expansion, and the contributions from small loop momenta on each side of (3.20) will match with the tree level coefficient $C_j^{(0)}$. The contributions from large loop momenta, however, will modify C_j by adding terms $\alpha/(4\pi) \cdot C_j^{(1)} \ldots$ to $C_j^{(0)}$. Yet these UV momenta are not sensitive to the small internal masses and small external momenta.

When the heavy top quark is involved in the amplitude of interest, it must also be integrated out like the W–boson.

In the discussion above we have made plausible the following properties of the operator product expansion:

i) The C_j's do not depend on the infrared structure of the Standard Model amplitude.

ii) The Wilson coefficients C_j depend only on the heavy mass scales M_W and m_{top} and on μ, while the matrix elements contain the light masses. Large logarithms such as $\ln(m_c/M_W)$ are split into $\ln(\mu/M_W) + \ln(m_c/\mu)$. The former logarithm resides in the Wilson coefficient and the latter is contained in the matrix elements.

iii) RG methods are applicable to C_j allowing for the summation of the logarithm in all orders of perturbation theory. With the boundary conditions of the RG evolution being $\mu = M_W$ and $\mu = m_c$ one sums the large logarithm $\ln(m_c/M_W)$ of the Standard Model amplitude.

iv) The C_j's are independent of the external states.

Hence we have overcome the problems i) to iv) mentioned in sect. 3.3. The short distance coefficients C_j are physically sensible quantities, which can be obtained in perturbation theory. Clearly in the end one has to cope with hadronic matrix elements, which must be evaluated by nonperturbative methods such as lattice gauge theory, $1/N$ expansion or sum rule techniques. Yet one can sometimes find them from experimental data and insert the obtained values into predictions for other observables of interest. The dimensions of the $\widehat{Q}_j$'s in (3.18) now manifest themself in powers of the hadronic scale Λ_{QCD}.

The price paid for the factorization of short and long distance effects in (3.18) is the inclusion of only finite powers of m_{light}^2/M_W^2. These powers are modified by logarithms which come with powers of α and can be summed to all orders in α by use of the RG. Since the light quark masses are much smaller than M_W in most cases only the operator with the smallest dimension in (3.18) is sufficient. When μ passes the flavour thresholds m_b or m_c, however, we repeat the factorization process. Below m_c the OPE is an expansion in Λ_{QCD}/m_c and higher dimension operators may become important.

3.4.1. Renormalization of Composite Operators

Since composite operators involve products of interacting fields at the same space–time point, they require a renormalization in addition to that of the fields they are composed of. This operator renormalization has been worked out by Zimmermann [38], who called renormalized operators normal products.
The unrenormalized field product composed of unrenormalized fields will be denoted by the superscript *bare*. We will frequently be concerned with four–fermion operators:

$$\widehat{Q}_k^{\rm bare} \;=\; \overline{\psi}^{\rm bare} q_k \psi^{\rm bare} \cdot \overline{\psi}^{\rm bare} \tilde{q}_k \psi^{\rm bare}, \qquad \text{no sum on } k, \tag{3.23}$$

where q_k and $\tilde{q}_k$ are strings of Dirac matrices. We will only need four–fermion operators which are Lorentz singlets or pseudosinglets, i.e. all Lorentz indices in $Q_k = q_k \otimes \tilde{q}_k$ are contracted. Colour and flavour indices are suppressed in (3.23), we will make them explicit where necessary. Next in the matrix elements the fields creating the external states are conventionally not displayed. After expressing the bare fields in (3.23) in terms of renormalized fields as in (2.34), the matrix elements are still divergent. The necessary operator renormalization of $\widehat{Q}_k^{\rm bare}$ can require counterterms proportional to other operators $\widehat{Q}_j^{\rm bare}$. This phenomenon is called operator mixing. We say that $\widehat{Q}_j$ *mixes into* $\widehat{Q}_k$, if $\widehat{Q}_j^{\rm bare}$ requires a counterterm proportional to $\widehat{Q}_k$. Hence the multiplicative renormalization involves matrices renormalizing vectors of operators $\vec{\widehat{Q}}$. The renormalized operator reads

$$\widehat{Q}_j(x) \;=\; \widehat{Q}_j^{\rm ren}(x) \;=\; Z_{jk}^{-1} \widehat{Q}_k^{\rm bare}(x). \tag{3.24}$$

As in (2.36) a quantity without superscript is understood to be renormalized. In cases where this may be confusing (such as in chapter 4) we will mark renormalized quantities with *ren*. In the phenomenological sections also the caret on the operators will be omitted. A set of operators which renormalize each other in (3.24) is said to *close under renormalization*.
In (3.24) the standard definition of $\widehat{Q}_j^{\rm ren}$ has been given. It would be more useful to include the field renormalization into the defintion of $\widehat{Q}_j^{\rm ren}$, so that $\widehat{Q}_j^{\rm ren}$ would be expressed in terms of renormalized fields instead of bare fields. Again, in ambiguous places completely renormalized (i.e. finite) Green's functions will get a superscript *ren*:

$$\langle \widehat{Q}_j \rangle \;=\; \langle \widehat{Q}_j^{\rm ren} \rangle^{\rm ren} \;=\; Z_\psi^2 \langle \widehat{Q}_j^{\rm ren} \rangle^{\rm bare} \;=\; Z_\psi^2 Z_{jk}^{-1} \langle \widehat{Q}_k^{\rm bare} \rangle^{\rm bare}. \tag{3.25}$$

We will also have to discuss the mixing of four–fermion operators with operators containing only two external quark lines, but additional gluon or ghost legs. They involve the product of the corresponding field renormalization constants in (3.25) instead of four quark field constants $Z_\psi^{1/2}$.

3.5. Effective Field Theories

The operator product expansion in terms of some inverse heavy mass described in the previous section has a complementary interpretation in terms of an effective field theory:

Since the Wilson coefficients C_j on the RHS of (3.20) are independent of the external states we may consider them as coupling constants multiplying four–fermion couplings in some effective Lagrangian:

$$\begin{aligned}\mathcal{L}^{\rm I} &= C_j(\mu)\widehat{Q}_j^{\rm ren}(x,\mu) \;=\; C_j(\mu)Z_{jk}^{-1}(\mu)\widehat{Q}_k^{\rm bare}(x)\\ &= C_j\, Z_{jk}^{-1}Z_\psi^2\,\overline{\psi}_1(x)q_k\psi_2(x)\overline{\psi}_3(x)\tilde{q}_k\psi_4(x)\end{aligned} \tag{3.26}$$

Clearly the S–matrix

$$\mathbf{T}\,\exp\left[\mathrm{i}\int \mathrm{d^4x}\left(\mathcal{L}_{\rm QCD}(\mathrm{x})+\mathcal{L}^{\rm I}(\mathrm{x})\right)\right] \tag{3.27}$$

derived from (3.26) yields to first order in the effective coupling constants C_j and to all orders in the QCD coupling constant g the RHS of (3.20). We may compare the effective Lagrangian (3.26) with the QCD Lagrangian (2.36): The last line in (3.26) corresponds to a renormalized interaction vertex expressed in terms of renormalized fields. We may view Z_{jk}^{-1} as renormalizing the effective coupling constant C_j instead of the composite operator. Yet the concept of an effective field theory must allow for going beyond the first order in the effective interaction in (3.27). This is possible as we know from the work of Witten [39]. The Green's functions of second order in the effective interaction involve

$$\langle -\frac{1}{2}\int d^Dx\int d^Dy\,\mathbf{T}\,\mathcal{L}^{\rm I}(x)\mathcal{L}^{\rm I}(y)\rangle.$$

These *bilocal structures* are in general divergent even in the absence of QCD interactions as can be seen from fig. 5.4. Hence one must add counterterms proportional to local operators to $\mathcal{L}_{\rm QCD}+\mathcal{L}^{\rm I}$ in order to obtain a finite result. Although the effective theory is not renormalizable by power counting, this is possible in all orders of both the effective and the QCD interaction, because after subtracting subdivergences the remaining divergences are polynomial in the momenta. The non–renormalizable interaction, however, forces us to introduce new counterterms in every order of perturbation theory. Hence we cannot include all–order effects in the effective action as we can do with the RG summation of the QCD interaction. Yet ordinary perturbation theory works well for the weak interaction, so that working to finite order in the effective coupling is perfectly sufficient.
In this thesis we will work up to the second order in the effective couplings. After adding the local operator counterterms to $\mathcal{L}^{\rm I}$ one ends up with:

$$\begin{aligned}\mathcal{L}^{\rm II} &= \mathcal{L}^{\rm I}+C_k(\mu)C_{k'}(\mu)\;Z_{kk',l}^{-1}(\mu)\;\widetilde{Q}_l^{\rm bare}+\widetilde{C}_r(\mu)\;\widetilde{Z}_{rl}^{-1}(\mu)\;\widetilde{Q}_l^{\rm bare}\\ &= C_j\;Z_{jk}^{-1}Z_\psi^2\;\overline{\psi}(x)q_k\psi(x)\,\overline{\psi}(x)\tilde{q}_k\psi(x)\\ &\quad +C_kC_{k'}\;Z_{kk',l}^{-1}\;Z_\psi^2\;\overline{\psi}(x)q_l^{\rm loc}\psi(x)\,\overline{\psi}(x)\tilde{q}_l^{\rm loc}\psi(x)\\ &\quad +\widetilde{C}_l\;\widetilde{Z}_{lr}^{-1}Z_\psi^2\;\overline{\psi}(x)q_r^{\rm loc}\psi(x)\,\overline{\psi}(x)\tilde{q}_r^{\rm loc}\psi(x)\end{aligned} \tag{3.28}$$

with $\widetilde{Q}_l \;=\; \overline{\psi}(x)q_l^{\rm loc}\psi(x)\overline{\psi}(x)\tilde{q}_l^{\rm loc}\psi(x)$, no sum on l, being the local operators needed as counterterms to the bilocal structures. In $\mathrm{K^0}-\overline{\mathrm{K^0}}$–mixing the $\widehat{Q}_k$'s are $|\Delta\mathrm{S}|=1$ operators

and the $\widetilde{Q}_l$'s are $|\Delta S|=2$ operators. In (3.26) and (3.28) we have for simplicity only displayed four–fermion operator counterterms. If none of the quark fields in $\widehat{Q}_k$, $\widetilde{Q}_l$ has the same flavour quantum number as one of the antiquark fields, only four–quark counterterms appear in $\mathcal{L}^{\mathrm{II}}$. Yet in the general case so called *penguin diagrams* lead to a mixing of four–quark operators into other operators as depicted in figs. 5.8 (p. 69) and 5.11 (p. 70). From (3.28) we realize the advantage of the effective lagrangian picture: The extra terms in (3.28) exactly look like renormalization factors for the effective couplings $\widetilde{C}_j$, but now both in terms of the effective interaction and of QCD:

$$\widetilde{C}_l^{\mathrm{bare}} \;=\; \widetilde{Z}_{rl}^{-1}\widetilde{C}_r + Z_{kk',l}^{-1}C_kC_{k'} + \ldots .$$

This form resembles the QCD coupling renormalization in (2.36). Further the effective lagrangian form allows for a simple inclusion of the correct wave function renormalization, which is simply taken into account by the corresponding counterterm Feynman rules derived from $\mathcal{L}_{\mathrm{QCD}} + \mathcal{L}^{\mathrm{II}}$. Finally the renormalization group equations for the C_k's and $\widetilde{C}_l$'s to be discussed in sect. 3.8 are very easily found from (3.26) and (3.28).

3.6. Appelquist–Carrazone Theorem

The decoupling theorem of Appelquist and Carrazone [40] deals with the effect of heavy virtual particles on low energy processes: If we can remove some heavy particle field from the lagrangian without spoiling the renormalizability[4], the loop effects of the heavy particle can be absorbed in the renormalization constants of the low energy lagrangian (without the heavy particle field) and into additive terms which are suppressed by powers (times logarithms) of the heavy particle mass.

The Appelquist–Carrazone theorem puts some hierarchical order into field theory: It has allowed to discover QED without knowing about its embedding into the Standard Model and it allows to study Standard Model predictions at LEP energies without knowing the physics at, say, $10^{16}\,\mathrm{GeV}$.

We will be concerned with the Appelquist–Carrazone theorem in a twofold way: First we will use that quark fields and clearly also the W field do decouple with respect to the strong interaction: QCD works with 5 flavours as well as with 6, hence we can remove the top quark from the lagrangian when passing with the renormalization scale μ below its mass. We repeat this with the W mass and then when crossing the b– and c–threshold. We could even incorporate these inverse power corrections by taking into account operators with higher dimension in (3.28) and we can use the RG to sum the logarithms accompanying these powers together with powers of the strong coupling constant.

The weak interaction, however, is a prominent example for non–decoupling: The heavy top–quark is clearly needed as an isospin partner of the bottom quark and after removing the W–boson we are faced with non–renormalizable effective four–fermion couplings. The

[4]We will use the term *renormalizability* for two different properties: It either refers to the locality of counterterms, in this sense we also call an effective theory renormalizable, or it means *renormalizability by power counting* such that all couplings have non–negative dimension.

non–decoupling allows to study the weak interaction in hadronic processes, although their energy scale $\Lambda_{\rm QCD}$ is much lower than the scale M_W, at which the weak transition takes place.

3.7. Initial Condition for the Wilson Coefficients

RG improved perturbation theory starts with the definition of the initial condition for the Wilson coefficients. This is done by matching the Standard Model amplitude to the effective theory as prescribed in (3.20). For definiteness we will consider some weak four–fermion amplitudes.

3.7.1. Single Operator Insertion

Let's look at some weak tree level process such as a $|\Delta S|=1$ transition, which is mediated by the exchange of one W boson. The corresponding Standard Model amplitude factorizes order by order in $1/M_W^2$ into a Wilson coefficient vector $\vec{C} = (C_1, \dots C_n)^T$ and matrix elements $\langle\vec{\widehat{Q}}\rangle$. For illustration we only display the dependence on the renormalization scale μ, the W mass M_W and a light quark mass m:

$$-iG_4^{(2)\,tc}(M_W,\mu,m) \;=\; C_j(M_W,\mu)\langle\widehat{Q}_j\rangle(\mu,m). \tag{3.29}$$

A $|\Delta S|=1$ four–quark operator is depicted in fig. 5.7 on p. 69.
To obtain (3.29) one has to calculate the Standard Model amplitude and the matrix element in perturbation theory to the desired order in the QCD coupling g. By comparing both results one finds $C_j(M_W,\mu)$. For a meaningful perturbative result for C_j the factorization scale $\mu = \mu_0$ must be chosen to be of the order M_W to keep the logarithm $\alpha\ln(\mu/M_W)$ in C_j small. Thereby one obtains the initial value for $C_j(M_W,\mu_0)$ with respect to the RG evolution. With the RG evolution of C_j from $\mu = \mu_0$ down to $\mu = \mu_m \approx m$ described in the following section we want to sum $\ln(\mu_m/\mu_0) \approx \ln(m/M_W)$ present in the LHS of (3.29) to all orders. As indicated one is not forced to choose $\mu_m = m, \mu_0 = M_W$ exactly. The two large logarithms $\ln(\mu_m/\mu_0)$ and $\ln(m/M_W)$ differ by a small logarithm of the order of magnitude of the remaining non–summed radiative correction. Changing μ_0 and μ_m modifies the result by terms of the order of the uncalculated higher order corrections. These scale dependences are inherent to RG improved perturbation theory and may be viewed as an estimate of the accuracy of the truncated perturbation series. For the rest of this section we choose $\mu_0 = M_W$ and $\mu_m = m$ for clarity.
From the matching procedure one can count the powers of the summed logarithms: In LO the matching is done in the order $\alpha^0\ln^0(m/M_W)$, and the LO RG will sum

$$\alpha^n \ln^n \frac{m}{M_W}, \qquad n = 0, 1, 2, \dots .$$

In NLO we will sum the log's with one additional power of α. Hence the matching is done in the order $\alpha^1\ln^0(m/M_W)$, which requires the calculation of the one–loop diagrams of fig. 4.1 on p. 43.

3.7.2. Double Operator Insertion

Next we will look at a process which appears in the second order of the effective couplings. Clearly we have in mind the $|\Delta S|=2$ transition with light internal quarks. Its Standard Model amplitude is described in LO by fig. 5.1 (p. 61) and the effective theory matrix element is shown in fig. 5.4 (p. 66). We will often refer to fig. 5.4 as the prototype for a matrix element with two insertion of four–fermion operators, although we will later also discuss matrix elements containing one other operator such the one depicted in fig. 5.9 (p. 69) or 5.11 (p. 70).
Here the matching condition reads

$$-iG_4^{(2)\,tc} \;=\; C_k C_{k'} \left\langle \left[\frac{i}{2} \int \mathbf{T}\, \widehat{Q}_k \widehat{Q}_{k'} \right]^{\mathrm{ren}} \right\rangle^{\mathrm{ren}} + C_l \left\langle \widetilde{Q}_l \right\rangle . \tag{3.30}$$

Here the square brackets around the two operators shall denote the inclusion of the local operator counterterms in $\mathcal{L}^{\mathrm{II}}$ in (3.28).
Next let us comment on the powers of the logarithm. There are two different cases, both of which appear in $\mathrm{K}^0-\overline{\mathrm{K}^0}$–mixing:

Case I:
This generic case is the following situation:
The diagram in fig. 5.4 is divergent and requires local operator counterterms depicted in fig. 5.3 (p. 64). In the example of $\mathrm{K}^0-\overline{\mathrm{K}^0}$–mixing these local operators $\widetilde{Q}_l$ are $|\Delta S|=2$ operators. With the divergence comes $\ln(\mu/m)$ in the finite part even in the absence of QCD corrections. Its twin in the Standard Model amplitude is $\ln(m/M_W)$. In the LO we can simply do the matching from these logarithms and the leading log summation comprises

$$\alpha^n \ln^{n+1} \frac{m}{M_W}, \qquad n = 0, 1, 2, \ldots .$$

Consequently in NLO we can still do the matching from the one–loop graphs figs. 5.1 and 5.4, but now from the $\alpha^0 \ln^0(m/M_W)$ parts. Here we must also take into account the coefficients of the $\widetilde{Q}_l$'s.
Case I will appear in the calculation of η_3 in (1.1) in chapter 6. Cf. also the NLO calculation of rare K decays in [41].

Case II:
The insertion of two local operators into the diagram of fig. 5.4 is convergent. This situation appears when there are several contributions of the form in fig. 5.4 combining such that the divergences of the individual contributions cancel. With the cancellation of the divergences also the $\ln \mu$'s will disappear, so that there is no large log in the corresponding one–loop amplitude of fig. 5.1. Hence the leading log summation will comprise

$$\alpha^n \ln^n \frac{m}{M_W}, \qquad n = 0, 1, 2, \ldots$$

and the matching has to be done in the order $\alpha^0 \ln^0(m/M_W)$. Consequently we are forced to perform the NLO matching in the order $\alpha^1 \ln^0(m/M_W)$. This requires the calculation of the finite parts of the diagrams of fig. 5.2 (p. 64) and of those of fig. 5.5 (p. 66).
Case II appears in the calculation of η_1. The cancellation of the large logs in the corresponding Standard Model amplitude is caused by the GIM mechanism: The divergence of the diagram in fig. 5.4 is multiplied with the product of two columns of the CKM matrix, which is zero due to the unitarity of the latter. The finite part is of the order m^2/M_W^2 and one speaks of a *hard* GIM suppression. One could even term this suppression *superhard*, because there is even no $\ln(m^2/M_W^2)$ multiplying m^2/M_W^2 and the RG enhancement is thereby suppressed by one power of α compared to case I.

3.8. Renormalization Group for Operators and Coefficients

3.8.1. Single Operator Insertion

In this section we will set up the RG formalism for matrix elements with single insertions of composite operators, which can be derived from $\mathcal{L}^{\mathrm{I}}$ in (3.26).

Anomalous Dimension Matrix

The anomalous dimension matrix γ is defined by

$$\begin{aligned} \gamma_{ij}(g(\mu)) &= -\left[\mu\frac{d}{d\mu}Z_{ik}^{-1}\right]Z_{kj} = Z_{ik}^{-1}\mu\frac{d}{d\mu}Z_{kj} \\ &= Z_{ik}^{-1}\beta(g)\frac{d}{dg}Z_{kj}. \end{aligned} \tag{3.31}$$

From (3.24) one simply obtains the RG equation for the renormalized operator:

$$\left[\mu\frac{d}{d\mu}\delta_{jk}+\gamma_{jk}\right]\widehat{Q}_k(\mu) = 0. \tag{3.32}$$

We expand Z_{jk} as usual in g and ε as shown in (2.35). The anomalous dimension matrix

$$\gamma_{jk} = \gamma_{jk}^{(0)}\frac{g^2}{16\pi^2}+\gamma_{jk}^{(1)}\frac{g^4}{(16\pi^2)^2}+O(g^6) \tag{3.33}$$

is related to Z_{jk} as follows:

$$\begin{aligned} \gamma^{(0)} &= -2Z_1^{(1)}-2\varepsilon Z_0^{(1)} \\ \gamma^{(1)} &= -4Z_1^{(2)}+2\left\{Z_0^{(1)},Z_1^{(1)}\right\}-2\beta_0 Z_0^{(1)}+O(\varepsilon). \end{aligned} \tag{3.34}$$

In (3.33) and in (3.34) we have only kept the terms relevant for NLO calculations. We have allowed for a finite renormalization $Z_0^{(1)}$ as well. The structure of (3.34) reveals that one

obtains the correct $\gamma^{(1)}$ by inserting the finite one–loop counterterms with a factor of 1/2 instead of 1 into the one–loop counterterm diagrams. (3.34) can be easily derived from the insertion of (3.33) into (3.31), see e.g. [43]. Alternatively one can recall that γ_{ij} is related to the coefficient of $\ln \mu$ in $\langle \widehat{Q} \rangle$. In dimensional regularization the $\ln \mu$'s enter the finite parts of Green's functions via

$$(\mu^{2\varepsilon} - 1)\frac{1}{\varepsilon} \quad = \quad 2 \ln \mu,$$

where the -1 stems from counterterm diagrams. Hence e.g. in lowest order the coefficient of $\ln \mu$ is simply twice the coefficient of the divergence.
In the same way one finds for β_0 in (3.9):

$$\beta_0 \quad = \quad -2 Z_{g,1}^{(1)}. \tag{3.35}$$

As mentioned before, the different coefficients of Z are not independent. In NLO one has the relation

$$4 Z_2^{(2)} + 2\beta_0 Z_1^{(1)} - 2 Z_1^{(1)} Z_1^{(1)} \quad = \quad 0. \tag{3.36}$$

(3.36) is a consequence of the renormalizability, i.e. of the locality of the counterterms [42]. Since in mass independent schemes the divergence of each diagram plus its subloop counterterm diagrams is polynomial in the momenta and masses, any dependence on $\ln \mu$ also cancels from the divergent parts. The two–loop diagrams involve $\mu^{4\varepsilon} Z_2^{(2)}/\varepsilon^2$, while the one–loop counterterm diagrams involve $\mu^{2\varepsilon} Z_1^{(1)}/\varepsilon$ times either $Z_1^{(1)}/\varepsilon$ or $Z_{g,1}^{(1)}/\varepsilon = -\beta_0/(2\varepsilon)$. The vanishing of $\ln \mu$ enforces (3.36). We will use this argument in a different context in a formal proof on evanescent operators, which vanish in $D = 4$ dimensions, in chapter 4. Relation (3.36) is tightly related to the finiteness of anomalous dimensions, which has been used for an elegant proof of (3.36) in [43].

Solution of the RG Equations

Let us first derive the RG equation for the Wilson coefficients: From $\mu \frac{d}{d\mu} \mathcal{L}^{\mathrm{I}} = 0$ in (3.26) one immediately obtains:

$$\left[\mu \frac{d}{d\mu} \delta_{jk} - \gamma_{jk} \right] C_j \quad = \quad 0, \tag{3.37}$$

thus the RG equation for the Wilson coefficient vector $\vec{C}$ involves the transpose of γ. The solution of (3.37) is given by

$$C_j(\mu_1) \quad = \quad \left[U(\mu_1, \mu_0) \right]_{jk} C_k(\mu_0) \tag{3.38}$$

where $U(\mu_1, \mu_0)$ is the *evolution matrix*:

$$U(\mu_1, \mu_0) \quad = \quad \mathbf{T_g} \exp \left[\int_{g(\mu_0)}^{g(\mu_1)} dg' \frac{\gamma^T(g')}{\beta(g')} \right]. \tag{3.39}$$

Here $\mathbf{T}_g$ means that the matrices $\gamma(g'), \gamma(g'') \ldots$ in the expanded exponential are ordered such that the couplings $\left\{ \begin{array}{ll} \text{increase from right to left} & \text{for } g(\mu_0) < g(\mu_1) \\ \text{decrease from right to left} & \text{for } g(\mu_0) > g(\mu_1) \end{array} \right\}$.
The LO solution of (3.39) is

$$U^{(0)}(\mu_1, \mu_0) \;=\; \exp\left[d \ln \frac{\alpha(\mu_0)}{\alpha(\mu_1)} \right] \tag{3.40}$$

with

$$d \;=\; \frac{\gamma^{(0)}}{2\beta_0}. \tag{3.41}$$

In the diagonal basis of d the LO evolution matrix $U^{(0)}$ is simply a diagonal matrix with diagonal elements $[\alpha(\mu_0)/\alpha(\mu_1)]^{d_j}$, where the d_j's are the eigenvalues of d.
The NLO solution of (3.39) reads:

$$U(\mu_1, \mu_0) \;=\; \left(1 + \frac{\alpha(\mu_1)}{4\pi} J \right) U^{(0)}(\mu_1, \mu_0) \left(1 - \frac{\alpha(\mu_0)}{4\pi} J \right). \tag{3.42}$$

Here clearly the NLO running α has to be used in $U^{(0)}$. J in (3.42) is a solution of the matrix equation [44]:

$$J + \left[\frac{\gamma^{(0)\,T}}{2\beta_0}, J \right] \;=\; -\frac{\gamma^{(1)\,T}}{2\beta_0} + \frac{\beta_1}{2\beta_0^2} \gamma^{(0)\,T}. \tag{3.43}$$

In practical calculations it is not useful to solve (3.43) by transforming into the diagonal basis. On better solves (3.43) directly: Since it is a system of linear equations for the elements of J, the entries of J are simply rational functions of N and f.
For the LO evolution matrix it is useful to transform to the diagonal form, as this saves computation time, because $U^{(0)}$ has to be calculated newly for every new pair (μ_0, μ_1). In our phenomenological analysis of chapter 7, however, we have simply exponentiated the matrix in (3.40), because the computer algebra system MATHEMATICA provides a fairly fast numerical matrix exponentiation algorithm.

3.8.2. Double Operator Insertion

The local operator counterterms $Z^{-1}_{kk',l}(\mu)\ \widetilde{Q}_l$ in $\mathcal{L}^{\mathrm{II}}$ do not influence the RG evolution of the coefficients C_k, but they modify the running of $\widetilde{C}_l$. We will investigate this in the following. Often one does not insert the full set of operators in $\mathcal{L}^{\mathrm{I}}$ into both places in fig. 5.4, but limits oneself to a subset which closes under renormalization. Hence k and k' in $Z^{-1}_{kk',l}$ may run over different ranges. This will be so in the case of η_3.

Anomalous Dimension Tensor and RG Equations

The evolution of the Wilson coefficients in $\mathcal{L}^{\rm I}$ is fixed with (3.38). Now $\mathcal{L}^{\rm II}$ contains new local operator counterterms with coefficients $\widetilde{C}_l$. It has become standard to define the operators $\widetilde{Q}_l$ with two inverse powers of g, e.g. $\widetilde{Q} = m^2/(g^2\overline{\mu}^{2\varepsilon}) \cdot \gamma_\mu (1-\gamma_5) \otimes \gamma^\mu (1-\gamma_5)$, to avoid operator mixing in the order g^0. Then $Z^{-1}_{kn,l} = O(g^2)$ and the mixing matrices start in the order g^2.
From $\mu\frac{d}{d\mu}\mathcal{L}^{\rm I} = 0$ and $\mu\frac{d}{d\mu}\mathcal{L}^{\rm II} = 0$ one finds with (3.28):

$$0 \;=\; \mu\frac{d}{d\mu}\left[C_k(\mu)C_{k'}(\mu)\; Z^{-1}_{kk',l}(\mu) + \widetilde{C}_r(\mu)\; \widetilde{Z}^{-1}_{rl}(\mu)\right].$$

This can be compactly rewritten as

$$\mu\frac{d}{d\mu}\widetilde{C}_l(\mu) \;=\; \widetilde{C}_{l'}(\mu)\widetilde{\gamma}_{l'l} + C_k(\mu)C_{k'}(\mu)\gamma_{kk',l} \tag{3.44}$$

with the *anomalous dimension tensor*

$$\begin{aligned}\gamma_{kn,l} &= \frac{g^2}{16\pi^2}\gamma^{(0)}_{kn,l} + \left(\frac{g^2}{16\pi^2}\right)^2 \gamma^{(1)}_{kn,l} + \ldots \\ &= -\left[\gamma_{kk'}\delta_{nn'} + \delta_{kk'}\gamma_{nn'}\right] Z^{-1}_{k'n',l'}\widetilde{Z}_{l'l} - \left[\mu\frac{d}{d\mu}Z^{-1}_{kn,l'}\right]\widetilde{Z}_{l'l}.\end{aligned}$$

The analogue of (3.34) is found as

$$\begin{aligned}\gamma^{(0)}_{kn,l} &= 2\left[Z_1^{-1,(1)}\right]_{kn,l} + 2\varepsilon\left[Z_0^{-1,(1)}\right]_{kn,l} \\ \gamma^{(1)}_{kn,l} &= 4\left[Z_1^{-1,(2)}\right]_{kn,l} + 2\beta_0\left[Z_0^{-1,(1)}\right]_{kn,l} \\ &\quad -2\left[Z_0^{-1,(1)}\right]_{kn,l'}\left[\widetilde{Z}_1^{-1,(1)}\right]_{l'l} - 2\left[Z_1^{-1,(1)}\right]_{kn,l'}\left[\widetilde{Z}_0^{-1,(1)}\right]_{l'l} \\ &\quad -2\left\{\left[Z_0^{-1,(1)}\right]_{kk'}\delta_{nn'} + \delta_{kk'}\left[Z_0^{-1,(1)}\right]_{nn'}\right\}\left[Z_1^{-1,(1)}\right]_{k'n',l} \\ &\quad -2\left\{\left[Z_1^{-1,(1)}\right]_{kk'}\delta_{nn'} + \delta_{kk'}\left[Z_1^{-1,(1)}\right]_{nn'}\right\}\left[Z_0^{-1,(1)}\right]_{k'n',l} + O(\varepsilon).\end{aligned} \tag{3.45}$$

Solution of the RG Equations

The solution of the inhomogeneous RG equation (3.37) for the running Wilson coefficient $\widetilde{C}(\mu)$ reads:

$$\begin{aligned}\widetilde{C}_l(g(\mu)) &= \widetilde{U}^{(0)}_{ll'}(g(\mu), g_0)\,\widetilde{C}_{l'}(g_0) \\ &\quad + \left[\delta_{ll'} + \frac{g^2(\mu)}{16\pi^2}\widetilde{J}_{ll'}\right] \cdot \int_{g_0}^{g(\mu)} dg'\; \widetilde{U}^{(0)}_{l'k}(g(\mu), g')\left[\delta_{kk'} - \frac{g'^2}{16\pi^2}\widetilde{J}_{kk'}\right] \\ &\qquad \cdot \left[\delta_{nn'} + \frac{g'^2}{16\pi^2}J_{nn'}\right] U^{(0)}_{n't}(g', g_0)\left[\delta_{tt'} - \frac{g'^2}{16\pi^2}J_{tt'}\right] C_{t'}(g_0)\end{aligned}$$

$$\cdot \left[\delta_{mm'} + \frac{g'^2}{16\pi^2} J_{mm'}\right] U^{(0)}_{m'v}(g', g_0) \left[\delta_{vv'} - \frac{g'^2}{16\pi^2} J_{vv'}\right] C_{v'}(g_0)$$
$$\cdot \left\{ -\frac{\gamma^{(0)}_{nm,k'}}{\beta_0} \frac{1}{g'} + \left[\frac{\beta_1}{\beta_0^2} \gamma^{(0)}_{nm,k'} - \frac{\gamma^{(1)}_{nm,k'}}{\beta_0}\right] \frac{g'}{16\pi^2} \right\}. \tag{3.46}$$

Here $\widetilde{U}^{(0)}$ and $\widetilde{J}$ are the RG quantities related to single insertions of $\widetilde{Q}$ as defined in (3.40) and (3.43). Further the Wilson coefficients and evolution matrices have been labeled with $g(\mu)$ rather than μ to comply with the integration variable g'. The coupling at the scale μ_0 at which the initial condition is defined is denoted by $g_0 = g(\mu_0)$.
The first term in (3.46) is solely related to matrix elements with single insertions of $\widetilde{Q}$. There are no factors involving $\widetilde{J}$ here, because the initial coefficients $\widetilde{C}_l(g_0)$ start at the order g^2.
(3.46) nicely reveals the structure of the RG in bilocal matrix elements: First the two Wilson coefficients $C_{l'}$ and $C_{\nu'}$ run from μ_0 down to the intermediate scale μ' with $g(\mu') = g'$. Then they are linked by the anomalous dimension tensor to a single coefficient $\widetilde{C}_{k'}$, which runs further down with the NLO evolution matrix $\widetilde{U}(\mu, \mu')$. The integral sums over all intermediate scales μ'.
For formal analyses as those in chapter 4 the form (3.46) is well suited. In a practical calculation, however, the solution of the integral in (3.46) requires to transform the $\widetilde{Q}_l$'s to the diagonal basis of $\widetilde{\gamma}$. The same must be done for the $\widehat{Q}_k$'s of at least one of the two operator bases corresponding to the double operator insertion.
Consider the case that the two operator bases feeding fig. 5.4 (p. 66) have K and K' elements, while L linearly independent operators $\widetilde{Q}_l$ are needed as counterterms to fig. 5.4. In the calculation of η_3 we will have $K = 2$, $K' = 6$ and $L = 1$. The simplest way to solve (3.44) is to label the product $C_k C_{k'}$ with a single index running from 1 to $K \cdot K'$. We obtain the form as in (3.37) and can proceed as in the case of single operator insertions. The evolution matrix has $K \cdot K' + L$ rows and columns. Yet this method hides the different sources of RG admixtures to $\widetilde{C}_l$.
Next one can transform to the diagonal basis for one set of operators $\widehat{Q}_k$: The RG evolution then decomposes into K separate sectors each involving $(K' + L) \times (K' + L)$ matrices. This is similar to the method used in the LO analysis of $\mathrm{K}^0 - \overline{\mathrm{K}^0}$–mixing of Gilman and Wise [45]. If this method is used beyond the leading order, however, *the mixing matrices of different orders must commute*, if the standard formalism of sect. 3.8.1 shall apply: Only if $\left[\gamma^{(0)}, \gamma^{(1)}\right] = 0$, the NLO matrix J does not induce a mixing of the different sectors of the LO evolution. In the calculation of η_3, where $K = 2$, this is indeed the case for the relevant LO and NLO mixing matrices given in the literature [43].
The discussion above stresses the advantage of commuting LO and NLO mixing matrices, especially for the case of multiple operator insertions. It is noticeable that one can indeed always achieve this situation by a finite renormalization, because $\gamma^{(1)}$ is scheme dependent. In the context of four–fermion operators scheme transformations involving a set of continuos real parameters naturally enter the scene due to the presence of evanescent operators. We will look at this in chapter 4.

Of course one can further decompose the RG evolution by transforming the remaining operator sets to the diagonal basis, too. Yet this does neither significantly improve the algorithm nor does it provide more insight into physics.
The K sectors each having a $(K'+L)\times(K'+L)$ evolution matrix contain some redundancy, because all K of them encode the running of the $K'+L$ other operators. This redundancy can be removed by replacing the $\widetilde{C}_l$'s by $\widetilde{C}_l^{(k)}$'s which are obtained by dividing the $\widetilde{C}_l$'s by the C_k's of the diagonalized basis. This results in a matrix evolution for a coefficient vector with $K' + K \cdot L$ components. We have used this method in the calculation of η_3 thereby reducing the problem to a single 8×8 evolution matrix instead of using four such matrices as in [45].
We finally remark that the evolution matrix has a block–triangular form, because the coefficients $\widetilde{C}_l$ of the local operators $\widetilde{Q}_l$ cannot mix into the products $C_k \cdot C_{k'}$. Since such block–triangular matrices appear in many contexts, their discussion deserves a separate section.

3.8.3. Block–triangular Mixing Matrix

We will frequently encounter block–triangular anomalous dimension matrices:

$$\gamma \;=\; \begin{pmatrix} \gamma_a & \gamma_b \\ 0 & \gamma_c \end{pmatrix} \tag{3.47}$$

with submatrices γ_a, γ_b and γ_c. This form leads to a block–triangular LO evolution matrix:

$$U^{(0)}(\mu_1,\mu_0) \;= \begin{pmatrix} U_a^{(0)}(\mu_1,\mu_0) & 0 \\ U_{\rm inh}^{(0)}(\mu_1,\mu_0) & U_c^{(0)}(\mu_1,\mu_0) \end{pmatrix} = \begin{pmatrix} \exp\left[d_a \ln\frac{\alpha(\mu_0)}{\alpha(\mu_1)}\right] & 0 \\ * & \exp\left[d_c \ln\frac{\alpha(\mu_0)}{\alpha(\mu_1)}\right] \end{pmatrix} \tag{3.48}$$

with d_a, d_c defined analogously to (3.41). Hence the diagonal blocks of the LO evolution matrix exponentiate separately. The RG evolution of the Wilson coefficients of the subspace $\mathrm{S_a}$ corresponding to γ_a is not affected by the coefficients of the other subspace $\mathrm{S_c}$. The Wilson coefficient vectors in $\mathrm{S_c}$, however, satisfy a RG equation to which an inhomogeneous term is added involving the solution of the RG equation of subspace $\mathrm{S_a}$.
This invariance of $\mathrm{S_a}$ persists in NLO: (3.47) leads to a block–triangular J matrix in (3.43) protecting $\mathrm{S_a}$ from admixtures.
We will be confronted with the case that γ_c is a 1×1 matrix. Then one can also solve $U_{\rm inh}^{(0)}$ in terms of $\gamma_c^{(0)}$, the submatrix $n \times n$ matrix $\gamma_a^{(0)}$ and the column vector $\gamma_b^{(0)}$:

$$U_{\rm inh}^{(0)} \;=\; d_b \cdot \exp\left[U_a^{(0)}(\mu_1,\mu_0) - \mathsf{1}_n U_c^{(0)}(\mu_1,\mu_0)\right] \cdot \left[(d_a - \mathsf{1}_n d_c)\ln\frac{\alpha(\mu_0)}{\alpha(\mu_1)}\right]^{-1}, \tag{3.49}$$

which is a row vector due to $d_b = \gamma_b^{(0)\,T}/(2\beta_0)$. $\mathsf{1}_n$ is the $n \times n$ unit matrix.

A similar relation for

$$J \;=\; \begin{pmatrix} J_a & 0 \\ J_b & J_c \end{pmatrix}$$

can be derived from (3.43) for the case that J_c is just a number:

$$J_b \;=\; \left[-\frac{\gamma_b^{(1)}}{2\beta_0} + \frac{\beta_1}{\beta_0} d_b - d_b J_a + J_c d_b\right] \left[(1+d_c)\,\mathbf{1}_n - d_a\right]^{-1} \tag{3.50}$$

The relations (3.49) and (3.50) are useful to check the RG evolution in the calculation of η_3 in chapter 6, because the subspace $\mathrm{S_a}$ is related to the Wilson coefficients for $|\Delta \mathrm{S}|=1$ transitions which is known to NLO from [44].

3.9. Scheme Dependence of Coefficients and Anomalous Dimension

General aspects of renormalization scheme dependences have already been discussed in sect. 3.1. In the framework of effective field theories scheme dependences appear in a new context: Even when keeping the scheme in the full Standard Model lagrangian fixed there is still the freedom to invoke a finite renormalization on the operator renormalization matrix (3.24) in analogy to (3.1). From now on we will only discuss such scheme dependences related to the effective theory.
Collecting some results of [44] let us write the matrix element in the form:

$$\langle \vec{\tilde{Q}} \rangle \;=\; \langle \vec{\tilde{Q}} \rangle^{(0)} + \frac{g^2}{16\pi^2} \langle \vec{\tilde{Q}} \rangle^{(1)} + O(g^4) \tag{3.51}$$

$$\;=\; \left[1 + \frac{g^2}{16\pi^2} r + O(g^4)\right] \langle \vec{\tilde{Q}} \rangle^{(0)} \tag{3.52}$$

If the matrix r obtained in two schemes a and b differs by $\Delta r = r_b - r_a$, one finds the corresponding finite renormalization as

$$Z_a \;=\; Z_b \left[1 + \frac{g^2}{16\pi^2} \Delta r + O(g^4)\right] + O(\varepsilon) \tag{3.53}$$

This leads to the scheme independence of $\gamma^{(0)}$, while $\gamma^{(1)}$ transforms as

$$\gamma_b^{(1)} \;=\; \gamma_a^{(1)} + \left[\Delta r, \gamma^{(0)}\right] + 2\beta_0 \Delta r. \tag{3.54}$$

This yields for J defined in (3.43):

$$J_b \;=\; J_a - \Delta r^T, \tag{3.55}$$

so that $J + r^T$ is scheme independent.

From (3.51) also the scheme transformation of the Wilson coefficient is clear:

$$\vec{C}_b^T = \vec{C}_a^T \left[1 - \frac{g^2}{16\pi^2} \Delta r + O(g^4) \right]. \tag{3.56}$$

With (3.38),(3.42),(3.56) and (3.55) one finds the scheme dependence related to the upper end μ_0 of the RG evolution canceled in the RG improved Wilson coefficient (3.38). The scheme dependence of the lower end μ has to cancel with a corresponding dependence in the hadronic matrix element.
Now one is often confronted with the situation that one calculates the matrix element (3.51) with different *renormalization prescriptions*. This is related to the fact that in many cases mathematical structures such as the Dirac algebra defined in 4 dimensions cannot unambiguosly be extended to D dimensions. This phenomenon is related to the evanescent redefinitions mentioned in sect. 3.1: A priori one can modify any D–dimensional quantity by terms of order ε without changing its limit for $D \to 4$. One then has to check which of the D–dimensional definitions leads to a consistent renormalizable theory complying with the observed symmetries of the described physics. Hence one has to prove that two different renormalization prescriptions leading to different r's in (3.51) really correspond to renormalization schemes. A necessary condition is that the change in the renormalization prescription is equivalent to a finite renormalization as in (3.53). This has been done for the important question of how to treat γ_5 in D dimensions in e.g. [43], [44] and [46] and will be done in chapter 4 for the question of how to define evanescent operators.

3.10. Unphysical Operators

Effective lagrangians also contain unphysical operators. We have already alluded to the presence of evanescent operators, which will be analyzed in detail in chapter 4.

3.10.1. Equation of Motion and BRS Exact Operators

Another set of unphysical operators is related to the Euler–Lagrange equation of motion (EOM) derived from the lagrangian. In classical physics one can simply drop terms which vanish by the field equation of motion. In a quantized field theory the issue is more difficult, because the path integral involves the integration over all field configurations, not just those which obey the EOM. The second subtlety stems from the fact that in Green's functions of operators containing derivatives the latter must always be understood to act on the time ordering $\mathbf{T}$ as well. This is necessary for the Green's function to be a correctly defined operator–valued distribution. (Otherwise it could not be Fourier–transformed to momentum space giving the familiar $-ik^\mu$ for each ∂^μ.) The third difficulty concerns the renomalization process, as two operators whose difference vanishes by the EOM may have bare Green's functions with a different forest structure.
The correct implementation of the EOM in quantum field theory also depends on the regularization, in BPHZ renormalization the use of the EOM requires oversubtractions, while this is not so for dimensional regularization.

First analyses of the subject used the EOM derived from the lagrangian (2.15). Yet for perturbative calculations the lagrangian (2.36) containing a gauge fixing term and Faddeev–Popov (FP) ghosts should be used. In the following we will collect the results obtained with this modern approach [51–53,58]. We recommend [54] for a nice explanation of the subject. Hence the EOM we use will always include the terms from $\mathcal{L}_{\rm gf}$ and $\mathcal{L}_{\rm FP}$
The necessary theorems we will be exemplified with operators of the forthcoming calculation of $\mathrm{K}^0-\overline{\mathrm{K}^0}$–mixing. We will be confronted with the following $|\Delta \mathrm{S}|=1$ operator:

$$\widehat{Q}_{\rm EOM} \;=\; \overline{s}\gamma_\mu L T^a d\cdot\left[-\frac{\delta\mathcal{L}_{\rm QCD}}{\delta A^a_\mu}+\partial_\nu\frac{\delta\mathcal{L}_{\rm QCD}}{\delta\left(\partial_\nu A^a_\mu\right)}\right] \tag{3.57}$$

with $L=1-\gamma_5$. This operator with the EOM of the gluon field attached to the $|\Delta \mathrm{S}|=1$ current contains the couplings depicted in fig. 5.9 (p. 69), and in the right pictures of fig. 5.10 (p. 70) and fig. 5.11 (p. 70). Four–fermion Green's functions with one insertion of $\widehat{Q}_{\rm EOM}$ vanish [52]. This statement holds for both bare and renormalized Green's functions. If external gluons are involved, the matrix element of $\widehat{Q}_{\rm EOM}$ equals a sum of matrix elements of $\overline{s}\gamma_\mu L T^a d$ in each of which one of the external gluon fields is missing. These *contact terms* vanish after the LSZ reduction (2.25), because they miss a gluon pole. Hence $\widehat{Q}_{\rm EOM}$ is termed *on–shell equivalent* to the zero operator. The same, of course, is true for any operator vanishing by the EOM for the fermion fields.
Another class of unphysical operators is related to $\mathcal{L}_{\rm FP}$ and the BRS invariance discussed in sect. 2.4.2. We will involve the following operator:

$$\widehat{Q}_{\rm BRS} \;=\; \frac{1}{g}\frac{1}{\xi}\,\overline{s}\gamma_\mu L T^a d\cdot\partial^\mu\partial_\nu A^\nu_a+\overline{s}\gamma_\mu L T^a d\cdot\left(\partial^\mu\overline{\eta}_b\right)\eta_c f_{abc}. \tag{3.58}$$

$\widehat{Q}_{\rm BRS}$ is the BRS variation of some other operator:

$$\widehat{Q}_{\rm BRS} \;=\; \delta_{\rm BRS}\widehat{Q}' \;=\; \delta_{\rm BRS}\left(\frac{1}{g}\,\overline{s}\gamma_\mu L T^a d\cdot\partial^\mu\overline{\eta}_a\right), \tag{3.59}$$

i.e. it is *BRS–exact*. From (2.32) one obtains:

$$\langle 0|\widehat{Q}^{\rm bare}_{\rm BRS}\overline{s}(x_1)d(x_2)\overline{\psi}(x_3)\psi(x_4)|0\rangle \;=\; -\langle 0|\widehat{Q}'^{,\rm bare}\delta_{\rm BRS}\left(\overline{s}(x_1)d(x_2)\overline{\psi}(x_3)\psi(x_4)\right)|0\rangle, \tag{3.60}$$

which also does not survive LSZ reduction thereby being zero on–shell.
From the discussion it is clear that $\widehat{Q}_{\rm EOM}$ and $\widehat{Q}_{\rm BRS}$ do not contribute to the matching of Green's functions with single operator insertions, because the matching can (though need not) be done on–shell.

3.10.2. Mixing

In order for the coefficients of $\widehat{Q}_{\rm EOM}$ and $\widehat{Q}_{\rm BRS}$ to be irrelevant one has to verify the block–triangular form of the mixing matrix to ensure that $\widehat{Q}_{\rm EOM}$ and $\widehat{Q}_{\rm BRS}$ do not mix into physical operators.

To discuss the mixing it is useful to introduce three classes of operators:
$\underline{\mathcal{P}}$: The set of gauge invariant operators which do not vanish by the EOM. Hence P contains physical and evanescent operators.
$\underline{\mathcal{E}}$: The set of operators vanishing by the EOM such as $\widehat{Q}_{\rm EOM}$.
$\underline{\mathcal{B}}$: The set of BRS–exact operators. The operator $\widehat{Q}_{\rm BRS}$ belongs to this class.
Now the renormalization matrix has the following form [52, 58]:

$$Z^{-1} \;=\; \begin{pmatrix} * & * & * \\ 0 & * & * \\ 0 & 0 & * \end{pmatrix} \qquad \text{corresponding to} \qquad \begin{pmatrix} \mathcal{P} \\ \mathcal{B} \\ \mathcal{E} \end{pmatrix}, \tag{3.61}$$

i.e. the renormalized version of (3.60) involves operators from $\mathcal{B} \oplus \mathcal{E}$ as counterterms.
The block–triangular form of (3.61) allows to ignore the operators from $\mathcal{E}$ and $\mathcal{B}$, because they neither contribute to the matching nor do their coefficients mix into the coefficients of the operators from $\mathcal{P}$. The lagrangian with the renormalized operators of $\mathcal{B} \oplus \mathcal{E}$ removed is sometimes called *reduced* lagrangian. In a calculation beyond one–loop, however, the operators of $\mathcal{B} \oplus \mathcal{E}$ appear in subloop counterterm diagrams. On can even avoid operators from $\mathcal{B}$ altogether by using a *background field gauge*. In our case of $\mathrm{K}^0 - \overline{\mathrm{K}^0}$–mixing the use of a background field gauge does not simplify the calculation.
Of course there are other non–gauge invariant operators which belong to none of the three classes. But since the initial values of their coefficients are zero and none of the operators from $\mathcal{P} \oplus \mathcal{B} \oplus \mathcal{E}$ mixes into them, they clearly do not affect any physical coefficient.

3.10.3. Double Insertions

For double insertion the issue is more complex, because now the operators in $\mathcal{B} \oplus \mathcal{E}$ give a non–zero contribution. For a four–fermion matrix element containing one insertion of $\widehat{Q}_{\rm EOM}$ one finds [52]:

$$\begin{aligned} &\langle \iint d^D x d^D y \, \mathbf{T}\, \widehat{Q}_{\rm EOM}(x) \widehat{Q}(y) \rangle \;= \\ &\quad i \sum_{\Lambda=1, \partial_\nu, \partial_\nu \partial_\rho} (-1)^{P_\Lambda} \langle \iint d^D x d^D y \, \mathbf{T}\, \Lambda \, [\overline{s} \gamma_\mu L T^a d(x)] \, \frac{\delta}{\delta \left(\Lambda \left[A^a_\mu(x) \right] \right)} \widehat{Q}(y) \rangle . \end{aligned} \tag{3.62}$$

Here the sum extends over all gluon field derivatives present in $\widehat{Q}_{\rm EOM}$. P_Λ means the number of derivatives in Λ. The main point in (3.62) is that the variation of $\widehat{Q}(y)$ with respect to $A^a_\mu(x)$ is proportional to $\delta^{(D)}(x-y)$. Hence the matrix element in (3.62) is identical to the matrix element of a single local operator $\widetilde{Q}_k(y)$. Since this holds for both bare and renormalized operators, we can reduce the effective lagrangian $\mathcal{L}^{\rm II}$ by substituting $\widetilde{Q}_k$ for $\widehat{Q}_{\rm EOM}$. If we kept both of them, the anomalous dimension tensor defined in sect. 3.8.2 would have a degenerate eigenvalue. The product of the two Wilson coefficients corresponding to the operators of the RHS of (3.62) would evolve parallely to the coefficient $\widetilde{C}_l$ of $\widetilde{Q}_l$ under the RG flow, and we could do the reduction of the effective lagrangian at any scale. The

method to perform the reduction, i.e. to construct the local operator $\widetilde{Q}_k$ is decribed e.g. in [54]. In a practical calculation, however, it is sufficient to know that we can drop $\widehat{Q}_{\rm EOM}$ from the operator basis, because we have to do the matching and mixing calculation anyway with all operators of the desired dimension in $\mathcal{L}^{\rm II}$, including the $\widetilde{Q}_l$'s.
Next for the operators from $\mathcal{B}$ one finds with (2.32):

$$\begin{aligned}\langle Q^{\rm bare}_{\rm BRS}\widehat{Q}^{\rm bare}\rangle &= \langle\Big(\delta_{\rm BRS}\widehat{Q}'^{\,\rm bare}\Big)\,\widehat{Q}^{\rm bare}\rangle \;=\; -\langle\widehat{Q}'^{\,\rm bare}\delta_{\rm BRS}\widehat{Q}^{\rm bare}\rangle \\ &\quad +\text{on–shell vanishing terms.}\end{aligned} \tag{3.63}$$

Here the RHS immediately vanishes, if $\widehat{Q}\in\mathcal{P}\oplus\mathcal{E}$, because gauge–invariant operators are BRS–invariant. For $\widehat{Q}\in\mathcal{B}$ we involve $\delta^2_{\rm BRS}$ on the RHS, which is either zero or yields an operator vanishing by the EOM of the ghost field. Recalling further that the renormalized version of (3.63) involves only operators from $\mathcal{B}\oplus\mathcal{E}$ one finally realizes that one can also trade the renormalized operators from $\mathcal{B}$ for suitable $\widetilde{Q}_l$'s.

4. Evanescent Operators

4.1. Motivation

When effective field theories containing four–fermion interactions are regularized dimensionally, evanescent operators, which vanish for $D = 4$, enter the scene. A prominent example is connected to the Fierz transformation: Since it is allowed only for $D = 4$, the difference of some D–dimensional operator and its Fierz transformed one is an evanescent operator. Since the lagrangian is a D-dimensional object, it also contains these evanescent operators. The whole issue would be trivial, if the evanescent sector was decoupled from the physical sector in the matching and mixing process.
Yet when calculating radiative corrections in a SU(N) gauge theory to some matrix element of a physical operator one has to face evanescent operators both in the matching procedure (3.29) and among the operator counterterms in (3.24). Let us exemplify this with the current–current operator $\widehat{Q}$ corresponding to the Dirac structure

$$Q \;=\; \gamma_\mu\,(1-\gamma_5)\otimes\gamma^\mu\,(1-\gamma_5)\,. \tag{4.1}$$

We will use this example frequently in this section together with an anticommuting γ_5 (NDR scheme). The consistency of this scheme in NLO QCD short distance calculations has been demonstrated in [43], [44] and [46] for cases without closed fermion loops. In the diagrams of the effective field theory the latter can be avoided by passing to a Fierz transformed operator basis. The use of an anticommuting γ_5 in a renomalizable field theory has been justified in [47]. The general arguments in this chapter, however, are not restricted to the NDR scheme.

Figure 4.1: One–loop current–current type radiative corrections to $\langle\widehat{Q}_k\rangle$.

Now consider the one–loop matrix elements of $\widehat{Q}$ depicted in fig. 4.1. The Dirac structure of the result is easily expressed in terms of a linear combination of Q and an evanescent Dirac structure:

$$E_1\,[Q] \;=\; \gamma_\mu\gamma_\nu\gamma_\vartheta(1-\gamma_5)\otimes\gamma^\vartheta\gamma^\nu\gamma^\mu(1-\gamma_5) - (4+a\varepsilon)\gamma_\mu(1-\gamma_5)\otimes\gamma^\mu(1-\gamma_5). \tag{4.2}$$

From the basis decomposition of the four–dimensional Dirac algebra we know that (4.2) vanishes in four dimensions. Nevertheless (4.2) appears with a factor of $1/\varepsilon$ in bare matrix elements and therefore in counterterms to physical operators. Depending on the flavour

structure of $\widehat{Q}$ one must take into account also the penguin–type diagrams of fig. 5.10 (p. 70). They do not contribute to the coefficients of evanescent operators in the one–loop order. Hence $\widehat{Q}$ mixes into some evanescent operator $\widehat{E}_1[Q]$. After inserting $\widehat{E}_1[Q]$ into the diagrams of fig. 4.1 another evanescent operator $\widehat{E}_2[Q]$ with five Dirac matrices in each string comes into play. Hence one realizes that one must deal with an infinite set of evanescent operators, because the Dirac algebra is infinite dimensional in dimensional regularization. With the real parameter a in (4.2) we have displayed the arbitrariness in the definition of $E_1[Q]$. One can a priori add ε times any physical operator (not only proportional to $\widehat{Q}$) to any evanescent operator. Indeed, in the literature one finds different definitions of the evanescents.
Let us display the evanescent operators in the effective lagrangian (3.26) in the following way:

$$\begin{aligned}\mathcal{L}^{\mathrm{I}} &= C_k Z^{-1}_{kl} \widehat{Q}^{\mathrm{bare}}_l + C_k Z^{-1}_{kE_{rl}} \widehat{E}_r \left[Q_l\right]^{\mathrm{bare}} \\ &\quad + C_{E_{jk}} Z^{-1}_{E_{jkl}} \widehat{Q}^{\mathrm{bare}}_l + C_{E_{jk}} Z^{-1}_{E_{jkE_{rl}}} \widehat{E}_r \left[Q_l\right]^{\mathrm{bare}} . \end{aligned} \tag{4.3}$$

Here and in the following we will distinguish the renormalization constants related to some evanescent operator $E_j[Q_m]$ by denoting the corresponding index with E_{jm}.
Buras and Weisz were the first to recognize that evanescents cannot simply be neglected but influence physical quantities [43]. They focused on the evanescent operators' contribution to the matching (3.29) and found that the one–loop matrix elements of $E_1[Q]$ involve finite components proportional to physical operators. In [43] it has been proposed to cancel these components, which are local, by a finite renormalization of $E_1[Q]$. By this the evanescent operators do not contribute to the matching in (3.29) anymore and their undetermined coefficients $C_{E_{jk}}$ are irrelevant at the matching scale μ_0. From (3.34) the authors of [43] found the influence of this finite renormalization on the physical part of the NLO anomalous dimension matrix $\gamma^{(1)}$.
To insure that evanescent operators remain irrelevant at any scale one must insure that the evanescents do not mix into physical operators. As discussed in sect. 3.8.3 such a block–triangular anomalous dimension matrix protects the physical coefficients C_k in (4.3) from admixtures of the $C_{E_{jk}}$. This has been noticed first by Dugan and Grinstein in [48]. They, however, have used a definition of the evanescents different from that of [43], i.e. a different a in (4.2). We do not need to repeat the definitions used in [43] and [48] in this introductory section to understand the issue. The authors of [48] proved that the anomalous dimension matrix indeed has the desired block–triangular form using their special definition of the evanescents, if the finite renormalization of [43] is performed. Yet it is not clear at all that these features holds for any definition of the evanescents: An evanescent redefinition of e.g. $E_1[Q]$ in (4.2) by adding $\varepsilon \cdot \delta a \cdot Q$ to it modifies the components of the divergent parts of the bare two–loop matrix elements proportional to physical operators. Hence we are immediately confronted with the question:
Does the definition of the evanescents employed in [43] also yield a block–triangular anomalous dimension matrix?
We will answer this question affirmatively in sect. 4.3. There we will also generalize the

method of [43]. Especially one is not forced to use the definition of the evanescent operators proposed in [48], whose implementation is quite cumbersome.
Then the next point to discuss is:
Is the dependence on a in (4.2) spurious or does it influence the physical Wilson coefficients C_k and the physical portion of the anomalous dimension matrix γ?
We will find in sect. 4.4 that the latter is the case. Here we will also find that evanescent redefinitions corresponding to a change of a in (4.2) imply a renormalization scheme dependence in the physical sector, i.e. we will be able to find a quantitity Δr such that the Wilson coefficients and the mixing matrix transforms as in (3.56) and (3.54). This touches a non–trivial aspect: It is not clear from the beginning that the change of the definition of the evanescents does not spoil renormalizability of the theory, i.e. the locality of the divergences. Yet in NLO it is trivial that renormalizability holds for any definition of the E_{jk}'s, because a redefiniton as in (4.2) only reshuffles local terms in the divergences of the bare matrix elements. When going beyond NLO terms of order ε^2, etc., in (4.2) become important, and these terms might be constrained by the condition of maintaining renormalizability. We will not discuss this point. In fact we will extend the discussion only beyond NLO when addressing the all–order argument of [48] for the block–triangular mixing matrix.
A main subject of this thesis is the correct renormalization of bilocal structures with two coloured operators. Clearly for this we have to answer the question:
What is the correct method to handle evanescent operators in matrix elements with two operator insertions?
This point will be the subject of sections 4.5 and 4.6, where four–fermion processes and inclusive decays will be discussed.

4.2. Preliminaries and Notation

Let us consider a set of physical four–quark operators $\{\widehat{Q}_k = \overline{\psi} q_k \psi \cdot \overline{\psi} \widetilde{q}_k \psi,\ k = 1, 2, 3, \ldots\}$ as shown in (3.23). For simplicity we restrict the basis to dimension-six operators. As usual we are interested in the Green's functions of a SU(N) gauge theory with insertions of $\widehat{Q}_k$ renormalized in a mass-independent scheme. For simplicity of the notation we pick minimal subtraction (MS). The arguments are easily generalized to other schemes like $\overline{\text{MS}}$. The dirac structures $Q_k = q_k \otimes \widetilde{q}_k$ corresponding to $\widehat{Q}_k$ are considered to form a basis of the space of Lorentz singlets and pseudosinglets for $D = 4$. Neither the Lorentz indices of q_k and $\widetilde{q}_k$ are displayed nor any flavour or colour indices, which are irrelevant for the discussion of the subject. $[\Gamma \otimes 1]\, Q_k\, [1 \otimes \Gamma']$ means $\Gamma q_k \otimes \widetilde{q}_k \Gamma'$.
For the purpose of this chapter we define the perturbative expansion of the matrix elements of $\widehat{Q}_k$ differently from (3.51):

$$Z_\psi^2 \langle \widehat{Q}_k^{\text{bare}} \rangle \;=\; \sum_{j \geq 0} \left(\frac{g^2}{16\pi^2} \right)^j \langle \widehat{Q}_k^{\text{bare}} \rangle^{(j)}. \tag{4.4}$$

We have extracted the wave function renormalization here, because it is not related to the issue of the mixing of evanescent operators.
Now the insertion of $\widehat{Q}_k$ into the one-loop diagrams of fig. 4.1 yields a linear combination of the $\widehat{Q}_l$'s and a new operator with the Dirac structure $Q'_k = [\gamma_\rho\gamma_\sigma \otimes 1]\, Q_k\, [1 \otimes \gamma^\sigma\gamma^\rho]$:

$$\langle \widehat{Q}_k^{\rm bare}\rangle^{(1)} \;=\; d_{kl}^{(1)}\langle \widehat{Q}_l\rangle^{(0)} + d_{k,Q'_k}^{(1)}\langle \widehat{Q}'_k\rangle^{(0)} \quad \text{no sum on } k, \tag{4.5}$$

where $\langle\ldots\rangle^{(0)}$ denote tree level matrix elements. Both coefficients have a term proportional to $1/\varepsilon$ and a finite part. $\widehat{Q}'_k$ is now decomposed into a linear combination of the $\widehat{Q}_l$'s and an evanescent operator:

$$\widehat{Q}_k'^{\rm bare} \;=\; (f_{kl} + a_{kl}\varepsilon)\, \widehat{Q}_l^{\rm bare} + \widehat{E}_1[Q_k]^{\rm bare} + O(\varepsilon^2). \tag{4.6}$$

Here the f_{kl}'s are uniquely determined by the Dirac basis decomposition in $D = 4$ dimensions. The a_{kl}'s, however, are arbitrary, and a different choice for the a_{kl}'s corresponds to a different definition of $\widehat{E}_1[Q_k] = \widehat{E}_1[Q_k, \{a_{rs}\}]$. When going beyond the one-loop order new evanescent operators $\widehat{E}_2[Q_k], \widehat{E}_3[Q_k], \ldots$ will appear. Their precise definition is irrelevant for the moment and will be given after (4.16).
Now in the framework of dimensional regularization the renormalization of some physical operator $\widehat{Q}_k$ requires counterterms proportional to physical and evanescent operators: From (4.3) we find

$$Z_\psi^2\langle \widehat{Q}_k^{\rm bare}\rangle \;=\; Z_{kl}\langle \widehat{Q}_l^{\rm ren}\rangle + Z_{k,E_{jm}}\langle \widehat{E}_j[Q_m]^{\rm ren}\rangle \quad . \tag{4.7}$$

(4.5) and (4.6) imply that $Z_{kl}^{(1)}$ depends on the a_{rs}'s, while $Z_{k,E_{jm}}^{(1)}$ is independent of them. The definition of the coefficients in the expansion of Z in terms of the gauge coupling constant g has been given in (2.35).
Next we describe the method of Buras and Weisz [43] for the treatment of evanescent operators: They have determined the a_{kl}'s by choosing some set of Dirac structures $M = \{\gamma^{(1)} \otimes \widetilde{\gamma}^{(1)}, \ldots \gamma^{(10)} \otimes \widetilde{\gamma}^{(10)}\}$, which forms a basis for $D = 4$, and contracting all elements in M with Q'_k and Q_l in (4.6):

$$\begin{aligned}\mathrm{tr}\left(\gamma^{(m)} q'_k \widetilde{\gamma}^{(m)} \widetilde{q}'_k\right) \;&=\; (f_{kl} + a_{kl}\varepsilon)\,\mathrm{tr}\left(\gamma^{(m)} q_l \widetilde{\gamma}^{(m)} \widetilde{q}_l\right) + O(\varepsilon^2),\\ &\qquad\qquad \text{no sum on } k \text{ and on } m{=}1,\ldots,\,10.\end{aligned} \tag{4.8}$$

The solution of the equations (4.8) uniquely defines the $f_{kl} + a_{kl}\varepsilon$. In other words, $E_1[Q_k]$ obeys the equations:

$$E_1[Q_k]_{ijrs}\gamma_{si}^{(m)}\widetilde{\gamma}_{jr}^{(m)} \;=\; O(\varepsilon^2) \qquad \text{for } m{=}1,\ldots,10, \tag{4.9}$$

where i, j, r, s are Dirac indices.
Our arguments will not depend on the scheme used for the treatment of γ_5. The use of a totally anticommuting γ_5 does not cause any ambiguity in the trace operation in (4.8), because all Lorentz indices are contracted, so that the traced Dirac string is a linear combination of γ_5 and the unit matrix.

E.g. the choice of

$$\begin{aligned} M &= \{1\otimes 1, 1\otimes\gamma_5, \gamma_5\otimes 1, \gamma_5\otimes\gamma_5, \gamma_\mu\otimes\gamma^\mu, \gamma_\mu\otimes\gamma^\mu\gamma_5, \\ &\quad \gamma_5\gamma_\mu\otimes\gamma^\mu, \gamma_5\gamma_\mu\otimes\gamma^\mu\gamma_5, \sigma_{\mu\nu}\otimes\sigma^{\mu\nu}, \gamma_5\sigma_{\mu\nu}\otimes\sigma^{\mu\nu}\} \end{aligned} \tag{4.10}$$

gives for Q in (4.1)

$$Q' = \gamma_\rho\gamma_\sigma\gamma_\mu\,(1-\gamma_5)\otimes\gamma^\mu\gamma^\sigma\gamma^\rho\,(1-\gamma_5) = (4-8\varepsilon)Q + E_1[Q] + O(\varepsilon^2) \tag{4.11}$$

as in [43]. We remark that this choice $a=-8$ respects the Fierz symmetry, which relates the first to the second diagram in fig. 4.1.
A basis different from M in (4.10) yields the same $f_{k,l}$'s, but different a_{kl}'s. For example by replacing the sixth and eighth element of M in (4.10) by $\gamma_\alpha\gamma_\beta\gamma_\delta\otimes\gamma^\alpha\gamma^\beta\gamma^\delta$ and $\gamma_5\gamma_\alpha\gamma_\beta\gamma_\delta\otimes\gamma^\alpha\gamma^\beta\gamma^\delta$ one finds

$$Q' = 4Q + 16\varepsilon(1+\gamma_5)\otimes(1-\gamma_5) + E_1'[Q_k] + O(\varepsilon^2),$$

instead of (4.11), i.e. a different evanescent operator. The Dirac algebra is infinite dimensional for non-integer D and is spanned by M and an infinite set of evanescent Dirac structures. Hence one can reverse the above procedure and first arbitrarily choose the a_{kl}'s and then add properly adjusted linear combinations of the evanescent structures to the elements of M such as to obtain the chosen a_{kl}'s.
Yet the so defined evanescent operators do not decouple from the physics in four dimensions: In [43] it has been observed that their one-loop matrix elements generally have nonvanishing components proportional to the physical operators Q_k:

$$\begin{aligned} \langle\widehat{E}_1[Q_k]^{\text{bare}}\rangle^{(1)} &= \left[Z_0^{(1)}\right]_{E_{1k},l}\langle\widehat{Q}_l\rangle^{(0)} + \frac{1}{\varepsilon}\left[Z_1^{(1)}\right]_{E_{1k},E_{1k}}\langle\widehat{E}_1[Q_k]\rangle^{(0)} \\ &\quad + \frac{1}{\varepsilon}\left[Z_1^{(1)}\right]_{E_{1k},E_{2k}}\langle\widehat{E}_2[Q_k]\rangle^{(0)} + O(\varepsilon). \end{aligned} \tag{4.12}$$

Here a second evanescent operator $\widehat{E}_2$, which will be discussed in a moment, has appeared. Clearly no sum on k is understood in (4.12) and in following analogous places. In (4.12) $[Z_0^{(1)}]_{E_{1k},l}$ is local, because it originates from the local $1/\varepsilon$–pole of the tensor integrals and a term proportional to ε stemming from the evanescent Dirac algebra. For the same reason there is no divergence in the term proportional to $\langle\widehat{Q}_l\rangle^{(0)}$. Now in [43] it has been proposed to renormalize $\widehat{E}_1$ by a finite amount to cancel this component:

$$\begin{aligned} \widehat{E}_1[Q_k]^{\text{ren}} &= \widehat{E}_1[Q_k]^{\text{bare}} + \frac{g^2}{16\pi^2}\Big\{-\left[Z_0^{(1)}\right]_{E_{1k},l}\widehat{Q}_l \\ &\quad -\frac{1}{\varepsilon}\left[Z_1^{(1)}\right]_{E_{1k},E_{1k}}\widehat{E}_1[Q_k] \\ &\quad -\frac{1}{\varepsilon}\left[Z_1^{(1)}\right]_{E_{1k},E_{2k}}\widehat{E}_2[Q_k]\Big\} + O\left(g^4\right). \end{aligned} \tag{4.13}$$

With (4.13) the renormalized matrix elements of the evanescent operators are $O(\varepsilon)$, so that they do not contribute to the one-loop matching of some Green's function G^{ren} in the full renormalizable theory with matrix elements in the effective theory:

$$iG^{\text{ren}} = C_l \langle \widehat{Q}_l \rangle^{\text{ren}} + C_{E_{1k}} \langle \widehat{E}_1[Q_k] \rangle^{\text{ren}} + O\left(g^4\right), \tag{4.14}$$

i.e. the coefficients $C_{E_{1k}}$ are irrelevant, because they multiply matrix elements which vanish for $D = 4$. In [43] it has been further noticed that $Z_0^{(1)}$ in (4.13) influences the two-loop anomalous dimension matrix of the *physical* operators, so that the presence of evanescent operators indeed has an impact on physical observables.
Next we discuss $\widehat{E}_2[Q_k]$, which has entered the scene in (4.12): When inserting $\widehat{E}_1[Q_k]$ defined in (4.6) into the one-loop diagrams of fig. 4.1, one involves

$$\begin{aligned} Q_k'' &= [\gamma_\rho \gamma_\sigma \otimes 1]\, Q_k' \,[1 \otimes \gamma^\sigma \gamma^\rho] \\ &= [f + a\varepsilon]_{kl}^2\, Q_l + (f_{kl} + a_{kl}\varepsilon)\, E_1[Q_l] \\ &\quad + [\gamma_\rho \gamma_\sigma \otimes 1]\, E_1[Q_k]\, [1 \otimes \gamma^\sigma \gamma^\rho] \qquad (4.15) \\ &= \left\{ [f + a\varepsilon]_{kl}^2 + b_{kl}\varepsilon \right\} Q_l + E_2[Q_k] + O\left(\varepsilon^2\right), \qquad (4.16) \end{aligned}$$

which defines $E_2[Q_k] = E_2[Q_k, \{a_{rs}\}, \{b_{rs}\}]$. Only the last term in (4.15) can contribute to the new coefficients b_{kl}. If the projection is performed with e.g. M defined in (4.10), one finds $b_{kl} = 0$[1]. In our discussion we will keep b_{kl} arbitrary. Clearly, one has a priori to deal with the mixing of an infinite set of evanescent operators $\left\{\widehat{E}_j[Q_k]\right\}$ for each physical operator $\widehat{Q}_k$, where $\widehat{E}_{j+1}[Q_k]$ denotes the new evanescent operator appearing first in the one-loop matrix elements of $\widehat{E}_j[Q_k]$.
With the finite renormalization of $\widehat{E}_1[Q_k]$ in (4.13) the evanescent operators do not affect the physics at the matching scale, at which (4.14) holds. In order that this will be true at any scale μ, however, one must also ensure that the evanescent operators do not mix into the physical ones, as noticed first by Dugan and Grinstein in [48]. In their analysis they have introduced another way to define the evanescent operators, which is also frequently used: It is easy to see that one can restrict the operator basis $\{Q_k\}$ to the set of operators whose Dirac structures $q_k, \widetilde{q}_k$ are completely antisymmetric in their Lorentz indices. Dirac strings being antisymmetric in more than four indices vanish in four dimensions and are therefore evanescent. Operators with five antisymmetrized indices correspond to $\widehat{E}_1$ in our notation, and $\widehat{E}_2$ would be expressed in terms of a linear combination of Dirac structures with seven and with five antisymmetrized indices. Clearly this method also corresponds to some special choice for the a_{kl}'s and b_{kl}'s in (4.6) and (4.16). Now in [48] the authors have proven that with the use of those definitions and a finite renormalization analogous to (4.13) the anomalous dimension matrix indeed has the desired block-triangular form, so that the evanescent operators do not mix into the physical ones. While the anomalous dimension matrix is trivially block-triangular at one-loop level, the proof for the two-loop

[1] This is the case for any basis M in which for each $\gamma^{(m)} \otimes \gamma^{(m)} \in M$ the quantity $\gamma_\rho \gamma_\sigma \gamma^{(m)} \gamma^\sigma \gamma^\rho \otimes \gamma^{(m)}$ is a linear combination of the elements in M.

level was given in [48] by the use of the abovementioned special definition of the evanescent operators. The latter, however, has some very special features, which are absent for the general case with arbitrary a_{kl}'s and b_{kl}'s, e.g. the definition used in [48] automatically yields an anomalous dimension matrix which is tridiagonal in the evanescent sector.
This immediately raises the question whether the more general method of [43] also yields a block-triangular anomalous dimension matrix for any chosen projection basis, i.e. any chosen set $\{a_{kl}\}$. In the following section we will prove that this is indeed the case and, more generally, that one may also choose the b_{kl}'s in (4.16) completely arbitrary.

4.3. Block Triangular Anomalous Dimension Matrix

Consider some set of physical operators $\{\widehat{Q}_k\}$ which closes under renormalization together with the corresponding evanescent operators $\{\widehat{E}_j[Q_k] : j \geq 1\}$. Their $O(\varepsilon)$–parts $a_{rs}, b_{rs}, \ldots$ are chosen arbitrarily. We want to show that the block of the anomalous dimension matrix describing the mixing of $\widehat{E}_j[Q_k]$ into $\widehat{Q}_l$ equals zero,

$$[\gamma]_{E_{jk},l} \;=\; 0, \tag{4.17}$$

provided one uses the finite renormalization described in (4.13).
Our sketch will follow the outline of [48], where (4.17) has been proven by complete induction. At the one-loop level (4.17) is trivial, and the induction starts in two-loop order: The next-to-leading order contribution to the anomalous dimension matrix has been stated in (3.34). The nonzero contributions to (4.17) in two-loop order are

$$\begin{aligned}\left[\gamma^{(1)}\right]_{E_{jk},l} \;=\;& -4\left[Z_1^{(2)}\right]_{E_{jk},l} - 2\beta_0\left[Z_0^{(1)}\right]_{E_{jk},l} \\ & +2\left\{\left[Z_1^{(1)}\right]_{E_{jk},E_{rs}}\left[Z_0^{(1)}\right]_{E_{rs},l} + \left[Z_0^{(1)}\right]_{E_{jk},m}\left[Z_1^{(1)}\right]_{ml}\right\}. \end{aligned}\tag{4.18}$$

Here (4.18) contains terms which are absent when the special definition of the evanescent operators in [48] is used: In [48] one has $\left[Z^{(1)}\right]_{E_{jk},l} = 0$ for $j \geq 2$ contrary to the general case, where any evanescent operator can have counterterms proportional to physical operators. Next we look at $\left[Z_1^{(2)}\right]_{E_{jk},l}$, which stems from the $1/\varepsilon$–term of the $O(g^4)$–matrix elements of $\widehat{E}_j[Q_k]$. As discussed in [48], these $1/\varepsilon$–terms originate from $1/\varepsilon^2$–poles in the tensor integrals multiplying a factor proportional to ε stemming from the evanescent Dirac algebra. Now in each two-loop diagram the former are related to the corresponding one-loop counterterm diagrams by a factor of 1/2, because the non-local $1/\varepsilon$–poles cancel in their sum [42]. For this it is crucial that the one-loop counterterms are properly adjusted, i.e. that they cancel the $1/\varepsilon$–poles in the one-loop tensor integrals. In the one-loop matrix elements of evanescent operators the latter are multiplied with ε originating from the Dirac algebra. Hence the proper one-loop renormalization of the evanescent operators must be such as to give matrix elements of order ε, as shown for $E_1[Q_k]$ in (4.13).

From the one-loop counterterm graphs one simply reads off:

$$\left[Z_1^{(2)}\right]_{E_{jk},l} = \frac{1}{2}\left\{\left[Z_0^{(1)}\right]_{E_{jk},m}\left[Z_1^{(1)}\right]_{ml} + \left[Z_1^{(1)}\right]_{E_{jk},E_{rs}}\left[Z_0^{(1)}\right]_{E_{rs},l} - \beta_0\left[Z_0^{(1)}\right]_{E_{jk},l}\right\},$$

which yields the desired result when inserted into (4.18). Here the first two terms stem from insertions of physical and evanescent counterterms to $E_j[Q_k]$, while the term involving the coefficient of the one-loop β–function $\beta(g) = -g^3/(16\pi^2)\beta_0$ originates from the diagrams with coupling constant counterterms. The terms involving the wave function renormalization constants cancel with those stemming from the factor Z_ψ^2 in (4.7).
The inductive step in [48] proving (4.17) to any loop order does not use any special definition of the evanescent and therefore applies unchanged here.

4.4. Evanescent Scheme Dependences

In this section we will analyze the dependence of the physical part of $\gamma^{(1)}$ given in (3.34) and of the one-loop Wilson coefficients on a_{il} and b_{il}. In practical next-to-leading order calculations one often has to combine Wilson coefficients and anomalous dimension matrices obtained with different definitions of the evanescent operators and it is therefore important to have formulae allowing to switch between them (see e.g. appendix B of [49]).
We start with the investigation of the dependence of $\gamma^{(1)}$ on a_{il}. The bare one-loop matrix element

$$\begin{aligned}\langle\widehat{Q}_k^{\rm bare}\rangle^{(1)} &= \left\{\frac{1}{\varepsilon}\left[Z_1^{(1)}\right]_{kj} + \left[d_0^{(1)}\right]_{kj}\right\}\langle\widehat{Q}_j\rangle^{(0)} + \frac{1}{\varepsilon}\left[Z_1^{(1)}\right]_{k,E_{1k}}\langle\widehat{E}_1[Q_k]\rangle^{(0)} \\ &\quad + O(\varepsilon)\end{aligned} \tag{4.19}$$

is independent of a_{il}, which is evident from (4.5). $E_1[Q_k]$ depends linearly on a_{il} through its definition (4.6) with the coefficient

$$\frac{\partial}{\partial a_{il}}\widehat{E}_1[Q_k] = -\varepsilon\,\delta_{ki}\,\widehat{Q}_l, \tag{4.20}$$

so that (4.19) gives:

$$\frac{\partial}{\partial a_{il}}\left[d_0^{(1)}\right]_{kj} = \left[Z_1^{(1)}\right]_{k,E_{1k}}\delta_{ki}\delta_{lj}, \tag{4.21}$$

while $Z_1^{(1)}$ is independent of a_{il}.
In the same way on can obtain the a_{kl}–dependence of $Z_1^{(2)}$. (4.7) reads to two-loop order (cf. (4.4)):

$$\begin{aligned}\langle\widehat{Q}_k^{\rm bare}\rangle^{(2)} &= Z_{kj}^{(2)}\langle\widehat{Q}_j\rangle^{(0)} + Z_{k,E_{1m}}^{(2)}\langle\widehat{E}_1[Q_m]\rangle^{(0)} + Z_{k,E_{2m}}^{(2)}\langle\widehat{E}_2[Q_m]\rangle^{(0)} \\ &\quad + Z_{kr}^{(1)}\langle\widehat{Q}_r^{\rm ren}\rangle^{(1)} + Z_{k,E_{1k}}^{(1)}\langle\widehat{E}_1[Q_k]^{\rm ren}\rangle^{(1)} + \langle\widehat{Q}_k^{\rm ren}\rangle^{(2)}.\end{aligned} \tag{4.22}$$

From (4.16) we know

$$\frac{\partial}{\partial a_{il}}\widehat{E}_2[Q_m] \;=\; -\varepsilon\left[f_{mi}\delta_{lj}+\delta_{mi}f_{lj}\right]\widehat{Q}_j, \tag{4.23}$$

and from (4.19) one reads off:

$$\langle\widehat{Q}_r^{\rm ren}\rangle^{(1)} \;=\; \left[d_0^{(1)}\right]_{rj}\langle\widehat{Q}_j\rangle^{(0)}. \tag{4.24}$$

These relations and (4.21) allow to calculate the derivative of (4.22) with respect to a_{il}. Keeping in mind that the evanescent matrix elements are $O(\varepsilon)$ the $O(1/\varepsilon)$–part of the derivative yields:

$$\begin{aligned}\frac{\partial}{\partial a_{il}}\left[Z_1^{(2)}\right]_{kj} \;&=\; -\left[Z_1^{(1)}\right]_{ki}\left[Z_1^{(1)}\right]_{i,E_{1i}}\delta_{lj}+\left[Z_2^{(2)}\right]_{k,E_{1i}}\delta_{lj}\\ &\quad+\left[Z_2^{(2)}\right]_{k,E_{2m}}\left(\delta_{mi}f_{lj}+f_{mi}\delta_{lj}\right),\quad\text{no sum on } i.\end{aligned} \tag{4.25}$$

We pause here to stress that (4.25) is local showing that an evanescent redefinition does not spoil the renormalizability of the physical sector in NLO.
Next we extract $\left[Z_2^{(2)}\right]$ from the one-loop counterterm diagrams as described in the preceding section:

$$\begin{aligned}\left[Z_2^{(2)}\right]_{k,E_{1i}} \;&=\; \frac{1}{2}\left[Z_1^{(1)}\right]_{ki}\left[Z_1^{(1)}\right]_{i,E_{1i}}+\frac{1}{2}\left[Z_1^{(1)}\right]_{i,E_{1i}}\left[Z_1^{(1)}\right]_{E_{1i},E_{1i}}\delta_{ki}\\ &\quad-\frac{1}{2}\beta_0\left[Z_1^{(1)}\right]_{i,E_{1i}}\delta_{ki},\qquad\text{no sum on } i\\ \left[Z_2^{(2)}\right]_{k,E_{2m}} \;&=\; \frac{1}{2}\left[Z_1^{(1)}\right]_{k,E_{1k}}\left[Z_1^{(1)}\right]_{E_{1k},E_{2k}}\delta_{km},\qquad\text{no sum on } k.\end{aligned} \tag{4.26}$$

After inserting (4.26) into (4.25) we want to substitute the last term in (4.25). For this we derive both sides of (4.12) with respect to a_{il} giving:

$$\begin{aligned}&\left[Z_1^{(1)}\right]_{E_{1k},E_{2k}}\left(\delta_{ki}f_{lj}+f_{ki}\delta_{lj}\right) \;=\\ &\quad\frac{\partial}{\partial a_{il}}\left[Z_0^{(1)}\right]_{E_{1k},j}+\left[Z_1^{(1)}\right]_{lj}\delta_{ki}-\left[Z_1^{(1)}\right]_{E_{1k},E_{1k}}\delta_{ki}\delta_{lj},\quad\text{no sum on } k.\end{aligned} \tag{4.27}$$

Finally one has to insert the expression for (4.25) obtained by the described substitutions into

$$\frac{\partial}{\partial a_{il}}\left[\gamma^{(1)}\right]_{kj} \;=\; -4\frac{\partial}{\partial a_{il}}\left[Z_1^{(2)}\right]_{kj}+2\left[Z_1^{(1)}\right]_{k,E_{1k}}\frac{\partial}{\partial a_{il}}\left[Z_0^{(1)}\right]_{E_{1k},j},\quad\text{no sum on } k,$$

which follows from (3.34). The result reads:

$$\begin{aligned}\frac{\partial}{\partial a_{il}}\left[\gamma^{(1)}\right]_{kj} \;&=\; -2\left[Z_1^{(1)}\right]_{lj}\left[Z_1^{(1)}\right]_{i,E_{1i}}\delta_{ki}+2\left[Z_1^{(1)}\right]_{ki}\left[Z_1^{(1)}\right]_{i,E_{1i}}\delta_{lj}\\ &\quad+2\beta_0\left[Z_1^{(1)}\right]_{i,E_{1i}}\delta_{ki}\delta_{lj},\qquad\text{no sum on } i.\end{aligned} \tag{4.28}$$

Since the quantities on the right hand side of (4.28) do not depend on a_{il}, one can easily integrate (4.28) to find the desired relation between two γ's corresponding to different choices for a_{kl} in (4.6). To write the result in matrix form we recall the expression for the physical one-loop anomalous dimension matrix

$$\left[\gamma^{(0)}\right]_{lj} \;=\; -2\left[Z_1^{(1)}\right]_{lj}$$

and introduce the diagonal matrix D with

$$D_{im} \;=\; \left[Z_1^{(1)}\right]_{i,E_{1i}}\delta_{im}, \qquad \text{no sum on } i. \tag{4.29}$$

Hence

$$\gamma^{(1)}(a') \;=\; \gamma^{(1)}(a) + \left[D\cdot(a'-a),\gamma^{(0)}\right] + 2\,\beta_0\,D\cdot(a'-a), \tag{4.30}$$

where the summation in the row and column indices only runs over the physical submatrices.
(4.30) exhibits the familiar structure of the scheme dependence of $\gamma^{(1)}$ as given in (3.54). The matrix J in (3.55) consequently reads:

$$J(a') \;=\; J(a) - \left[D\cdot(a'-a)\right]^T. \tag{4.31}$$

Hence we have found a scheme dependence which is caused by an evanescent redefinition of a *bare* operator basis (i.e. of the bare evanescent operators).
The dependence of the one-loop matrix elements on a can be found easily from (4.24) and (4.21):

$$\langle\vec{Q}\rangle^{\rm ren}(a') \;=\; \left[1+\frac{g^2}{16\pi^2}D\cdot(a'-a)\right]\langle\vec{Q}\rangle^{\rm ren}(a) + O(g^4). \tag{4.32}$$

Since in (4.14) G does not depend on a and the evanescent matrix element is $O(\varepsilon)$, the corresponding relation for the Wilson coefficients at the matching scale reads:

$$\vec{C}^T(a') \;=\; \vec{C}^T(a)\left[1-\frac{g^2}{16\pi^2}D\cdot(a'-a)\right] + O(g^4). \tag{4.33}$$

Thus also the Wilson coefficient transforms correctly as in (3.56) and the scheme dependence cancels between coefficients and anomalous dimension matrix.
In the same way one can investigate the dependence of $\gamma^{(1)}$ on b_{il} given in (4.16): While $Z_1^{(2)}$ and $Z_0^{(1)}$ depend on b_{il}, this dependence cancels in (3.34). Hence neither $\gamma^{(1)}$ nor the one-loop Wilson coefficient are affected by the choice of b_{il}. Thus in NLO the b_{il}'s do not induce a scheme dependence. By keeping b_{il} arbitrary in a practical calculation one has a non–trivial check of the correct handling of the evanescents: The b_{il}'s disappear from the result only after inserting the evanescent counterterms with a factor of 1/2.

The nice feature of (4.32), (4.33) and (4.30) is that the summed matrix indices only run over the physical subset. From (3.54) and (3.56) we could have expected a formula where the summation runs over the whole operator basis including the evanescents. This is why we could not simply deduce (4.30) from (4.32) using (3.53) and (3.54). Possible contributions from summations over evanescent operator indices cannot be inferred from (4.32), because there they would multiply vanishing matrix elements.
We have already stressed in the end of sect. 3.8.1 that it is advantageous to have a $\gamma^{(1)}$ which commutes with $\gamma^{(0)}$. Now one can use (4.30) to simplify $\gamma^{(1)}$: By going to the diagonal basis for $\gamma^{(0)} = \mathrm{diag}\left(\gamma_i^{(0)}\right)$ one can easily find solutions for $a' - a$ in (4.30) which even give $\gamma^{(1)}(a') = 0$ provided that all $Z_{k,E_{1k}}$'s are nonzero and all eigenvalues of $\gamma^{(0)}$ satisfy $\left|\gamma_i^{(0)} - \gamma_j^{(0)}\right| \neq 2\beta_0$. We will exemplify this in a moment.
A choice for a_{il} which leads to a $\gamma^{(1)}$ commuting with $\gamma^{(0)}$ has been done implicitly in [43]: There the mixing of the two operators $Q_+ = Q\left(1 + \widetilde{1}\right)/2$ and $Q_- = Q\left(1 - \widetilde{1}\right)/2$ has been considered, where 1 and $\widetilde{1}$ denote colour singlet and antisinglet and Q was introduced in (4.1). Now Q_+ is self-conjugate under the Fierz transformation, while Q_- is anti-self-conjugate, so that $\gamma^{(0)}$ is diagonal to maintain the Fierz symmetry in the leading order renormalization group evolution. As remarked after (4.11), the definition of $E_1[Q]$ in (4.11) is necessary to ensure the Fierz symmetry in the one-loop matrix elements. Consequently with (4.11) also $\gamma^{(1)}$ has to obey the Fierz symmetry preventing the mixing of Q_+ and Q_-, i.e. yielding a diagonal $\gamma^{(1)}$. A different definition of $E_1[Q]$ would result in non-Fierz-symmetric matrix elements, but in renormalization scheme independent expressions they would combine with a non-diagonal $\gamma^{(1)}$ such as to restore Fierz symmetry.
Let us consider the example above to demonstrate that one can pick a' such that $\gamma^{(1)}(a') = 0$: In [43] the definitions

$$\begin{aligned} E_1[Q_\pm] &= \left(\pm 1 - \frac{1}{N}\right)[\gamma_\rho\gamma_\sigma\gamma_\nu(1-\gamma_5) \otimes \gamma^\nu\gamma^\sigma\gamma^\rho(1-\gamma_5) \\ &\quad -(4-8\varepsilon)\ \gamma_\nu(1-\gamma_5) \otimes \gamma^\nu(1-\gamma_5)], \end{aligned}$$

i.e. $a_{++} = 8(1/N-1), a_{--} = 8(1/N+1), a_{+-} = a_{-+} = 0$, were adopted yielding a diagonal $\gamma^{(1)}(a) = \mathrm{diag}\left(\gamma_+^{(1)}(a), \gamma_-^{(1)}(a)\right)$. From the insertion of Q_+ and Q_- into the diagrams of fig. 4.1 one finds $Z_{+,E_{1+}} = Z_{-,E_{1-}} = 1/4$. Hence if we pick $a'_{\pm\pm} = a_{\pm\pm} - 2/\gamma_\pm^{(1)}(a)/\beta_0$ and $a'_{\pm\mp} = 0$, (4.30) will imply $\gamma^{(1)}(a') = 0$.

4.5. Double Insertions

4.5.1. Motivation

From the preceding sections we know that the coefficients $C_{E_{jk}}$ of properly renormalized evanescents in (4.3) are irrelevant for physical quantities and remain undetermined. In the following we will extend these results to 4-fermion Green's functions with two insertions of local operators.

For the discussion of Green's functions with insertion of two local operators as depicted in fig. 5.4 we first display the evanescents in $\mathcal{L}^{\rm II}$ in (3.28):

$$\mathcal{L} = \mathcal{L}^{\rm I} + \mathcal{L}^{\rm II} \tag{4.34}$$

$$\begin{aligned}\mathcal{L}^{\rm II} &= C_k C_{k'} \left\{ Z^{-1}_{kk',l} \widetilde{Q}^{\rm bare}_l + Z^{-1}_{kk',E_{rl}} \widetilde{E}_r \left[\widetilde{Q}_l\right]^{\rm bare} \right\} \\ &\quad + C_k C_{E_{j'k'}} \left\{ Z^{-1}_{kE_{j'k'},l} \widetilde{Q}^{\rm bare}_l + Z^{-1}_{kE_{j'k'},E_{rl}} \widetilde{E}_r \left[\widetilde{Q}_l\right]^{\rm bare} \right\} \\ &\quad + C_{E_{jk}} C_{E_{j'k'}} \left\{ Z^{-1}_{E_{jk}E_{j'k'},l} \widetilde{Q}^{\rm bare}_l + Z^{-1}_{E_{jk}E_{j'k'},E_{rl}} \widetilde{E}_r \left[\widetilde{Q}_l\right]^{\rm bare} \right\} \\ &\quad + \widetilde{C}_k \widetilde{Z}^{-1}_{kl} \widetilde{Q}^{\rm bare}_l + \widetilde{C}_k \widetilde{Z}^{-1}_{kE_{rl}} \widetilde{E}_r \left[\widetilde{Q}_l\right]^{\rm bare} \\ &\quad + \widetilde{C}_{E_{jk}} \widetilde{Z}^{-1}_{E_{jk}l} \widetilde{Q}^{\rm bare}_l + \widetilde{C}_{E_{jk}} \widetilde{Z}^{-1}_{E_{jk}E_{rl}} \widetilde{E}_r \left[\widetilde{Q}_l\right]^{\rm bare} \end{aligned} \tag{4.35}$$

Since the $\widehat{Q}_k$'s have dimension six, the $\widetilde{Q}_l$'s are dimension–eight operators. For simplicity, we assume the $\widetilde{Q}_l$'s to be linearly independent from the $\widehat{Q}_k$'s, e.g. the $\widehat{Q}_k$'s represent $\Delta S = 1$ operators and the $\widetilde{Q}_l$'s denote $\Delta S = 2$ operators. The $E_r\left[\widetilde{Q}_l\right]$ in (4.35) are defined analogously to (4.6) with new coefficients $\widetilde{f}_{kl}$, $\widetilde{a}_{kl}$, $\widetilde{b}_{kl}$, etc. Hence new arbitrary constants $\widetilde{a}_{kl}$, $\widetilde{b}_{kl}$ potentially causing scheme dependences enter the scene.
Clearly the following questions arise here:

1. Are the coefficient functions $C_{E_{jk}}$ irrelevant also for the double insertions; i.e. do

$$\left\langle \int \mathbf{T}\, \widehat{E}\widehat{Q} \right\rangle \qquad \text{and} \qquad \left\langle \int \mathbf{T}\, \widehat{E}\widehat{E} \right\rangle \tag{4.36}$$

   contribute to the matching procedure and the operator mixing?

2. Does one need a *finite* renormalization in the evanescent sector of double insertions; if yes, how does this affect the anomalous dimension tensor?

3. How do the $\widetilde{C}_l$ and anomalous dimension matrices depend on the a_{kl}, b_{kl}, $\widetilde{a}_{kl}$, $\widetilde{b}_{kl}$?

4. Are the RG improved observables scheme independent?

4.5.2. Scheme Consistency

In this section we will carry out the program of section 4.3 for the case of double insertions to answer questions 1 and 2 of page 54.
We have mentioned already in sect. 3.7.2 that two cases have to be distinguished: The matrix element of the double insertion of the two local renormalized operators can be divergent or finite:

$$\left\langle \frac{i}{2} \int \mathbf{T}\, \widehat{Q}_k \widehat{Q}_{k'} \right\rangle = \begin{cases} \text{divergent} & , \ \text{case 1} \\ \text{finite} & , \ \text{case 2} \end{cases} . \tag{4.37}$$

Therefore we need or do not need a separate renormalization for the double insertion

$$Z^{-1}_{kk',l} \begin{cases} \neq & 0 \quad , \quad \text{case 1} \\ = & 0 \quad , \quad \text{case 2} \end{cases} . \tag{4.38}$$

Let us start the discussion with the matching procedure 3.30:

$$\begin{aligned} -iG^{\text{ren}} &= C_k C_{k'} \left\langle \left[\frac{i}{2} \int \mathbf{T}\, \widehat{Q}_k \widehat{Q}_{k'} \right]^{\text{ren}} \right\rangle + C_k C_{E_{i'k'}} \left\langle \left[i \int \mathbf{T}\, \widehat{Q}_k \widehat{E}_{i'} \left[Q_{k'} \right] \right]^{\text{ren}} \right\rangle \\ &\quad + C_{E_{ik}} C_{E_{i'k'}} \left\langle \left[\frac{i}{2} \int \mathbf{T}\, \widehat{E}_i \left[Q_k \right] \widehat{E}_{i'} \left[Q_{k'} \right] \right]^{\text{ren}} \right\rangle + C_l \left\langle \widetilde{Q}_l \right\rangle \\ &\quad + \widetilde{C}_{E_{jl}} \left\langle \widetilde{E}_j \left[\widetilde{Q}_l \right] \right\rangle , \end{aligned} \tag{4.39}$$

where G^{ren} corresponds e.g. to the box–function shown in fig. 5.1 and the radiative corrections depicted in fig. 5.2.
Since the coefficients $C_{E_{jk}}$ must be irrelevant for this matching procedure, one must have

$$Z_\psi^2 \left\langle \left[\frac{i}{2} \int \mathbf{T}\, \widehat{E}_j \left[Q_k \right] \widehat{Q}_{k'} \right]^{\text{ren}} \right\rangle \stackrel{!}{=} \begin{cases} O\left(\varepsilon^0\right) & \text{in case 1 (LO)} \\ O\left(\varepsilon^1\right) & \text{in case 1 (NLO and higher)} \\ O\left(\varepsilon^1\right) & \text{in case 2} \end{cases} \tag{4.40}$$

and the analogous relation for two insertions of evanescent operators. Recall from sect. 3.7.2 that in case 1 the LO matching is performed by the comparison of the coefficients of logarithms of the full theory amplitude and the effective theory matrix element (4.40) (the latter being trivially related to the coefficient of the divergence), while the NLO matching is obtained from the finite part and also involves the matrix elements of the local operators. In case 2 the matching is performed with the finite parts in all orders. In both cases the condition (4.40) is trivially fulfilled in LO, because the evanescent Dirac algebra gives an additional ε compared to the case of the insertion of two physical operators. Therefore a finite renormalization for the double insertion turns out to be unnecessary at the LO level. This statement remains valid at the NLO level only in case 2, in case 1 condition (4.40) no longer holds if one only subtracts the divergent terms in the matrix elements containing a double insertion. With the argumentation preceding (4.13) one finds that in this case the finite term needed to satisfy the condition (4.40) is local and therefore can be provided by a finite counterterm.
The operator mixing can be analyzed analogously to section 4.3. Using the finite renormalization enforcing (4.40) and the locality of counterterms, one shows for the anomalous dimension tensor (3.45):

$$\gamma^{(0)}_{E_{rk}l,n} = \gamma^{(1)}_{E_{rk}l,n} = 0 \qquad \text{and} \qquad \gamma^{(0)}_{E_{rk}E_{sl},n} = \gamma^{(1)}_{E_{rk}E_{sl},n} = 0, \tag{4.41}$$

i.e. a double insertion containing at least one evanescent operator does not mix into physical operators. Together with the statement that evanescent operators do not contribute to the

matching this proves our method to be consistent at the NLO level. As in the case of single insertions one can pick the $\widetilde{a}_{kl}$, $\widetilde{b}_{kl}$,... completely arbitrary and then has to perform a finite renormalization for the double insertions containing an evanescent operator in (4.36). This statement remains valid also in higher orders of the SU(N) interaction, which can be proven analogously to the proof given by Dugan and Grinstein [48] for the case of single insertions. Now we use the findings above to show the nonvanishing terms in (3.45) explicitly for the physical submatrix:

$$\begin{aligned}\gamma^{(1)}_{kn,l} &= 4\left[Z_1^{-1,(2)}\right]_{kn,l} - 2\left[Z_1^{-1,(1)}\right]_{kn,E_{1l'}}\left[\widetilde{Z}_0^{-1,(1)}\right]_{E_{1l'}l} \\ &\quad -2\left[Z_1^{-1,(1)}\right]_{kE_{1k'}}\left[Z_0^{-1,(1)}\right]_{E_{1k'}n,l} - 2\left[Z_1^{-1,(1)}\right]_{nE_{1n'}}\left[Z_0^{-1,(1)}\right]_{kE_{1n'},l}\end{aligned} \tag{4.42}$$

The last equation encodes the following rule for the correct treatment of evanescent operators in NLO calculations: *The correct contribution of evanescent operators to the NLO physical anomalous dimension tensor is obtained by inserting the evanescent one-loop counterterms with a factor of* $\frac{1}{2}$ *instead of* 1 *into the counterterm graphs.* Hence the finding of [43] for a single operator insertion generalizes to Green's functions with double insertions. Here the second term in (4.42) corresponds to the graphs with the insertion of a local evanescent counterterm into the graphs depicted in fig. 4.1, while the last to terms correspond to the diagrams of fig. 5.4 with one physical and one evanescent operator.

4.5.3. Double Insertions: Evanescent Scheme Dependences

In this section we will answer questions 3 and 4 on page 54. Let us first look at the dependence of the anomalous dimension tensor $\gamma_{kk',l}$ on the coefficients a_{rs}. First one notices, that the LO $\gamma^{(0)}_{kk',l}$ is independent of the choice of the a_{rs}. Similarly to the procedure of section 4.4 one derives the following NLO relation:

$$\gamma^{(1)}_{kk',l}(a') = \gamma^{(1)}_{kk',l}(a) + [D\cdot(a'-a)]_{ks}\,\gamma^{(0)}_{sk',l} + [D\cdot(a'-a)]_{k's}\,\gamma^{(0)}_{sk,l} \tag{4.43}$$

with the diagonal matrix D from (4.29). Note again that the indices only run over the physical subspace.
The variation of the anomalous dimension tensor $\gamma_{kk',l}$ with the coefficients $\widetilde{a}_{rs}$ again vanishes in LO, in NLO we find the transformation

$$\begin{aligned}\gamma^{(1)}_{kk',l}(\widetilde{a}') &= \gamma^{(1)}_{kk',l}(\widetilde{a}) + \gamma^{(0)}_{kk',i}\left[\widetilde{Z}_1^{-1,(1)}\right]_{iE_{1i}}[\widetilde{a}'-\widetilde{a}]_{il} - 2\beta_0\left[Z_1^{-1,(1)}\right]_{kk',\widetilde{E}_{1i}}[\widetilde{a}'-\widetilde{a}]_{il} \\ &\quad + \left[\gamma^{(0)}_{kj}\delta_{k'j'} + \delta_{kj}\gamma^{(0)}_{k'j'}\right]\left[Z_1^{-1,(1)}\right]_{jj',\widetilde{E}_{1i}}[\widetilde{a}'-\widetilde{a}]_{il} \\ &\quad - \left[Z_1^{-1,(1)}\right]_{kk',\widetilde{E}_{1i}}[\widetilde{a}'-\widetilde{a}]_{is}\,\widetilde{\gamma}^{(0)}_{sl}\end{aligned} \tag{4.44}$$

As in the case of single insertions, up to the NLO level there exists no dependence of γ on the coefficients b_{rs} and also no one on the $\widetilde{b}_{rs}$. This provides a nontrivial check of the treatment of evanescent operators in a practical calculation, when the b_{rs}, $\widetilde{b}_{rs}$ are kept arbitrary: the

individual renormalization factors Z each exhibit a dependence on the coefficients b_{rs}, $\widetilde{b}_{rs}$ but all this dependence cancels, when the Z's get combined to γ. This has been done in the calculation of η_3 in chapter 6.
Next we verify the scheme independence of RG improved physical observables. From the solution of the inhomogeneous RG equation (3.46) we find the local operators' Wilson coefficients $\widetilde{C}_l$ independent under the transformations (4.33), (4.31) and (4.43).
In a similar way one treats the scheme dependence stemming from the coefficients $\widetilde{a}_{kl}$. Here some work has been necessary to prove the cancellation of the scheme dependence connected to $g'^2 \widetilde{J}_{kk'}$ and $\gamma^{(1)}_{nm,k'}$ in (3.46): Although it is not possible to perform the integration in (3.46) without transforming some of the operators to the diagonal basis, one can do the integral for the scheme dependent part of (3.46), because the part of the integrand depending on $\widetilde{a}_{kl}$'s is a total derivative with respect to g. There is one important difference compared to the dependence on the a_{kl}'s: A scheme dependence of the Wilson coefficient related to the lower end of the RG evolution μ in (3.46) still remains. This residual $\widetilde{a}_{kl}$ dependence must be canceled by a corresponding one in the hadronic matrix element. If the matrix elements are obtained in the parton model, the dependence of the $\widetilde{C}_l$'s on $\widetilde{a}_{kl}$ cancels due to (4.32). Finally, as in the case of single insertions [44], one can define a scheme–independent Wilson coefficient for the local operator

$$\overline{\widetilde{C}_l(\mu)} \;=\; \left[\delta_{ll'} + \frac{g^2(\mu)}{16\pi^2}\cdot \widetilde{r}_{l'l}\right] \widetilde{C}_{l'} + \frac{g^2(\mu)}{16\pi^2}\cdot \widetilde{r}_{nm,l}\cdot C_n^{(0)}(\mu)\, C_m^{(0)}(\mu) + O\left(g^4\right), \tag{4.45}$$

which multiplies a scheme independent matrix element defined accordingly. It contains the analogue of $\widehat{r}$ in (3.52) for the double insertion

$$\left\langle \frac{i}{2}\int \mathbf{T}\, Q_n Q_m \right\rangle^{(0)} \;=\; \frac{g^2}{16\pi^2}\cdot \widetilde{r}_{nm,l}\cdot \left\langle \widetilde{Q}_l \right\rangle^{(0)}. \tag{4.46}$$

4.6. Inclusive Decays

Inclusive decays are calculated either by calculating the exclusive process and performing a subsequent phase space integration and a summation over final polarizations etc. (referenced as method 1) or by use of the optical theorem, which corresponds to taking the imaginary part of the self-energy diagram depicted in fig. 4.2 (method 2). This figure shows that inclusive decays are in fact related to double insertions, but in contrast to the case of section 4.5 they do not involve local four-quark operators as counterterms for double insertions. In fact, even local two-quark operator counterterms would only be needed to renormalize the real part, but the imaginary part of their matrix elements clearly vanishes. The only scheme dependence to be discussed is therefore the one associated with the a_{kl}'s, b_{kl}'s, etc., as there are no $\widetilde{a}_{kl}$'s $\widetilde{b}_{kl}$'s, etc. involved.
To discuss the dependence on the a_{kl}'s it is nevertheless advantageous to consider method 1, i.e. the exclusive process plus the subsequent phase space integration. From section 4.4 we

already know most of the properties of the exclusive process: At the upper renormalization scale the properly renormalized evanescent operators do not contribute and the scheme dependence cancels. Further we know from (4.31) the scheme dependence of the (RG improved) Wilson coefficients at the lower renormalization scale. What we are left with is the calculation of the properly renormalized operators in perturbation theory, i.e. with on-shell external momenta. Clearly the form of the external states does not affect the scheme dependent terms of the matrix elements, they are again given by (4.32) and therefore cancel trivially between the Wilson coefficients and the matrix elements, because the scheme dependent terms are independent of the external momenta. Since we now have a finite amplitude which is scheme independent, we may continue the calculation in four dimensions and may therefore forget about the evanescent operators. The remaining phase space integration and summation over final polarizations does not introduce any new scheme dependence, therefore we end up with a rate independent of the a_{kl}'s, b_{kl}'s, etc. [2]
Alternatively one may use the approach via the optical theorem (method 2). Then one has to calculate the imaginary parts of the diagram in fig. 4.2 plus gluonic corrections. Of

Figure 4.2: The lowest order self-energy diagram needed for the calculation of inclusive decays via the optical theorem (method 2).

course the properly renormalized operators have to be plugged in:

$$\mathrm{Im}\left\langle \widehat{O}_k^{\mathrm{ren}} \widehat{O}_l^{\mathrm{ren}} \right\rangle \tag{4.47}$$

One immediately ends up with a finite rate. What is left to show is the consistency of the optical theorem with the presence of evanescent operators and with their arbitrary definition proposed in (4.6), (4.16): The result must not depend on whether the evanescent operators are kept in the basis inserted into the diagram of fig. 4.2 or whether they have been removed knowing the above result of method 1. This means that evanescent operators must not contribute to the rate, i.e. diagrams containing an insertion of one or two evanescent operators must be of order ε

$$\mathrm{Im}\left\langle \widehat{E}_i \left[O_k\right]^{\mathrm{ren}} \widehat{O}_l^{\mathrm{ren}} \right\rangle = O\left(\varepsilon\right) \quad \text{and} \quad \mathrm{Im}\left\langle \widehat{E}_i \left[O_k\right]^{\mathrm{ren}} \widehat{E}_j \left[O_l\right]^{\mathrm{ren}} \right\rangle = O\left(\varepsilon\right). \tag{4.48}$$

As in the previous sections one can discuss tensor integrals and Dirac algebra separately leading to (4.48).

4.7. Summary and Outlook

Let us list the results of this chapter:

[2] We discard problems due to infrared singularities and the Bloch-Nordsiek theorem. At least in NLO one can use a gluon mass, because no three-gluon vertex contributes to the relevant diagrams

i) It is allowed to redefine any *bare* evanescent operator by $(D-4)$ times any physical operator without affecting the block-triangular form of the anomalous dimension matrix, which ensures that properly renormalized evanescent operators (as described in [43]) do not mix into physical ones.

ii) We have analyzed the renormalization scheme dependence associated with the redefinition transformation in the next-to-leading order in renormalization group improved perturbation theory. The formulas transforming between different schemes have been derived. It is meaningless to give some anomalous dimension matrix or some Wilson coefficients beyond leading logarithms without specifying the definition of the evanescent operators used during the calculation. In physical observables, however, this renormalization scheme dependence cancels between Wilson coefficients and the anomalous dimension matrix. One may take advantage of this feature by defining the evanescent operators such as to achieve a simple form for the anomalous dimension matrix.

iii) We have extended the work of [43] and [48] and the results of i) and ii) to the case of Green's functions with two operator insertions. This analysis is necessary for the correct treatment of evanescents in particle–antiparticle mixing and rare decays. Scheme-independent Wilson coefficients have been defined.

iv) Finally we have analyzed the role of evanescents in inclusive decay rates.

The issue of the renormalization of composite operators in dimensional regularization is not restricted to four–quark operators. We suggest that one may investigate to what extent evanescent redefinitions are useful to gain insight into the renormalization scheme dependences of other operators. If, for example, some current j is handled with two renormalization prescriptions denoted by j_1 and j_2, one could try to reabsorb the scheme dependence by an evanescent redefinition $j_1 \to j_1' = (1 + a\varepsilon + \ldots)j_1 + \varepsilon \cdot (\text{other currents})$. I.e. j_1' yields with prescription 1 the same finite parts of physical amplitudes as j_2 renormalized with prescription 2.

5. Effective Lagrangian for Flavour Changing Processes

In this chapter we will set up the operator basis needed for the calculation of the $K^0-\overline{K^0}$–mixing described in chapter 6. We will also explain the general structure of the effective lagrangian and of the calculations which are necessary to obtain its RG improved coefficients. The basic framework is very similar for the general case of particle–antiparticle mixing. We will sometimes comment on differences between the considered $|\Delta S|=2$ transitions and $|\Delta B|=2$ or $|\Delta C|=2$ amplitudes.
First the Standard Model diagrams contributing to the $K^0-\overline{K^0}$–mixing will be analyzed. Since $|\Delta S|=2$ transitions involving light quarks contain $|\Delta S|=1$ processes as substructures, sect. 5.3 will discuss them in detail. Here we will notice that the definition of the correct $|\Delta S|=1$ operator basis involved in $|\Delta S|=2$ amplitudes is much more complicated than the one needed to describe the four quark amplitudes appearing in $|\Delta S|=1$ weak decays. The analysis of the operator basis requires the careful application of the theorems of sect. 3.10 on the use of the field equations of motion and on BRS–exact operators.

5.1. $|\Delta S|=2$ transition in the Standard Model

The $|\Delta S|=2$ transition is a flavour–changing neutral current (FCNC) process and therefore forbidden at tree level. The lowest order contribution to it is depicted in fig. 5.1.

Figure 5.1: The lowest order box diagrams mediating a $|\Delta S|=2$ transition. The zigzag lines stand for W–bosons or ficticious Higgs particles. The diagrams rotated by 90° must also be considered.

5.1.1. Notations and Conventions

Before writing down the result for the diagram of fig. 5.1, we set up the notations used in the following.
The different contributions from the internal quarks involve different CKM factors $\lambda_j = V_{jd}V_{js}^*$. The GIM mechanism $\lambda_t + \lambda_c + \lambda_u = 0$ allows for the elimination of λ_u. Hence we can split up the Standard Model Green's function as

$$\widetilde{G} \;=\; \lambda_c^2\widetilde{G}^{cc} + \lambda_t^2\widetilde{G}^{tt} + 2\lambda_c\lambda_t\widetilde{G}^{ct}, \tag{5.1}$$

which is understood to be truncated, connected and Fourier–transformed into momentum space. We will sometimes use the abbrevation $x_i = m_i^2/M_W^2$ for the squared ratio of some quark mass and the W mass. For the W propagator the 't Hooft–Feynman gauge will be used, while we keep the QCD gauge parameter ξ arbitrary. As only open fermion lines appear in the calculation, we can safely use a naive anticommuting γ_5 (NDR scheme) with $L = 1 - \gamma_5$ and $R = 1 + \gamma_5$. N is the number of colours, and $\mathbb{1}$ and $\widetilde{\mathbb{1}}$ denote colour singlet and antisinglet[1], i.e. $(L \otimes R) \cdot \widetilde{\mathbb{1}}$ stands for $\overline{s}_i(1-\gamma_5)d_j \cdot \overline{s}_j(1+\gamma_5)d_i$ with j and k being colour indices. The $SU(N)$ Casimir factor involved will be $C_F = (N^2-1)/(2N)$.
The result of fig. 5.1 is proportional to the tree–level matrix element of

$$\widetilde{Q}_{S2} \;=\; (\overline{s}d)_{V-A}(\overline{s}d)_{V-A}\mathbb{1} \;=\; (\overline{s}\gamma_\mu(1-\gamma_5)d)(\overline{s}\gamma^\mu(1-\gamma_5)d)\cdot\mathbb{1} \tag{5.2}$$

shown in fig. 5.3. In four dimensions the Fierz transformation maps $\widetilde{Q}_{S2}$ onto an operator with the same Dirac structure, but $\mathbb{1}$ replaced by $\widetilde{\mathbb{1}}$. Hence if we substituted $\mathbb{1}$ by $\widetilde{\mathbb{1}}$ or by $(\mathbb{1}+\widetilde{\mathbb{1}})/2$ in the definition (5.2), we would redefine $\widetilde{Q}_{S2}$ by an evanescent operator proportional to $(\overline{s}d)_{V-A}(\overline{s}d)_{V-A}(\widetilde{\mathbb{1}}-\mathbb{1})$. If the evanescent operator $E_1[\widetilde{Q}_{S2}]$ is defined as in (4.11), the Fierz symmetry is maintained on the loop level and the replacement $\mathbb{1} \to \widetilde{\mathbb{1}}$ does not change the two–loop anomalous dimension.
The expansion of matrix elements in terms of α has already been defined in (3.51). Analogously we will expand the $\widetilde{G}$'s in (5.1),

$$\widetilde{G}^j \;=\; \widetilde{G}^{j,(0)} + \frac{\alpha}{4\pi}\widetilde{G}^{j,(1)} + O(\alpha^2), \tag{5.3}$$

and the Wilson coefficients:

$$C_k \;=\; C_k^{(0)} + \frac{\alpha}{4\pi}C_k^{(1)} + O(\alpha^2). \tag{5.4}$$

The $\widetilde{G}^{j,(1)}$'s involve infrared (mass) singularities, which will be regularized by small quark masses.
Finally the weak coupling constant g_w will be traded for the Fermi constant G_F according to (3.21).

5.1.2. Zeroth Order Amplitude

In the leading order of $m_{\text{light}}/m_{\text{heavy}}$, where m_{heavy} stands for m_t or M_W and m_{light} denotes any other massive parameter, one can neglect the external momenta in (5.1).
One finds for the mixed top–charm contribution in (5.1):

$$i\widetilde{G}^{ct,(0)} \;=\; \frac{G_F^2}{16\pi^2}M_W^2 S(x_c,x_t)\langle\widetilde{Q}_{S2}\rangle^{(0)}. \tag{5.5}$$

Here the *Inami–Lim function* [14] $S(x_j,x_k)$ is defined as

$$S(x_j,x_k) \;=\; \widetilde{S}(x_j,x_k) - \widetilde{S}(x_j,0) - \widetilde{S}(x_k,0) + \widetilde{S}(0,0), \tag{5.6}$$

[1] This is clearly a misnomer from a group theoretical point of view.

where the result of the box diagram with internal quarks j and k is denoted by $\widetilde{S}(x_j, x_k)$ and the u–quark mass is set to zero. For $j = c, t$ one finds:

$$i\widetilde{G}^j \;=\; \frac{G_F^2}{16\pi^2} M_W^2 S(x_j) \langle \widetilde{Q}_{S2} \rangle^{(0)}, \tag{5.7}$$

with $S(x_j) = S(x_j, x_j)$. Here one realizes that the effect of the GIM mechanism is not only to forbid FCNC's at tree level, but also to cancel the constant terms in the $\widetilde{S}$'s and to nullify $\mathrm{K}^0 - \overline{\mathrm{K}^0}$–mixing in the case of degenerate quark masses.
The reminder of the thesis will deal with RG improved short distance QCD corrections in (5.1), which are parametrized by

$$\begin{array}{lllll} \eta_1 & \text{on the RHS of (5.7)} & \text{for} & \widetilde{G}^c, & \\ \eta_2 & \text{on the RHS of (5.7)} & \text{for} & \widetilde{G}^t & \text{and} \\ \eta_3 & \text{on the RHS of (5.5)} & \text{for} & \widetilde{G}^{ct}. & \end{array}$$

I.e. we want to derive the low energy hamiltonian given in (1.1).
Let us first look at the three contributions (5.5) and (5.7) to (5.1) with emphasis on large logarithms:

$$S(x_t) \;=\; x_t \left[\frac{1}{4} + \frac{9}{4} \frac{1}{1-x_t} - \frac{3}{2} \frac{1}{(1-x_t)^2} \right] - \frac{3}{2} \left[\frac{x_t}{1-x_t} \right]^3 \ln x_t \tag{5.8}$$

clearly involves no large logarithm because of $\ln x_t \approx 1.5$. After multiplying with $\alpha(M_W)/(4\pi)$ this is of the order 10^{-2}.

$$S(x_c) \;=\; x_c + O(x_c^2) \tag{5.9}$$

Here we have only kept terms which are larger than those of order $(m_s m_c)/M_W^2$ neglected by setting the external momenta to zero. As we will see in the following section one would naturally expect a large logarithm $\ln x_c$ multiplying x_c here. Its absence is due to the GIM mechanism.

$$S(x_c, x_t) \;=\; -x_c \ln x_c + x_c \left[\frac{x_t^2 - 8x_t + 4}{4(1-x_t)^2} \ln x_t + \frac{3}{4} \frac{x_t}{x_t - 1} \right] + O(x_c^2 \ln x_c) \tag{5.10}$$

Here we encounter a large logarithm $|\ln x_c| \approx 8$. According to our discussion in sect. 3.7.2 we can sum $\ln x_c (\alpha \ln x_c)^n, n = 0, 1, 2, \ldots$ with the help of factorization and RG techniques. $S(x_t)$ is much larger than $S(x_c)$ and $S(x_c, x_t)$, but it is CKM suppressed in (5.1). Yet this is not so in $|\Delta B|=2$ transitions, where $S(x_t)$ and its radiative corrections comprised in η_2 are clearly dominating.

Figure 5.2: The classes of diagrams constituing the $O(\alpha)$–contribution to $\widetilde{G}$ in (5.1); the remaining diagrams are obtained by left–right and up–down reflections. The curly lines denote gluons. Also QCD counterterm diagrams have to be included. Diagram F_8 equals 0 for zero external momenta.

Figure 5.3: The diagram for the matrix element of $\widetilde{Q}_{S2}$ in the effective three–quark theory to order α^0. The cross denotes the insertion of the effective $\Delta S = 2$ operator.

5.1.3. O(α) Radiative Corrections

Since we are worried about the absence of the logarithm in $S(x_c)$, let us look at the one–loop radiative corrections to $\widetilde{G}^c$ depicted in fig. 5.2.
These diagrams have been calculated for arbitrary internal quark masses in [15]:

$$i\widetilde{G}^{c\,(1)}(\mu) \;=\; \frac{G_F^2}{16\pi^2}\lambda_c^2 m_c^2(\mu)\left\{\langle\widetilde{Q}_{S2}\rangle^{(0)}\widetilde{h}\,(\mu) + \langle T\rangle^{(0)}h_T + \langle U\rangle^{(0)}h_U\right\}. \tag{5.11}$$

In (5.11) new operators have emerged:

$$\begin{aligned}
\hat{T} &= (L\otimes L + R\otimes R - \sigma_{\mu\nu}\otimes\sigma^{\mu\nu})\cdot\frac{N-1}{2N}\mathbb{1},\\
\hat{U} &= \frac{1}{2}(\gamma_\mu L\otimes\gamma^\mu R + \gamma_\mu R\otimes\gamma^\mu L)\cdot\left(\frac{N^2+N-1}{2N}\mathbb{1} - \frac{1}{2N}\widetilde{\mathbb{1}}\right)\\
&\quad -(L\otimes R + R\otimes L)\cdot\left(\frac{N^2+N-1}{2N}\widetilde{\mathbb{1}} - \frac{1}{2N}\mathbb{1}\right),
\end{aligned} \tag{5.12}$$

We have written $\hat{U}$ and $\hat{T}$ in a manifestly Fierz self–conjugate way. The functions in (5.11) are:

$$\begin{aligned}
\widetilde{h}(\mu) &= C_F\left[-1-6\log\frac{m_c^2}{\mu^2} + \xi\left(2 - 2\frac{m_s^2\log(m_s^2/\mu^2) - m_d^2\log(m_d^2/\mu^2)}{m_s^2-m_d^2}\right)\right]\\
&\quad +\frac{N-1}{2N}\left[-11+\frac{4}{3}\pi^2 + 12\log\frac{m_c^2}{M_W^2} + 3\log\frac{m_d^2m_s^2}{\mu^4} - 6\log\frac{m_c^2}{\mu^2}\right.\\
&\quad \left. +\xi\left(2+\log\frac{m_d^2m_s^2}{\mu^4} - 2\frac{m_s^2\log(m_s^2/\mu^2) - m_d^2\log(m_d^2/\mu^2)}{m_s^2-m_d^2}\right)\right]\\
h_T &= (-3-\xi)\\
h_U &= \frac{3+\xi}{2}\frac{m_dm_s}{m_s^2-m_d^2}\log\frac{m_s^2}{m_d^2},
\end{aligned} \tag{5.13}$$

Let us discuss (5.11) in more detail: First (5.11) is obviously unphysical, because it is gauge dependent. This is an artefact of the use of small quark masses to regularize the infrared singularities while at the same time using zero on–shell quarks for the external states. For the same reason we encounter the new operators T and U. When factorizing (5.11) to extract the Wilson coefficients C_k, these unphysical parts will match their counterparts in the effective theory with the zeroth order coefficient $C_k^{(0)}$. Hence they do not contribute to the C_k's. Yet we can anticipate this by noticing that the terms involving T, U and ξ are independent of M_W, which sets the scale for the short distance physics. An alternative method to treat the infrared singularities is to keep the quark masses exactly equal to zero and to rely on dimensional regularization to cope with both IR and UV singularities. This gives a different result, as the limit $m\to 0$ is non–uniform owing to the fact that $m^\varepsilon/\varepsilon$ has a zero mass limit, while the expanded version $1/\varepsilon + \ln m$ diverges in this limit. If we had used such an on–shell IR regularization, the additional operators T and U would be

absent. Since further the wave function renormalization constant Z_ψ equaled zero then, (5.11) would turn out to be gauge independent, too. The use of small quark masses for regularization has the advantage that the vanishing of the otherwise invisible IR terms from the C_k's provides a check of the calculation. Yet one may argue that this method requires a more complicated calculation. In fact this is not so as we will see in chapter 6.
Having in mind the RG evolution down to scales μ_c of order m_c we have arranged the logarithms in $\widetilde{h}$ in (5.13) such that one can easily distinguish those which are small for $\mu \simeq m_c$ from the large logarithm $\log(m_c^2/M_W^2)$. For this we have abstinated from using x_c, but have turned to m_c. We will do this again without warning. Due to the magic of factorization the coefficient of $\ln(m_c^2/M_W^2)$ is a linear combination of the anomalous dimensions of composite operators of some effective field theory.
Let us finally remark on the μ–dependent terms in $\widetilde{h}$: The colour octet term proportional to $(N-1)/(2N)$ is μ-independent. In the colour singlet part proportional to C_F one identifies $\gamma_m^{(0)} = 6C_F$ as the coefficient of $\ln \mu^2$, which stems from the running charm quark mass in (5.7). Likewise $2C_F\xi \ln \mu^2$ originates from the wave function renormalization.

5.2. General Structure of the RG Improvement

After integrating out the heavy top quark and the W–boson one is left with an effective field theory containing a lagrangian of the form (3.28). Now we extract the Fermi constant out of the Wilson coefficients to render them dimensionless:

$$\mathcal{L}_{\text{eff},1}^{|\Delta S|=2} = -\frac{G_F}{\sqrt{2}} V_{CKM,F} C_k Q_k^{(F)} - \frac{G_F^2}{2} V'_{CKM,F} \widetilde{C}_l^{(F)} \widetilde{Q}_l. \tag{5.14}$$

Here $V_{CKM,F}$ and $V'_{CKM,F}$ stand for products of CKM elements and F is a flavour index. The light internal quarks in fig. 5.1 and fig. 5.2 require to match the corresponding parts of G to matrix elements with two insertion of $|\Delta S|=1$ operators Q_k. Fig. 5.4 and fig. 5.5 show such diagrams for the case of two insertions of current–current operators. The $\widetilde{Q}_l$'s in

Figure 5.4: Diagram D_0 in the effective five–quark theory. The cross denotes the insertion of a $\Delta S = 1$ current–current operator.

Figure 5.5: The classes of diagrams giving the $O(\alpha)$ contribution to $\langle \mathcal{O}_{il} \rangle$ and $\langle \mathcal{R}_{ij} \rangle$ for $j = 1, 2$. The other members of a given class are obtained by left–right and up–down reflections. Also QCD counterterms have to be included. Diagram $D_8 = 0$ for zero external momenta.

(5.14) correspond to $|\Delta S|=2$ operators. In general their matrix elements also participate in the matching at the initial scale μ_W. We will be interested in the contribution of the lowest dimension operators: The Q_k's in (5.14) have dimension six and the $\widetilde{Q}_l$'s are dimension–eight operators. The remaining sections of this chapter will concern the correct reduced operator basis needed in (5.14).

Figure 5.6: The classes of diagrams in the effective three–quark theory contributing to $\langle \widetilde{Q}_{S2} \rangle$ to order α. The other members of a given class are obtained by left–right and up–down reflections. QCD counterterms have to be included.

Next one has to carry out the program of sect. 3.10, 3.7 and 3.8 consisting of the following steps:

i) Find a reduced operator basis for (5.14), from which renormalized operators of the types described in sect. 3.10 and properly renormalized evanescent operators have been removed.

ii) Match the Standard Model Green's function $\widetilde{G}$ in (5.1) to the matrix elements derived from (5.14) as shown in sect. 3.7. This is to be done at a scale μ_W satisfying $M_W \lesssim \mu_W \lesssim m_t$, but being arbitrary within this range.

iii) Follow sect. 3.8 to perform the RG evolution down to $\mu_c \approx m_c$ thereby summing $\ln(\mu_c/\mu_W)$ to all orders. When passing the b–quark threshold remove this degree of freedom from the calculation. This simply modifies the running coupling and trivially changes the penguin operators to be introduced in sect. 5.3.2. Strictly speaking one matches (5.14) to another lagrangian with the b–quark integrated out, but the structure of both lagrangians is essentially that of (5.14).

Hence $\mathcal{L}_{\rm eff,1}^{|\Delta S|=2}$ in (5.14) describes the physics between the scales μ_c and μ_W. At the scale μ_c one has to match the matrix elements derived from (5.14) to those of a new effective lagrangian $\mathcal{L}_{\rm eff,2}^{|\Delta S|=2}$ with the c–quark integrated out and to repeat steps i) to iii). This amounts to the matching of diagrams of the type of fig. 5.4, fig. 5.5 to those with a single local four–quark operator as depicted in fig. 5.3 and fig. 5.6. In fact the reduced $\mathcal{L}_{\rm eff,2}^{|\Delta S|=2}$ contains only a single physical dimension–six operator, which we have already met in (5.2):

$$\mathcal{L}_{\rm eff,2}^{|\Delta S|=2} \;=\; -\frac{G_F^2}{16\pi^2}\left(\widetilde{C}_{S2}^{(c)}\lambda_c^2 + \widetilde{C}_{S2}^{(t)}\lambda_t^2 + \widetilde{C}_{S2}^{(ct)}\lambda_c\lambda_t\right)\widetilde{Q}_{S2} \tag{5.15}$$

In the matching we equate dimension–eight Green's functions derived from $\mathcal{L}_{\rm eff,1}^{|\Delta S|=2}$ with dimension–six Green's functions from $\mathcal{L}_{\rm eff,2}^{|\Delta S|=2}$. Hence by power counting the $\widetilde{C}_{S2}^{(j)}$'s in (5.15) pick up two powers of $m_c(\mu_c)$. The subsequent RG improvement of the $\widetilde{C}_{S2}^{(j)}$'s from μ_c down to some scale μ will sum $\ln \mu_c/\mu$. The final scale μ must be large enough to trust into perturbation theory, this is roughly of the order of 1 GeV. The matrix element of $\widetilde{Q}_{S2}(\mu)$ must be evaluated between neutral K–meson states. The calculation of such QCD binding effects can be done in the framework of lattice gauge theory, $1/N$–expansion or with sum–rule techniques.
The observation that we need two powers of m_c in the matching greatly simplifies the finding of the correct set of dimension–eight operators $\widetilde{Q}_l$ needed in $\mathcal{L}_{\rm eff,1}^{|\Delta S|=2}$. The only

candidate is

$$\widetilde{Q}_7 \;=\; \frac{m_c^2}{g^2\overline{\mu}^{2\varepsilon}}\overline{s}\gamma_\mu Ld\cdot\overline{s}\gamma^\mu Ld, \tag{5.16}$$

which we already know from an example in sect. 3.8.2. To understand this recall that any other dimension–eight operator lacks the factor of m_c^2 and involves derivatives and/or gluon fields instead[2]. The matrix elements between s–quarks and d–quarks evaluated for the matching at μ_c cannot produce a factor of m_c^2: The c–quark can only enter matrix elements with single insertions of such operators through loops in gluon propagators, but the result is always proportional to $k^2g^{\mu\nu}-k^\mu k^\nu$ rather than m_c^2, where k^μ is the momentum flowing through the propagator. Hence the QCD gauge structure keeping the gluon massless provides us with unexpected help here. For the same reason other dimension–eight operators cannot mix into $\widetilde{Q}_7$ during the RG evolution from μ_W to μ_c. In principle operators with $\overline{\mu}^{-2\varepsilon}m_c^2/g^2$ multiplying other Dirac structures can also appear, but we will see that this is not the case due to the flavour structure of the problem. Let us drop some words on the factor $\overline{\mu}^{-2\varepsilon}$ in (5.16): Bare quantities must not depend on μ. Therefore the bare operator reads

$$\widetilde{Q}_7^{\text{bare}} \;=\; \frac{m_{c,\,\text{bare}}^2}{g_{\text{bare}}^2}\left[\overline{s}\gamma_\mu Ld\cdot\overline{s}\gamma^\mu Ld\right]^{\text{bare}}.$$

With (2.34) and (3.2) one is therefore lead to (5.16). It is also clear from fig. 5.4 that the dimension of $\widetilde{Q}_7$ is larger than the dimension of the Q_k's by $2-2\varepsilon$, because the loop integration gives a power of $D-2$. We have refrained from defining powers of $\mu^{2\varepsilon}$ into the C_k's, because this would lead to an unnecessary complication in the RG equations (3.44). The origin of these simplifications of $\mathcal{L}_{\text{eff},1}^{|\Delta S|=2}$ in (5.14) is the fact that the internal c–quark is heavier than the external s–quarks and d–quarks. The situation is therefore *completely different* for the case of the c–quark contributions to $|\Delta B|=2$ transitions or the effect of internal s–quarks in $|\Delta C|=2$ amplitudes. Here the external quarks are heavier and the dimension–eight operators containing derivatives dominate over the effect of $\overline{\mu}^{-2\varepsilon}m_c^2/g^2\cdot\gamma_\mu L\otimes\gamma^\mu L$ in $|\Delta B|=2$ amplitudes resp. $\overline{\mu}^{-2\varepsilon}m_s^2/g^2\cdot\gamma_\mu L\otimes\gamma^\mu L$ in $|\Delta C|=2$ amplitudes. Fortunately the former are phenomenologically uninteresting, as they are suppressed with m_b^2/m_t^2, and in the case of $|\Delta C|=2$ transitions there are other badly controllable long–distance effects in the game which most likely make short distance calculations of $D^0-\overline{D^0}$–mixing useless.

5.3. $|\Delta S|=1$ –Operator Basis

Let us now find a basis for the $|\Delta S|=1$ operators Q_k in (5.14), which closes under renormalization.

[2]Operators containing only one power of m_c can be removed by the use of the EOM for the fermion field according to the procedure described in sect. 3.10 giving $m_sm_c/g^2\cdot\gamma_\mu L\otimes\gamma^\mu L$.

5.3.1. Current–Current Operators

Consider first the matching procedure for the LO diagram fig. 5.1 with only light quarks in the intermediate state. Contracting the W boson lines yields the diagram of fig. 5.4 with two insertions of the current–current operator of fig. 5.7:

$$Q_2^{kl} \;=\; \overline{s}\gamma_\mu Lk \cdot \overline{l}\gamma_\mu Ld \cdot \mathbb{1}, \tag{5.17}$$

where k and l are u or c.

Figure 5.7: |ΔS|=1 current–current operator

For $k \neq l$ Q_2^{kl} only mixes with

$$Q_1^{kl} \;=\; \overline{s}\gamma_\mu Lk \cdot \overline{l}\gamma_\mu Ld \cdot \widetilde{\mathbb{1}}. \tag{5.18}$$

The corresponding diagrams are shown in fig. 4.1 on p. 43. The 2×2 mixing matrix in LO and NLO has been derived in [15]. If the corresponding evanescents are defined as in (4.11), the NLO anomalous dimension matrix commutes with the LO one. These matrices are diagonal in the basis containing the operators Q_+^{kl} and Q_-^{kl} defined by

$$Q_\pm^{kl} \;=\; \frac{1}{2}\left(Q_2^{kl} \pm Q_1^{kl}\right).$$

Their anomalous dimensions in the NDR scheme with (4.11) are

$$\gamma_\pm^{(0)} \;=\; \pm 6\frac{N \mp 1}{N}, \quad \gamma_\pm^{(1)(f)} \;=\; \frac{N \mp 1}{2N}\left(-21 \pm \frac{57}{N} \mp \frac{19}{3}N \pm \frac{4}{3}f\right). \tag{5.19}$$

5.3.2. Penguin Operators

We will focus first on the LO operator mixing. For $k = l$ the current–current operators mix with penguin operators. The simplest divergent one–particle irreducible penguin diagrams, into which $Q_{1/2}^{kk}$ can be inserted, are depicted in fig. 5.8. These diagrams require the gluon–

Figure 5.8: The mixing of a |ΔS|=1 current–current operator into gluon–foot penguin operators. Diagrams with crossed gluons compared to G_2 and G_3 must be included, too.

foot penguin operators Q_{g1}, Q_{g2} and Q_{g3} of fig. 5.9 as counterterms. We will encounter the

Figure 5.9: The gluon–foot penguin operators

basic penguin diagram G_1 later as a subdiagram, so that we comment on it here: Although

it is a dimension–two diagram, its result contains no term proportional to the square of the internal mass. One has instead

$$G_1 \quad \propto \quad \overline{s}\gamma_\mu LT^a d \cdot \left(p^\mu p^\nu - p^2 g^{\mu\nu}\right), \tag{5.20}$$

where ν and a are the open Lorentz and colour indices of the gluon line and p is the momentum flowing into the gluon vertex. (5.20) holds to all orders in $D-4$. Especially the inserted operators $Q^{kk}_{1/2}$ do not mix into an operator of the form $m^2\overline{s}\not{A}^a LT^a d$. Likewise the dimension–one diagram G_2 does not give a positive power of the internal mass.
In order to find a closed operator basis one now has to investigate into which operators G_1, G_2 and G_3 mix. One readily finds that e.g. G_1 mixes via box diagrams into new four–fermion operators. A box diagram with two fermion lines containing one Q_{g1} vertex and three QCD gluon–fermion vertices is divergent, because Q_{g1} involves two powers of the loop momentum due to (5.20). These new operators are fermion–foot penguin operators:

$$\begin{aligned}
Q_3 &= \overline{s}\gamma_\mu Ld \cdot \sum_{q=d,u,s,c,b} \overline{q}\gamma^\mu Lq \cdot \mathbb{1} \\
Q_4 &= \overline{s}\gamma_\mu Ld \cdot \sum_{q=d,u,s,c,b} \overline{q}\gamma^\mu Lq \cdot \widetilde{\mathbb{1}} \\
Q_5 &= \overline{s}\gamma_\mu Ld \cdot \sum_{q=d,u,s,c,b} \overline{q}\gamma^\mu Rq \cdot \mathbb{1} \\
Q_6 &= \overline{s}\gamma_\mu Ld \cdot \sum_{q=d,u,s,c,b} \overline{q}\gamma^\mu Rq \cdot \widetilde{\mathbb{1}}
\end{aligned} \tag{5.21}$$

We will be more interested in the mixing of $Q_{1/2}$ into them, which is shown in fig. 5.10. At this point we realize that our simple minded approach to the operator mixing leads

Figure 5.10: The mixing of a $|\Delta S|=1$ current–current operator into fermion–foot penguin operators depicted on the right.

to problems, as we could renormalize the divergence in fig. 5.10 either by a counterterm proportional to Q_{g1} or by one involving fermion foot operators. Further we obtain mixing into a third type of operator as depicted in fig. 5.11:

$$Q_{\rm FP} \quad = \quad \overline{s}\gamma_\mu LT^a d \cdot (\partial^\mu \overline{\eta}_b)\, \eta_c f_{abc}. \tag{5.22}$$

Figure 5.11: The mixing of a $|\Delta S|=1$ current–current operator into ghost–foot penguin operators depicted on the right.

Fortunately we can put order into the penguin zoo with the theorems of sect. 3.10. For this we first construct the dimension–six operators (with total ghost number zero) from class $\mathcal{B}$: The only possibility is given by $Q_{\rm BRS}$ from (3.58). It is related to $Q_{\rm FP}$ via

$$Q_{\rm BRS} \quad = \quad Q_{\rm FP} + Q_{\rm gf},$$

where $Q_{\rm gf}$ is the term on the LHS of (3.57) stemming from the gauge fixing part of the QCD lagrangian:

$$Q_{\rm gf} \;=\; \frac{1}{g}\frac{1}{\xi}\,\overline{s}\gamma_\mu L T^a d\cdot\partial^\mu\partial_\nu A^\nu_a. \tag{5.23}$$

Next we arrange the operators found so far into combinations belonging to class $\mathcal{E}$. Here only the EOM for the gluon field can give dimension–six operators related to the penguin zoo. The relevant operator has been introduced in (3.57). In terms of the operators defined in (5.21), (5.22) and (5.23) it reads:

$$Q_{\rm EOM} \;=\; \frac{1}{g}\cdot\overline{s}\gamma_\mu L T^a d\cdot D_{\nu\,a}F^{\mu\nu\,a} - \frac{1}{4}\left(Q_4+Q_6\right)+\frac{1}{4N}\left(Q_3+Q_5\right)-Q_{\rm gf}+Q_{\rm FP} \tag{5.24}$$

Now all other operators involved in the mixing must combine to gauge invariant operators, because they belong to class $\mathcal{P}$. We have already listed $Q_1^{kl},\dots Q_6$, the only other gauge invariant dimension–six operator is

$$\frac{1}{g}\cdot\overline{s}\gamma_\mu L T^a d\cdot D_{\nu\,a}F^{\mu\nu\,a} \;=\; Q_{g1}+Q_{g3}+Q_{g3}, \tag{5.25}$$

which we can drop from the basis, because it is a linear combination of $Q_{\rm EOM}$, $Q_{\rm BRS}$ and the other physical operators.
Hence the unreduced $|\Delta S|=1$ operator basis consists of $Q_1^{kl},\dots Q_6$, $Q_{\rm EOM}$, $Q_{\rm BRS}$ and of course of evanescent operators. This structure implies that the mixing of any operator into Q_{g1}, Q_{g2} and Q_{g3} must be the same. Indeed, the divergent parts of G_1, G_2 and G_3 all involve the same coefficient, as required by (5.25). The theorems of sect. 3.10 also explain the observation of (5.20), because there is no dimension–six operator in $\mathcal{P}\oplus\mathcal{E}\oplus\mathcal{B}$ involving $m^2\overline{\psi}\not{A}\psi$.
Due to sect. 3.10.2 and chapter 4 the reduced lagrangian for $|\Delta S|=1$ transitions is simply obtained by dropping the renormalized $Q_{\rm EOM}$, $Q_{\rm BRS}$ and the renormalized evanescents from the effective lagrangian.
The on–shell vanishing of $\langle Q_{\rm EOM}\rangle$ can be easily understood in terms of diagrams [54]. The Feynman rule for the one–gluon piece of $Q_{\rm EOM}$ depicted in Q_{g1} of fig. 5.9 involves an inverse gluon propagator:

$$\frac{1}{g}T^a\gamma_\mu L\left[p^2 g^{\mu\nu}-\frac{\xi-1}{\xi}p^\mu p^\nu\right]. \tag{5.26}$$

Hence in any diagram in which the gluon line of G_1 ends up in an internal vertex the gluon line is effectively shrunk to a point, because (5.26) is contracted with a gluon propagator. The resulting diagram is identical with a diagram containing one of the other operators in (5.24) and these contributions cancel. If the gluon of G_1 is an external line, the diagram vanishes after LSZ reduction. Care is necessary, however, if renormalization constants are calculated off–shell, because then $Q_{\rm EOM}$ and $Q_{\rm BRS}$ give non–zero contributions, which must

be properly taken into account. For example in fig. 5.10 one finds off–shell terms involving $\overline{s}\gamma_\mu Ld\cdot(p^\mu p^\nu/p^2)/\varepsilon$ which require a counterterm proportional to $Q_{\rm BRS}$.
Now for the case of the $|\Delta S|=1$ substructure of $|\Delta S|=2$ diagrams the situation is more complicated, because here the gluon of G_1 can end up in another Q_{g1}–vertex. Then we have one propagator hitting two inverse propagators and the result is non–vanishing. But from sect. 3.10.3 we know that this contact term is identical to the matrix element of a local dimension–eight $|\Delta S|=2$ operator $\widetilde{Q}_l$. Hence we can still restrict the renormalized Q_k's in (5.14) to the set $\{Q_1^{kl},\dots Q_6\}$.

5.4. Operator Basis for $|\Delta S|=2$ transitions

Let us now assign the correct CKM factors to the effective lagrangians $\mathcal{L}_{\rm eff,1}^{|\Delta S|=2}$ in (5.14) and $\mathcal{L}_{\rm eff,2}^{|\Delta S|=2}$ in (5.15).

5.4.1. Above μ_c

The reduced $|\Delta S|=1$ lagrangian can be taken from [44]:

$$\mathcal{L}^{|\Delta S|=1} \;=\; -\frac{G_F}{\sqrt{2}}\left[\sum_{i=1}^{2}\sum_{k,l=u,c} V_{ks}^* V_{ld} C_i Q_i^{kl} - \lambda_t \sum_{j=3}^{6} C_j Q_j\right]. \tag{5.27}$$

Here the coefficient λ_t originates from the fact that the matching of the penguin operators and the mixing of any four–quark operator into penguin operators involves the diagram of fig. 5.10 and radiative corrections to it all being proportional to $\lambda_u+\lambda_c=-\lambda_t$.
With the findings of sect. 5.2 the effective lagrangian $\mathcal{L}_{\rm eff,1}^{|\Delta S|=2}$ of (5.14) is found as

$$\begin{aligned}\mathcal{L}_{\rm eff,1}^{|\Delta S|=2} &= \mathcal{L}^{|\Delta S|=1} - \frac{G_F^2}{2}\frac{m_c^2}{g^2}\widetilde{C}_7\widetilde{Q}_7 \\ &= -\frac{G_F}{\sqrt{2}}\left[\sum_{i=1}^{2}\sum_{k,l=u,c} V_{ks}^* V_{ld} C_i Q_i^{kl} - \lambda_t \sum_{j=3}^{6} C_j Q_j\right] - \frac{G_F^2}{2}\frac{m_c^2}{g^2}\widetilde{C}_7\widetilde{Q}_7.\end{aligned}$$

We may ask where the contact terms from the reduction of the $|\Delta S|=2$ lagrangian have gone. Since diagrams with two insertions in which the two $|\Delta S|=1$ vertices are connected by a gluon line or by a ghost–loop cannot produce a factor of m_c^2, these terms are absorbed into other dimension–eight operators not containing m_c^2, which have been found to be irrelevant in sect. 5.2.
Since there are no more derivative couplings involved, we can pass to the more common hamiltonian formalism by simply flipping the sign: $H=-\mathcal{L}_{\rm eff,1}^{|\Delta S|=2}$. We will do further and define the $|\Delta S|=2$ hamiltonian such that it only contains terms of order G_F^2. For this we equate the first order term of the Gell-Mann–Low series $\exp[-i\int d^Dx H_1^{|\Delta S|=2}(x)]$ with the corresponding series involving $\mathcal{L}_{\rm eff,1}^{|\Delta S|=2}$:

$$\langle -i\int d^Dx H_1^{|\Delta S|=2}(x)\rangle|_{|\Delta S|=2} \;=\; \langle e^{i\int d^Dx \mathcal{L}_{\rm eff,1}^{|\Delta S|=2}(x)}\rangle|_{|\Delta S|=2} + O(G_F^3)$$

$$= \langle \frac{-1}{2} \iint d^D x d^D y \, \mathbf{T} \, \mathcal{L}^{|\Delta S|=1}(x) \mathcal{L}^{|\Delta S|=1}(y) - i \frac{m_c^2}{g^2} \int d^D x \widetilde{C}_7 \widetilde{Q}_7(x) \rangle |_{|\Delta S|=2} + O(G_F^3).$$

This notation is a bit sloppy, but useful. Let us write

$$H_1^{|\Delta S|=2} = H^c + H^t + H^{ct}.$$

One then obtains

$$\begin{aligned} H^c(x) &= \lambda_c^2 \frac{G_F^2}{2} \sum_{i,j=+,-} C_i C_j \mathcal{O}_{ij}(x) \\ H^t(x) &= \lambda_t^2 \frac{G_F^2}{16\pi^2} \widetilde{C}_{S2}^{(t)} \widetilde{Q}_{S2}(x) \\ H^{ct}(x) &= \lambda_c \lambda_t \frac{G_F^2}{2} \sum_{i=+,-} \sum_{j=1}^{6} C_i C_j \mathcal{R}_{ij}(x) + \lambda_c \lambda_t \frac{G_F^2}{2} \widetilde{C}_7 \widetilde{Q}_7(x) \end{aligned} \tag{5.28}$$

with

$$\begin{aligned} \mathcal{O}_{ij}(x) &= \frac{-i}{2} \int d^4 y \, \mathbf{T} \, \Big[Q_i^{cc}(x) Q_j^{cc}(y) + Q_i^{uu}(x) Q_j^{uu}(y) - Q_i^{cc}(x) Q_j^{uu}(y) \\ &\qquad - Q_i^{uu}(x) Q_j^{cc}(y) - Q_i^{uc}(x) Q_j^{cu}(y) - Q_i^{cu}(x) Q_j^{uc}(y) \Big] \, , \end{aligned}$$

$$\mathcal{R}_{ij}(x) = \begin{cases} \frac{-i}{2} \int d^4 y \, \mathbf{T} \, \Big[-Q_i^{uc}(x) Q_j^{cu}(y) - Q_i^{cu}(x) Q_j^{uc}(y) - Q_i^{uu}(x) Q_j^{cc}(y) \\ \qquad\qquad - Q_i^{cc}(x) Q_j^{uu}(y) + 2 Q_i^{uu}(x) Q_j^{uu}(y) \Big] \end{cases} \text{for j=1,2,} \\ \begin{cases} \frac{i}{2} \int d^4 y \, \mathbf{T} \, \left[\left(Q_i^{cc}(x) - Q_i^{uu}(x) \right) Q_j(y) \right. \\ \qquad\qquad \left. + Q_j(x) \left(Q_i^{cc}(y) - Q_i^{uu}(y) \right) \right] \end{cases} \text{for j=3,...6.} \tag{5.29}$$

The structure of (5.28) requires some explanation:

The top–top contribution $\mathbf{H^t}$

First there is only a $|\Delta S|=2$ operator involved in H^t. We have only listed the terms relevant for the leading term in the expansion in $1/m_{\text{heavy}}$. In the case of H^t this contribution comes from the internal top–quarks in fig. 5.1, which are matched at μ_W to the local operator $\widetilde{Q}_{S2}$. From (5.7) and (5.8) we know that $\widetilde{C}_{S2}^{(t)}$ is proportional to x_t, while the double penguin contributions can at most give a factor of x_b. Also the dimension–eight operators stemming from the contact terms in (3.62) and (3.63) can only give contributions proportional to m_{light}^2/M_W^2, because there is no more top–quark in the effective theory. The calculation of η_2 therefore only requires the consideration of matrix elements with a single $|\Delta S|=2$ operator. Yet the NLO matching has to be done from the finite parts of the two–loop diagrams in fig. 5.2. This calculation has been carried out by Buras, Jamin and Weisz [15].

The charm–charm contribution $\mathbf{H^c}$

Second there is no local $|\Delta S|=2$ operator involved in H^c. This feature is related to the absence of a large logarithm in (5.9). The GIM combination in $\mathcal{O}_{ij}$ in (5.29) leads to the cancellation of the divergences and thereby of the $\ln(\mu/M_W)$'s in the diagrams (5.4). The same holds true for the diagrams of (5.5) after the inclusion of counterterms for the $|\Delta S|=1$ operators and in fact to all orders in perturbation theory. This has been first observed by Witten [39]. Hence H^c belongs to case II of sect. 3.7.2. Yet we may conclude from sect. 3.7.2 only that there is no mixing into a local operator, but there could be a local operator involved in the matching at μ_W, which could evolve down to μ_c unaffected by the presence of the bilocal structures $\mathcal{O}_{ij}$. But in the case at hand the matching at μ_W can be made by the replacement $1/(M_W^2-k^2)\to 1/M_W^2$ in the diagrams of fig. 5.1 and fig. 5.2. This is allowed, if the renormalized Standard Model diagram does not become UV–divergent by shrinking the W line to obtain the effective diagrams of fig. 5.4 and fig. 5.5, because then the contribution of the UV momenta is suppressed. In H^c the GIM mechanism cancels the UV divergences in the effective theory, so that there is no room for a non–zero coefficient of $\widetilde{Q}_7$. This fact becomes very clear if one splits the loop integral connecting the two $|\Delta S|=1$ vertices into a part with momenta smaller than m_c and an UV part comprising loop momenta above m_c. For the first part we can use the factorization of the $|\Delta S|=1$ substructure yielding (5.29) up to terms of order m_c^2/M_W^2, and the UV momenta cannot give non–negative powers of M_W^2 to spoil this factorization, because the integral from m_c to ∞ vanishes in the limit $M_W\to\infty$ after forming the GIM combination $(c,c)-(c,u)-(u,c)+(u,u)$. Hence we only need to know the $|\Delta S|=1$ coefficients C_+ and C_-, which have been determined in [43]. No extra $|\Delta S|=2$ matching in necessary. From sect. 3.7.2, however, we know that we need the finite parts of the diagrams of fig. 5.5 for the NLO matching at the scale μ_c, so that we can check the absence of a local operator in H^c in (5.29) by comparing the matrix element of $H^c(\mu_W)$ in (5.28) with (5.7) and (5.11):

$$i\widetilde{G}^c(\mu_W)+O(x_c^2) \;=\; \langle H^c(\mu_W)\rangle \;=\; \lambda_c^2\frac{G_F^2}{2}C_i(\mu_W)C_j(\mu_W)\langle\mathcal{O}_{ij}(\mu_W)\rangle. \qquad (5.30)$$

On the other hand the operator mixing is simple and does not require new calculations. We have put the current–current operators in $\mathcal{O}_{ij}$ into the diagonal basis to simplify the RG evolution. The $|\Delta S|=1$ Wilson coefficients C_+ and C_- in (5.30) simply evolve down to $\mu=\mu_c$ according to [44].

The charm–top contribution $\mathbf{H^{ct}}$

H^{ct} involves the familiar large logarithm in (5.10), so that it belongs to case I of sect. 3.7.2. Hence both the LO and the NLO matching can be done from the one–loop graphs fig. 5.1 and fig. 5.4. Again we have chosen the diagonal basis in $\mathcal{R}_{ij}$ for the current–current vertex. For the other vertex we have chosen the operator basis $Q_1^{kl},\dots Q_6$ to use the results of [44]. Now the LO matching at $\mu=\mu_W$ is performed from the large logarithm $\ln x_c$ in $G^{c,(0)}$. In NLO we also equate the nonlogarithmic part of $G^{c,(0)}$ to the diagrams of the effective field

theory to obtain the initial value $\widetilde{C}_7(\mu_W)$. Since the initial value of the $|\Delta S|=1$ coefficients C_k are of order α for $k=1,3,4,5,6$ and $C_k = 1+O(\alpha)$ for $k=2,+,-$, the matching at the scale $\mu=\mu_W$ reads

$$\begin{aligned} iG^{ct\,(0)}(\mu_W) + O(x_c^2 \ln x_c) &= \langle H^{ct}(\mu_w)\rangle^{(0)} \\ &= \frac{G_F^2}{2}\lambda_c\lambda_t \left[\langle \mathcal{R}_{2,+}\rangle^{(0)} + \langle \mathcal{R}_{2,-}\rangle^{(0)} + \frac{\alpha(\mu_W)}{4\pi}\widetilde{C}_7^{(1)}(\mu_W)\langle \widetilde{Q}_7(\mu_W)\rangle^{(0)}\right]. \end{aligned} \tag{5.31}$$

Here we have accounted for the fact that $\widetilde{C}_7$ starts in order α due to the inverse power in the definition in $\widetilde{Q}_7$ giving $\langle \widetilde{Q}_7(\mu)\rangle^{(0)} = m_c^2(\mu)/(4\pi\alpha(\mu))\cdot\langle \widetilde{Q}_{S2}(\mu)\rangle^{(0)}$. Hence in LO there is nothing to adjust in (5.31) and the coefficients of the large logarithms must be the same on both sides. This is indeed the case. Further for the NLO matching only the diagrams in fig. 5.1 and the current–current diagrams of fig. 5.4 are needed. For later convenience we split H^{ct} up:

$$\begin{aligned} H^{ct}(\mu) &= H^{ct,+}(\mu) + H^{ct,-}(\mu) \\ H^{ct,\pm}(\mu) &= \frac{G_F^2}{2}\lambda_c\lambda_t\left[C_k(\mu)C_\pm(\mu)\mathcal{R}_{k,\pm}(\mu) + \widetilde{C}_7^\pm(\mu)\widetilde{Q}_7(\mu)\right] \end{aligned}$$

$H^{ct,+}$ and $H^{ct,-}$ evolve independently under the RG flow. Also $\widetilde{C}_7(\mu)$ is split into $\widetilde{C}_7^+(\mu) + \widetilde{C}_7^-(\mu)$, both of which receive different admixtures during the RG evolution. It is arbitrary which part of $\widetilde{C}_7(\mu_W)$ is put into $\widetilde{C}_7^\pm(\mu_W)$, as long as their sum fulfils the matching condition (5.31). We will choose $\widetilde{C}_7^{\pm,(1)}(\mu_W) = 1/2\cdot\widetilde{C}_7^{(1)}(\mu_W)$

The RG evolution is much more involved than in the case of H^c. With the well–known initial values of the $|\Delta S|=1$ coefficients [43,44] and with $\widetilde{C}_7(\mu_W)$ obtained from (5.31) one knows

$$\vec{C}^{(+)}(\mu_W) = \begin{pmatrix} C_+(\mu_W)C_1(\mu_W) \\ C_+(\mu_W)C_2(\mu_W) \\ C_+(\mu_W)C_3(\mu_W) \\ C_+(\mu_W)C_4(\mu_W) \\ C_+(\mu_W)C_5(\mu_W) \\ C_+(\mu_W)C_6(\mu_W) \\ \widetilde{C}_7^+(\mu_W) \end{pmatrix}, \qquad \vec{C}^{(-)}(\mu_W) = \begin{pmatrix} C_-(\mu_W)C_1(\mu_W) \\ C_-(\mu_W)C_2(\mu_W) \\ C_-(\mu_W)C_3(\mu_W) \\ C_-(\mu_W)C_4(\mu_W) \\ C_-(\mu_W)C_5(\mu_W) \\ C_-(\mu_W)C_6(\mu_W) \\ \widetilde{C}_7^-(\mu_W) \end{pmatrix} \tag{5.32}$$

to order α. These are the initial conditions for the NLO RG evolution. We will give the relevant expressions for $C_k(\mu_W)$ and $\widetilde{C}_7^\pm(\mu_W)$ in chapter 6, where the actual calculation is described.

In NLO all coefficients in H^{ct} have a non–zero initial value. The structure of the RG evolution has been described in sect. 3.8.2. In (3.46) the summation indices m, m', v and v' assume the values $+$ and $-$ and t, t', n and n' run from 1 to 6. The two terms of the summation over n correspond to $H^{ct,+}$ and $H^{ct,-}$ and the two coefficient vectors in (5.32).

The first term in (3.46) involving the initial value $\widetilde{C}_7(\mu_W)$ can obviously be arbitrarily distributed over $H^{ct,+}$ and $H^{ct,-}$.
The structure of the RG evolution is probably more transparent from (3.44): The anomalous dimension tensor $\gamma_{kn,l}$ describing the mixing of $|\Delta S|=1$ coefficients into the $|\Delta S|=2$ coefficient $\widetilde{C}_7$ contains 12 elements $\gamma_{n+,7}, \gamma_{n-,7}$, $n = 1, \ldots 6$, which we summarize into the row vectors

$$\begin{aligned} \gamma^T_{+,7} &= (\gamma_{1+,7}\ ,\ \gamma_{2+,7}\ ,\ \gamma_{3+,7}\ ,\ \gamma_{4+,7}\ ,\ \gamma_{5+,7}\ ,\ \gamma_{6+,7}) \\ \gamma^T_{-,7} &= (\gamma_{1-,7}\ ,\ \gamma_{2-,7}\ ,\ \gamma_{3-,7}\ ,\ \gamma_{4-,7}\ ,\ \gamma_{5-,7}\ ,\ \gamma_{6-,7}) \end{aligned} \tag{5.33}$$

Now (3.44) reads in the case at hand:

$$\mu\frac{d}{d\mu}\widetilde{C}_7 = \widetilde{\gamma}\widetilde{C}_7 + \gamma_{k+,7}\, C_k\, C_+ \ + \ \gamma_{k-,7}\, C_k\, C_- \tag{5.34}$$

which is split into

$$\begin{aligned} \mu\frac{d}{d\mu}\widetilde{C}^+_7 &= \widetilde{\gamma}\widetilde{C}^+_7 + \gamma_{k+,7}\, C_k\, C_+ \\ \mu\frac{d}{d\mu}\widetilde{C}^-_7 &= \widetilde{\gamma}\widetilde{C}^-_7 + \gamma_{k-,7}\, C_k\, C_-. \end{aligned}$$

Here $\widetilde{\gamma}$ is the anomalous dimension of $\widetilde{Q}_7$. This yields the RG equation for $\vec{C}^{(\pm)}$ defined in

$$\mu\frac{d}{d\mu}\vec{C}^{(\pm)}(\mu) = \begin{pmatrix} \gamma + \gamma_\pm \mathbf{1} & 0 \\ \gamma^T_{\pm,7} & \widetilde{\gamma} \end{pmatrix} \vec{C}^{(\pm)}(\mu), \tag{5.35}$$

where γ is the 6×6 $|\Delta S|=1$ anomalous dimension matrix and γ_+ and γ_- are the anomalous dimensions of Q_+ and Q_-. (5.35) leads to a block–triangular evolution matrix of the form (3.48) and one again recognizes that $\widetilde{C}_7(\mu) = \widetilde{C}^+_7(\mu) + \widetilde{C}^-_7(\mu)$ does not depend on how the initial value $\widetilde{C}_7(\mu_W)$ is distributed over $\widetilde{C}^+_7(\mu_W)$ and $\widetilde{C}^-_7(\mu_W)$.
The solution of (5.35) involves two 7×7 evolution matrices. They, however, encode redundant information, because each of them contains the full 6×6 $|\Delta S|=1$ evolution matrix. Now one can do better: Define the vector

$$\vec{D} = \begin{pmatrix} \vec{C} \\ \widetilde{C}^+_7/C_+ \\ \widetilde{C}^-_7/C_- \end{pmatrix}, \tag{5.36}$$

where $\vec{C} = (C_1, \ldots C_6)$ is the $|\Delta S|=1$ coefficient vector. From (5.34) one finds the RG equation for the seventh and eighth component of $\vec{D}$:

$$\begin{aligned} \mu\frac{d}{d\mu}D_7 &= (\widetilde{\gamma} - \gamma_+)D_7 + \gamma^T_{+,7}\cdot\vec{C}, \\ \mu\frac{d}{d\mu}D_8 &= (\widetilde{\gamma} - \gamma_-)D_8 + \gamma^T_{-,7}\cdot\vec{C}. \end{aligned} \tag{5.37}$$

Hence $\vec{D}$ satisfies the following RG equation:

$$\mu\frac{d}{d\mu}\vec{D} \;=\; \begin{pmatrix} \gamma & 0 & 0 \\ \gamma^T_{+,7} & \widetilde{\gamma}-\gamma_+ & 0 \\ \gamma^T_{-,7} & 0 & \widetilde{\gamma}-\gamma_- \end{pmatrix}\vec{D}. \tag{5.38}$$

After obtaining the 8×8 RG evolution matrix in the standard way one gets $\vec{D}(\mu)$ which has to be multiplied with $C_\pm(\mu)$ to obtain $\vec{C}^{(\pm)}(\mu)$ and

$$\begin{aligned} H^{ct,\pm}(\mu) \;&=\; \frac{G_F^2}{2}\lambda_c\lambda_t\sum_{n=+,-}\Big(\,\mathcal{R}_{1,n}(\mu),\ldots,\mathcal{R}_{6,n}(\mu),\widetilde{Q}_7(\mu)\,\Big)\cdot\vec{C}^{(n)}(\mu) \\ &= \frac{G_F^2}{2}\lambda_c\lambda_t\Big(C_+(\mu)\mathcal{R}_{1,+}(\mu)+C_-(\mu)\mathcal{R}_{1,-}(\mu),\ldots,C_+(\mu)\widetilde{Q}_7(\mu),C_-(\mu)\widetilde{Q}_7(\mu)\Big)\cdot\vec{D}(\mu) \end{aligned} \tag{5.39}$$

Hence we have switched from a $7\times 7'$ representation to an $8\times 1\times 1'$ representation of the renormalization group. We have programmed both the solution of (5.35) and (5.38) and checked that we obtain the same result. Of course, the program for (5.38) is much faster. Further the upper left 6×6 block–submatrix of the 8×8 evolution matrix is the $|\Delta S|=1$ evolution matrix of [44], which provides an additional check of the RG evolution.
Now the calculation of the elements $\gamma_{k\pm,7}$ of the LO and NLO anomalous dimension tensor has required the calculation of the divergent parts of the diagrams of fig. 5.4 and fig. 5.5, but now with insertions of $\mathcal{R}_{ij}$ for $j=1,2$, rather than $\mathcal{O}_{ij}$ and of the diagrams of fig. 5.12 and fig. 5.13 corresponding to matrix elements of $\mathcal{R}_{ij}$ for $j=3,\ldots 6$. Further there are

Figure 5.12: Diagram yielding the LO anomalous dimension tensor $\gamma^{(0)}_{k\pm,7}$ for $k=3\ldots 6$. The white cross denotes the insertion of a $\Delta S=1$ current–current operator. The dark cross stands for one of the $|\Delta S|=1$ penguin operators $Q_3,\ldots Q_6$.

diagrams in which the s–quark foot of the penguin operator is connected with the current–current vertex and likewise diagrams with the d–quark foot involved. An example is shown in fig. 5.14. For insertions of Q_5 and Q_6 these diagrams vanish by chirality. For insertions of Q_3 and Q_4 the diagrams are nonvanishing, but their sum cannot give a factor of m_c^2 in the divergent part. This follows from a subtle analysis exploiting (5.20) and the theorems on the mixing into gauge invariant operators.

Figure 5.13: The classes of diagrams contributing to $\langle\mathcal{R}_{ij}\rangle$ for $j=3,\ldots 6$, to $O(\alpha)$. The other members of a given class are obtained by left–right and up–down reflections. Also one–loop counterterms have to be included.

Figure 5.14: An example of a diagram involving the s–quark foot of the penguin operators.

5.4.2. Below μ_c

At the scale $\mu_c \approx m_c$ we remove the c–quark from the theory. Hence we are left with the single local operator $\widetilde{Q}_{S2}$. We have listed the low energy hamiltonian already in (1.1) and (5.15):

$$\begin{aligned} H &= H^c + H^t + H^{ct} \\ H^c(\mu) &= \frac{G_F^2}{16\pi^2}\lambda_c^2 \widetilde{C}_{S2}^{(c)}(\mu)\widetilde{Q}_{S2}(\mu) = \frac{G_F^2}{16\pi^2} M_W^2 \lambda_c^2 \eta_1 S(x_c) b(\mu) \widetilde{Q}_{S2}(\mu), \\ H^t(\mu) &= \frac{G_F^2}{16\pi^2}\lambda_t^2 \widetilde{C}_{S2}^{(t)}(\mu)\widetilde{Q}_{S2}(\mu) = \frac{G_F^2}{16\pi^2} M_W^2 \lambda_t^2 \eta_2 S(x_t) b(\mu) \widetilde{Q}_{S2}(\mu), \\ H^{ct}(\mu) &= \frac{G_F^2}{16\pi^2}\lambda_c\lambda_t \widetilde{C}_{S2}^{(ct)}(\mu)\widetilde{Q}_{S2}(\mu) = \frac{G_F^2}{16\pi^2} M_W^2 2\lambda_c\lambda_t \eta_3 S(x_c, x_t) b(\mu) \widetilde{Q}_{S2}(\mu). \end{aligned} \tag{5.40}$$

The only effect of the charm threshold for $\widetilde{C}_{S2}^{(t)}$ is the transition to the three–quark running α.
The coefficient $\widetilde{C}_{S2}^{(c)}(\mu_c)$ in (5.40) is determined by the matching of the matrix element of $H^c(\mu_c)$ in (5.28) to those of $H^c(\mu_c)$ in (5.40):

$$\langle H^c(\mu_c)\rangle = \frac{G_F^2}{2}\lambda_c^2 \sum_{i,j=+,-} C_i(\mu_c) C_j(\mu_c) \langle \mathcal{O}_{ij}(\mu_c)\rangle = \frac{G_F^2}{16\pi^2}\lambda_c^2\, \widetilde{C}_{S2}^{(c)}(\mu_c) \langle \widetilde{Q}_{S2}(\mu_c)\rangle \tag{5.41}$$

This yields $\widetilde{C}_{S2}^{(c)}(\mu_c)$ in terms of the RG improved $|\Delta S|=1$ Wilson coefficients $C_k(\mu_c)$. Here we verify the findings of sect. 3.7.2 that in the NLO the finite parts of fig. 5.6 and of the two–loop diagrams in fig. 5.5 are necessary.
The determination of $\widetilde{C}_{S2}^{(ct)}(\mu_c)$ requires the same procedure with H^{ct} of (5.28) and (5.40). Consider first the LO matching: The coefficient $\widetilde{C}_7(\mu_c)$ is nonzero due to admixtures from $C_2^{(0)}(\mu_W)$ picked up during the RG evolution from μ_W to μ_c. Hence the LO matching is done from the inverse power of $\alpha(\mu_c)$:

$$\widetilde{C}_{S2}^{(ct)}(\mu_c) = \frac{m_c^2(\mu_c)}{2}\frac{4\pi}{\alpha(\mu_c)}\widetilde{C}_7(\mu_c). \tag{5.42}$$

In the NLO matching all coefficients participate. We define

$$\langle \mathcal{R}_{ij}(\mu)\rangle = \frac{m_c^2(\mu)}{16\pi^2}\, 2\, r_{ij,S2}(\mu) \langle \widetilde{Q}_{S2}(\mu)\rangle^{(0)}. \tag{5.43}$$

Here the definition of $r_{ij,S2}$ differs from the one of $\widetilde{r}_{nm,l}$ given in (4.46) by a factor of 2. In NLO one therefore finds:

$$\widetilde{C}_{S2}^{(ct)}(\mu_c) = m_c^2(\mu_c)\left[\frac{1}{2}\frac{4\pi}{\alpha(\mu_c)}\widetilde{C}_7(\mu_c) + \sum_{i=+,-}\sum_{j=1}^{6} r_{ij,S2}(\mu_c) C_i(\mu_c) C_j(\mu_c)\right]. \tag{5.44}$$

On the side corresponding to the three–quark theory one expects the diagrams of fig. 5.3 and fig. 5.6 corresponding to $\langle \widetilde{Q}_{S2}\rangle^{(0)}$ and $\langle \widetilde{Q}_{S2}\rangle^{(1)}$ to be necessary. They, however, cancel with the terms accompanying $\langle \widetilde{Q}_7\rangle$ on the side of the four–quark theory.

Now one is left with the RG evolution from μ_c down to some scale μ at which the hadronic matrix element $\langle\overline{\mathrm{K}^0}|\widetilde{Q}_{S2}(\mu)|\mathrm{K}^0\rangle$ is obtained. The RG evolution of $\widetilde{Q}_{S2}$ is well–known [15,43], its anomalous dimension is γ_+ given in (5.19). In terms of (3.41) and (3.43) the NLO solution for $\widetilde{C}_{S2}^{(j)}(\mu)$, $j = c, t, ct$, reads:

$$\widetilde{C}_{S2}^{(j)}(\mu) \;=\; \widetilde{C}_{S2}^{(j)}(\mu_c)\left[\frac{\alpha(\mu_c)}{\alpha(\mu)}\right]^{d_+^{(3)}}\left(1 - J_+^{(3)}\frac{\alpha(\mu_c)-\alpha(\mu)}{4\pi}\right). \tag{5.45}$$

Finally we can express the NLO η_i's in (5.40) in terms of the coefficients:

$$\begin{aligned}
\eta_1 &= \frac{1}{m_c^2}\widetilde{C}_{S2}^{(c)}(\mu_c)\left[\alpha(\mu_c)\right]^{d_+^{(3)}}\left(1 - J_+^{(3)}\frac{\alpha(\mu_c)}{4\pi}\right)\\
\eta_2 &= \frac{1}{M_W^2 S(x_t)}\widetilde{C}_{S2}^{(t)}(\mu_c)\left[\alpha(\mu_c)\right]^{d_+^{(3)}}\left(1 - J_+^{(3)}\frac{\alpha(\mu_c)}{4\pi}\right)\\
\eta_3 &= \frac{1}{2M_W^2 S(x_c,x_t)}\widetilde{C}_{S2}^{(ct)}(\mu_c)\left[\alpha(\mu_c)\right]^{d_+^{(3)}}\left(1 - J_+^{(3)}\frac{\alpha(\mu_c)}{4\pi}\right).
\end{aligned} \tag{5.46}$$

The μ–dependence in (5.45) is absorbed into $b(\mu)$, which equals

$$b(\mu) \;=\; \left[\alpha(\mu)\right]^{-d_+^{(3)}}\left(1 + J_+^{(3)}\frac{\alpha(\mu)}{4\pi}\right) \tag{5.47}$$

in the NLO. The index (3) denotes that one has to set $f = 3$ in the corresponding quantities. From (5.46) it is evident that the η_i's depend on the definition of the masses. We will adopt the convention of [15, 17] that the running masses in (5.46) are evaluated at the scale at which they are integrated out, i.e. $m_c = m_c(\mu_c), m_t = m_t(\mu_W)$. Whenever the η_i's are defined such that they multiply $S(x_c(m_c))$, $S(x_t(m_t))$ and $S(x_c(m_c), x_t(m_t))$ in the effective hamiltonian in (5.40) we mark them with a star: η_i^*.
The hadronic matrix element $\langle\widetilde{Q}_{S2}\rangle$ is parametrized as

$$\langle\overline{K^0}\mid\widetilde{Q}_{S2}(\mu)\mid K^0\rangle \;=\; \frac{8}{3}B_K(\mu)f_K^2 m_K^2. \tag{5.48}$$

Here m_K and f_K are mass and decay constant of the neutral K meson. In (5.48) $B_K(\mu)$ measures the deviation from the vacuum insertion approximation $B_K(\mu) = 1$. It must combine with $b(\mu)$ in (5.47) to the RG invariant

$$B_K \;=\; B_K(\mu)b(\mu), \tag{5.49}$$

because physical observables are scale independent.

5.5. Why Working Beyond Leading Logarithms?

After all we may ask whether it is necessary to do the effort of a NLO calculation of $\mathrm{K}^0-\overline{\mathrm{K}^0}$–mixing instead of contenting oneself with the leading log approximation. Let us therefore close this chapter by listing the compelling reasons for passing to the next–to–leading order:

i) Only in NLO calculations it is possible to use the NLO quantity $\Lambda_{\overline{\rm MS}}$ defined in (3.15).

ii) The dependence of $\eta_3 S(x_c, x_t)$ on the top–quark mass first enters in the NLO.

iii) The LO results show a huge dependence on the scales μ_W and μ_c at which particles are integrated out. Such scale dependences are inherent to any RG improved calculation working with truncated perturbation series. It is caused by the fact that we can always subtract an arbitrary small logarithm (such as $\ln(\mu_W/M_W)$) from the summed large logarithm. By this one pushes small terms from the LO summation into the NLO. In the NLO the scale dependences therefore diminishes.

iv) One must go to the NLO to judge whether perturbation theory works, i.e. whether the radiative corrections are small. Further the corrections can be sizeable.

6. Calculation of η_1 and η_3

The following chapter is devoted to the description of some details of the NLO calculation of η_3 and η_1 and to the presentation of the analytical results.

6.1. The LO Analysis

The problem of RG improved short distance QCD correction to $K^0-\overline{K^0}$–mixing has been first addressed by Vaĭnsteĭn, Zakharov, Novikov and Shifman and by Vysotskiĭ [55]. They did not use the operator product expansion approach, but extracted the coefficients of the leading logarithms in a complicated way from the Standard Model amplitudes. Pioneering work in the development of the factorization method has been done by Gilman and Wise [45]. Their leading log results for η_1 and η_2 agreed with those of Vysotskiĭ, but they found his result for η_3 to be incorrect. In these early works the top–quark has been treated as light. Later Flynn [56] has redone the calculation for the case of a heavy top–quark. A good approximation neglecting flavour thresholds has been derived by Datta, Fröhlich and Paschos [57].
Let us comment on the LO calculation of η_3 of Gilman and Wise here: Their approach to the RG evolution is equivalent to the one described first in the paragraph on H^{ct} in sect. 5.4.1, i.e. they consider the mixing of $\mathcal{R}_{ij}$ into $\widetilde{Q}_7$ and work with coefficient vectors similar to (5.32). Yet their bilocal structures are defined in an inconvenient way, so that they need four evolution matrices instead of two. Further their operator basis is overcomplete resulting in 8×8 matrices rather than 7×7 ones. Indeed, the evolution matrices in [45] have a double eigenvalue.
With (3.45) we can simply read off the LO anomalous dimension tensor from the divergent parts of $\langle\mathcal{R}_{ij}\rangle^{(0)}$ depicted in fig. 5.4 and fig. 5.12. One finds

$$\gamma^{(0)}_{+,7} = \begin{pmatrix} -4(N+1) \\ -8 \\ -8(N+1) \\ -16 \\ 8(N+1) \\ 16 \end{pmatrix}, \qquad \gamma^{(0)}_{-,7} = \begin{pmatrix} 4(N-1) \\ 0 \\ 8(N-1) \\ 0 \\ -8(N-1) \\ 0 \end{pmatrix}. \tag{6.1}$$

We have expressed the result of [45] in terms of (6.1) and found agreement.

6.2. NLO Strategy

From the discussion of chapter 5 we know that we need the divergent parts of two–loop diagrams for the calculation of the NLO anomalous dimension tensor needed for η_3 and the finite parts of two–loop diagrams for the matching calculations in η_1. According to sect. 3.7 and 3.8 we can use any external state to perform the calculation and we choose massless external quarks with zero momentum. The QCD gauge parameter ξ is kept arbitrary. Its absence from the anomalous dimension tensor and the Wilson coefficients provides a check of the calculation. The same has to be true for the IR regulators, which are small masses m_s and m_d for the internal quarks. The problem therefore requires the calculation of the diagrams of fig. 5.5 and fig. 5.13. We remark here that the insertion of the right–handed penguin operators Q_5 and Q_6 into the diagrams of fig. 5.13 involves different integrals than that of the left–handed ones Q_3 and Q_4.
A further check of the result will be the absence of non–local terms involving $\ln \mu$ after the inclusion of subloop counterterm graphs.
Yet an incorrect treatment of the evanescent operators would pass all the checks mentioned above. In the calculation of η_3 we will therefore keep $\widetilde{a}_1$ and $\widetilde{b}_1$ parametrizing the order–ε term in the definition (4.6) and (4.16) of $E_1[\widetilde{Q}_7]$ and $E_2[\widetilde{Q}_7]$ arbitrary. While the individual Z–factors in (4.18) depend on $\widetilde{b}_1$'s in (4.16) this dependence cancels in $\gamma^{(1)}$. We will insert the evanescent counterterms with a factor of λ and with $\lambda = 1/2$ the dependence on $\widetilde{b}_1$ correctly vanishes. Conversely the non–local terms in the two–loop renormalization constants $Z^{(2)}_{k,E_{1k}}$ responsible for the mixing of physical operators into evanescents vanish for $\lambda = 1$.
Clearly the task at hand is simplified by an algorithm for the calculation of the two–loop diagrams. For the Dirac algebra the computer package Tracer [58] has been used. Further two–loop tensor vacuum bubble integrals up to rank six are involved. An algorithmic way to calculate them is described in the following section.

6.3. Master Formula for the Two–loop Integrals

We define the general two–loop vacuum bubble tensor integral as

$$\begin{aligned} T^{\nu_1\ldots\nu_s,\mu_1\ldots\mu_r}_{LNM}(\{m_j\},\{M_{1j}\},\{M_{2j}\}) \;=\; & \\ \frac{\mu^{4\varepsilon}e^{2\gamma_{\mathrm{E}}\varepsilon}}{\left[i\pi^{D/2}\right]^2}\iint d^Dk d^Dp \frac{p^{\nu_1}\cdots p^{\nu_s}\cdot k^{\mu_1}\cdots k^{\mu_r}}{(m_1^2-k^2)\cdots(m_L^2-k^2)\cdot(M_{11}^2-p^2)\cdots(M_{1N}^2-p^2)}\cdot & \\ \frac{1}{(M_{21}^2-(p+k)^2)\cdots(M_{2M}^2-(p+k)^2)}. & \end{aligned} \tag{6.2}$$

Here the M_{1j}'s and M_{2j}'s are arbitrary masses, while the m_j's are small masses to regulate IR singularities. This is the most complicated two–loop integral which can appear in the calculation of QCD corrections in light hadron systems. In our case of $\mathrm{K}^0-\overline{\mathrm{K}^0}$–mixing all cases with $0 \le L \le 4$ show up in the two–loop diagrams. Let us set T small masses exactly to zero while keeping $L-T$ of them nonzero. In practice one chooses T just as large that

Figure 6.1: The vacuum bubble diagram with two light masses m_1 and m_2. The tensor structure is arbitrary.

all the remaining $L-T$ masses suffice to regulate the IR singularities. In our calculation we needed at most two nonzero light masses, which were quark masses m_s and m_d. But also the case of on–shell dimensional IR regulators will be contained in the result, it simply corresponds to $L=T$. The heavy masses M_{1j} and M_{2j} in (6.2) correspond to the remaining masses in the problem, i.e. M_W, m_t, m_c and m_u in the Standard Model diagrams and m_c and m_u in the effective theory diagrams. We have only needed the latter, but for different combinations for the internal masses, so that we also keep them arbitrary.
For the scalar case $r=s=0$ the result for (6.2) is known for all masses being arbitrary [59], it involves a F_4 function and is not very useful for the situation at hand.
Finally the prefactor in (6.2) has been introduced for later convenience.
Let us now sketch the solution of (6.2): The first step consists of a decomposition into partial fractions of the propagators involving heavy masses:

$$T_{LNM}^{\nu_1\ldots\nu_s,\mu_1\ldots\mu_r}\left(\{m_j\},\{M_{1j}\},\{M_{2j}\}\right) = \sum_{l=1}^{M}\sum_{i=1}^{N}\left(\prod_{\substack{k=1\\k\neq l}}^{M}\frac{1}{M_{2k}^2-M_{2l}^2}\right)\left(\prod_{\substack{k=1\\k\neq i}}^{N}\frac{1}{M_{1k}^2-M_{1i}^2}\right) T_{L11}^{\nu_1\ldots\nu_s,\mu_1\ldots\mu_r}\left(\{m_j\},M_{1i},M_{2l}\right)$$

For equal heavy masses one finds derivatives of $T_{L11}^{\nu_1\ldots\nu_s,\mu_1\ldots\mu_r}$ with respect to M_{1i} or M_{2l} instead. $T_{L11}^{\nu_1\ldots\nu_s,\mu_1\ldots\mu_r}$ is depicted in fig. 6.1. We refrain from using partial fractions also in the line flown through by the loop–momentum k, because this would yield inverse powers of the infrared regulators m_j.
The first step to solve $T_{L11}^{\nu_1\ldots\nu_s,\mu_1\ldots\mu_r}$ is the expression of the sub–loop integral over p in (6.2) in terms of a Feynman parameter integral. The corresponding expression for a general one–loop tensor integral has been derived first by Davydychev [60]. Clearly only one Feynman parameter x is involved. Now one is faced with a sum of tensor integrals corresponding to all possibilities to build a rank–s tensor out of λ copies of the metric tensors and $s-2\lambda$ copies of the other momentum k. Each of the remaining integrals over k is proportional to the totally symmetric tensor

$$\left\{[g]^{\frac{r+s}{2}-\lambda}\right\}^{\nu_{\rho_{2\lambda+1}}\ldots\nu_{\rho_s},\mu_1\ldots\mu_r},$$

where $\{\rho_{2\lambda+1}\ldots\rho_s\}$ is a subset of $\{1,\ldots s\}$. The result reads

$$T_{L11}^{\nu_1\ldots\nu_s,\mu_1\ldots\mu_r} = \mu^{4\varepsilon}\sum_{\lambda=0}^{\left[\frac{s}{2}\right]}\sum_{\{\rho_1,\ldots\rho_{2\lambda}\}\cup\{\rho_{2\lambda+1},\ldots\rho_s\}=\{1,\ldots s\}}\left\{[g]^{\lambda}\right\}^{\nu_{\rho_1}\ldots\nu_{\rho_{2\lambda}}}\left\{[g]^{\frac{s+r}{2}-\lambda}\right\}^{\nu_{\rho_{2\lambda+1}}\ldots\nu_{\rho_s}\mu_1\ldots\mu_r}$$
$$(-1)^{\frac{3}{2}s+\frac{r}{2}}\left(\frac{1}{2}\right)^{\frac{s+r}{2}}\frac{\Gamma(-\lambda+\varepsilon)e^{2\varepsilon\gamma_{\rm E}}}{\Gamma\left(\frac{s+r}{2}+2-\lambda-\varepsilon\right)}\cdot\int_0^1 dx\,x^{s-2\lambda}\left[x(1-x)\right]^{\lambda-\varepsilon}\cdot$$

$$j_{1+\frac{s+r}{2}-\lambda-T,\lambda}(M(x), m_{T+1}, \ldots m_L).$$

Here the second sum runs over all $\left(\begin{array}{c} s \\ \rho_{2\lambda} \end{array} \right)$ possibilities to select $\rho_{2\lambda}$ numbers from the set $\{1, \ldots s\}$. Further $M^2(x) = M_{1j}^2/x - M_{2l}^2/(1-x)$ and the integration over $z = \sqrt{-k^2}$ is contained in

$$j_{p,q}(M, m_{T+1}, \ldots m_L) \;=\; \int_0^\infty dz \, \frac{z^{p-\varepsilon} \, (M^2+z)^{q-\varepsilon}}{(m_{T+1}^2+z) \cdots (m_L^2+z)} \tag{6.3}$$

Here the original IR singularities show up at the lower end $z = 0$ of the integration in the limit $m_i \to 0$. We have put T masses exactly to zero with $T \leq 1 + [(r+1)/2]$, so that the remaining masses regulate the IR singularity at $z = 0$. We can disentangle the IR regulators from the integral by noticing that the integration path in (6.3) connects two branch points of the integrand. Hence we can express the integral in (6.3) by a contour integral

$$\int_0^\infty dz \, z^{p-\varepsilon} f(z) \;=\; \frac{(-1)^p}{2i \sin(\pi\varepsilon)} \int_C dz \, (-z)^{p-\varepsilon} f(z),$$

where the contour C starts below the real axis at $z = +\infty$, encircles the point $z = 0$ clockwise and returns to $z = +\infty$ above the real axis. Here C is arbitrary as long as the poles $z = -m_{T+1}^2, \ldots z = -m_L^2$ and the third branch point $z = -M^2$ are to the left of C. Next one deforms C such that it encircles the other branch cut in (6.3) connecting $z = -M^2$ with $z = \infty$ along the negative real axis. When doing this one has to pull C over the poles thereby picking up $2\pi i$ times the sum of the residues of the integrand at $z = -m_{T+1}^2, \ldots z = -m_L^2$. One then obtains:

$$\begin{aligned} j_{p,q}(M, m_{T+1}, \ldots m_L) \;=\; & (-1)^{p+q} \int_0^\infty dz \, \frac{z^{q-\varepsilon} \, (M^2+z)^{p-\varepsilon}}{(-m_{T+1}^2+M^2+z) \cdots (-m_L^2+M^2+z)} \\ & + (-1)^p \frac{\pi}{\sin(\pi\varepsilon)} \sum_{l=T+1}^{L} \frac{(m_l^2)^{p-\varepsilon} (M^2-m_l^2)^{q-\varepsilon}}{\prod_{\substack{k=T+1 \\ k \neq l}}^{L} (m_k^2 - m_l^2)}. \end{aligned} \tag{6.4}$$

In the first integral we can safely set the small masses to zero and express the integral in terms of Euler's beta–function. This integral represents the result for the case of dimensional IR regularization. All IR regulators m_j are contained in an additive term. This must be so, because we know that IR terms in the full and effective theory factorize with the LO Wilson coefficient. If one kept small external momenta as IR regulators, they would appear in the same way in an additive term to the first integral (with $m_i = 0$) in (6.4). Now we can do the final integration over the Feynman parameter x yielding:

$$T_{L11}^{\nu_1 \ldots \nu_s, \mu_1 \ldots \mu_r} (\{m_j\}, M_{1j}, M_{2j}) \;=$$

$$\sum_{\lambda=0}^{\left[\frac{s}{2}\right]} \sum_{\{\rho_1,\ldots\rho_{2\lambda}\}\cup\{\rho_{2\lambda+1},\ldots\rho_s\}=\{1,\ldots s\}} \{[g]^{\lambda}\}^{\nu_{\rho_1}\ldots\nu_{\rho_{2\lambda}}} \{[g]^{\frac{s+r}{2}-\lambda}\}^{\nu_{\rho_{2\lambda+1}}\ldots\nu_{\rho_s}\mu_1\ldots\mu_r} \cdot$$
$$\left(\frac{1}{2}\right)^{\frac{s+r}{2}} \left[(-1)^{\frac{r-s}{2}} \frac{\Gamma(-2+L-\frac{s+r}{2}+2\varepsilon)e^{2\varepsilon\gamma_{\rm E}}}{\left(2-L+\frac{s+r}{2}-\lambda-\varepsilon\right)_L} h^{2-L+\frac{s+r}{2}}_{\frac{s-r}{2}+L-2-\lambda,\,-\frac{s+r}{2}+L-2+\lambda}(M_{2l},M_{1j}) \right.$$
$$\left. + T^{s,r,\lambda,T}_{L11,\rm IR}(\{m_j\},M_{1j},M_{2j})\right]. \tag{6.5}$$

Here $T^{s,r,\lambda,T}_{L11,\rm IR}$ is the part comprising the IR regulators. In (6.5) $(k)_l = k\cdot(k+1)\cdots(k+l-1)$ is the Pochhammer symbol. The function h in (6.5) reads:

$$\begin{aligned} h^p_{k,n}(M_i,M_j) &:= \mu^{4\varepsilon}\int_0^1 dx x^{k+\varepsilon}(1-x)^{n+\varepsilon}\left[x(M_i^2-M_j^2)+M_j^2\right]^{p-2\varepsilon} = h^p_{n,k}(M_j,M_i) \\ &= (M_j^2)^p\left(\frac{M_j^2}{\mu^2}\right)^{-2\varepsilon}{\rm B}(1+k+\varepsilon,1+n+\varepsilon) \\ &\quad {}_2{\rm F}_1(-p+2\varepsilon,1+k+\varepsilon,2+k+n+2\varepsilon,1-\frac{M_i^2}{M_j^2}). \end{aligned} \tag{6.6}$$

The second expression in terms of Gauß' hypergeometric function is useful for the case of one small mass M_i, e.g. $M_i = m_u$, in which case one can use Kummer's relations to transform to ${}_2F_1(.,.,.;M_i^2/M_j^2)$. In general the integral representation is more useful, because it can be more easily expanded in terms of ε. It further exhibits more symmetries and functional relations such as

$$\begin{aligned} h^p_{k,n}(M_i,M_j) &= h^p_{n,k}(M_j,M_i), \quad h^p_{k,n}(M_i,M_j) = h^p_{k+1,n}(M_i,M_j) + h^p_{k,n+1}(M_i,M_j) \\ \frac{\partial}{\partial M_j^2}h^p_{k,n}(M_i,M_j) &= (p-2\varepsilon)h^{p-1}_{k,n+1}(M_i,M_j). \end{aligned} \tag{6.7}$$

For equal masses one simply has

$$h^p_{k,n}(M,M) = \mu^{4\varepsilon}\left(M^2\right)^{p-2\varepsilon}B(1+k+\varepsilon,1+n+\varepsilon).$$

For different masses the expansion of the integral in (6.6) in terms of ε turns out to be the only cumbersome task to be done. One finds the familiar dilogarithm in the finite part and higher polylogarithms in the higher order terms in ε. Yet one only has to expand a few of the h's and one can obtain the others by the use of the functional equations (6.7). The expanded h–functions have been stored in a MATHEMATICA program to build a database. Now for a dimensional regularization of the IR singularities one finds $T^{s,r,\lambda,T}_{L11,\rm IR} = 0$. For the use of small masses as done by us one obtains:

$$T^{s,r,\lambda,T}_{L11,\rm IR}(\{m_j\},M_{1j},M_{2j}) =$$
$$(-1)^{r+1-T-\lambda}\frac{\pi}{\sin(\pi\varepsilon)}\frac{\Gamma(-\lambda+\varepsilon)e^{2\varepsilon\gamma_{\rm E}}\mu^{4\varepsilon}}{\Gamma(\frac{s+r}{2}+2-\lambda-\varepsilon)}\sum_{j=1}^{L-T}\sum_{l=0}^{L-2-\frac{s+r}{2}+\lambda}\frac{\left(m_j^2\right)^{1+\frac{s+r}{2}-T-\lambda+l-\varepsilon}}{\prod_{\substack{n=1\\n\neq j}}^{L-T}\left(m_n^2-m_j^2\right)}\cdot$$

$$\sum_{k=0}^{l} \left(\begin{array}{c} l \\ k \end{array} \right) (-1)^{k+l} \frac{1}{(\lambda+1-\varepsilon)_{s+k+1-2\lambda}} \cdot \frac{\partial^{s+k+l-2\lambda}}{\partial \left(M_{2l}^2\right)^{s+l+k-2\lambda}} \frac{\left(M_{2l}^2\right)^{s+k+1-\lambda-\varepsilon} - \left(M_{1j}^2\right)^{s+k+1-\lambda-\varepsilon}}{M_{2l}^2 - M_{1j}^2}. \tag{6.8}$$

In practice the summation indices only run over a small range, in the calculation of η_1 and η_3 only situations with $L - T \leq 2$ and $k = l = 0$ appeared.
We remark that the master formula (6.5) is a good investment into the future of short distance QCD corrections: First the formula holds in D dimensions. It can therefore be used for the matching calculations in a NNLO calculation and also for the two–loop counterterm diagrams in a n–loop calculation, which requires two–loop integrals up to the order $n-3$ in ε, if the divergent part is needed. Probably all calculations beyond NLO involve so many diagrams that a complete computerization is unavoidable. Then formulas of the type (6.5) also for higher loop integrals are indispensable. Further (6.5) can simply be extended to more powers in the small masses. Such integrals are needed in NLO calculations for the coefficients of higher dimension operators.

6.4. Result for the NLO Anomalous Dimension Tensor

In this section we list the result for the NLO anomalous dimension tensor $\gamma_{\pm,\mathbf{7}}^{\mathbf{T}}$.
From (5.28), (5.29) and (3.28) one readily finds the relation between the two–loop renormalization tensor $\left[Z^{-1,(2)}\right]_{ij,7}$ and the bare $O(\alpha)$ matrix elements of $\mathcal{R}_{ij}$:

$$\begin{aligned} -\left[Z^{-1,(2)}\right]_{ij,7} \langle \widetilde{Q}_7 \rangle^{(0)} \;=\; & \\ & \langle \mathcal{R}_{ij} \rangle^{(1),\text{bare}} + \frac{1}{\varepsilon} \left[2Z_{\psi,1}^{(1)} \delta_{ii'}\delta_{jj'} - \left[Z_1^{(1)}\right]_{ii'} \delta_{jj'} - \left[Z_1^{(1)}\right]_{jj'} \delta_{ii'} \right] \langle \mathcal{R}_{i'j'} \rangle^{(0),\text{bare}} \\ & + 2Z_{\psi,1}^{(1)} \frac{1}{\varepsilon^2} \left[Z_1^{-1,(1)}\right]_{ij,7} \langle \widetilde{Q}_7 \rangle^{(0)} + \frac{1}{\varepsilon^2} \left[Z_1^{-1,(1)}\right]_{ij,7} \langle \widetilde{Q}_7 \rangle^{(1),\text{bare}}, \end{aligned} \tag{6.9}$$

where we have used the notation (3.52) and (2.35) for the expanded matrix elements and Z–factors. Now one has to take into consideration that

$$\langle \widetilde{Q}_7 \rangle^{\text{bare}} \;=\; \langle \frac{m_{c,\,\text{bare}}^2}{g_{\text{bare}}^2} \widetilde{Q}_{S2} \rangle^{\text{bare}} \;=\; Z_m^2 Z_g^{-2} \frac{m_c^2}{g^2 \overline{\mu}^{2\varepsilon}} \langle \widetilde{Q}_{S2} \rangle^{\text{bare}}. \tag{6.10}$$

Hence

$$\langle \widetilde{Q}_7 \rangle^{(1),\text{bare}} \;=\; \frac{m_c^2}{g^2 \overline{\mu}^{2\varepsilon}} \left(2Z_{m,1}^{(1)} + \beta_0 \right) \frac{1}{\varepsilon} \langle \widetilde{Q}_{S2} \rangle^{(0)} + \frac{m_c^2}{g^2 \overline{\mu}^{2\varepsilon}} \frac{1}{\varepsilon} \langle \widetilde{Q}_{S2} \rangle^{(1),\text{bare}}. \tag{6.11}$$

Now the divergent parts of the diagrams of fig. 5.13 and fig. 5.5 and the corresponding subloop diagrams yield the terms in the first line of (6.9) and the last term in (6.11). The remaining divergences therefore correspond to

$$\left[Z_2^{-1,(2)} + \left(2Z_{m,1}^{(1)} + \beta_0 + 2Z_{\psi,1}^{(1)} \right) Z_1^{-1,(1)} \right]_{ij,7} \frac{1}{\varepsilon^2} + \left[Z_1^{-1,(2)} \right]_{ij,7} \frac{1}{\varepsilon} \tag{6.12}$$

Hence we can simply read off $Z_1^{-1,(1)}$ from the $1/\varepsilon$–divergences of the diagrams of fig. 5.5 and fig. 5.13 after the inclusion of subloop counterterms. We have also found that the dependence on ξ vanished from the $1/\varepsilon^2$–terms in (6.12) after subtracting the term involving $Z_{\psi,1}^{(1)}$. Further it has been checked that $Z_2^{-1,(2)}$ fulfills the relation to the $1/\varepsilon$ divergences of the one–loop renormalization constants.
Now $\gamma_{k\pm,7}^{(1)}$ is related to $\left[Z_1^{-1,(1)}\right]_{k\pm,7}$ via (3.45), i.e. the evanescents must be inserted with a factor of $1/2$.
To show the scheme dependence found in chapter 4 we keep the definitions of some evanescents arbitrary:

$$\begin{aligned}
E_1[Q_{1/2}] &= \gamma_\mu\gamma_\nu\gamma_\vartheta L \otimes \gamma^\vartheta\gamma^\nu\gamma^\mu L - (4-8\varepsilon)\gamma_\mu L \otimes \gamma^\mu L \\
E_1[Q_{3/4}] &= \gamma_\mu\gamma_\nu\gamma_\vartheta L \otimes \gamma^\vartheta\gamma^\nu\gamma^\mu L - (4+a_1\varepsilon)\gamma_\mu L \otimes \gamma^\mu L \\
E_1[Q_{5/6}] &= \gamma_\mu\gamma_\nu\gamma_\vartheta R \otimes \gamma^\vartheta\gamma^\nu\gamma^\mu L - (16+a_2\varepsilon)\gamma_\mu R \otimes \gamma^\mu L. \\
E_1[\widetilde{Q}_7] &= \gamma_\mu\gamma_\nu\gamma_\vartheta L \otimes \gamma^\vartheta\gamma^\nu\gamma^\mu L - (4+\widetilde{a}_1\varepsilon)\gamma_\mu L \otimes \gamma^\mu L
\end{aligned} \tag{6.13}$$

Insertions of Q_1 and Q_2 into the diagrams of fig. 5.5 also involve

$$E_2[\widetilde{Q}_7] = \gamma_\mu\gamma_\nu\gamma_\vartheta\gamma_\sigma\gamma_\rho L \otimes \gamma^\rho\gamma^\sigma\gamma^\vartheta\gamma^\nu\gamma^\mu L - \left[(4+\widetilde{a}_1\varepsilon)^2 + \widetilde{b}_1\varepsilon\right]\gamma_\mu L \otimes \gamma^\mu L. \tag{6.14}$$

Now one finds for $N = 3$:

$$\gamma_{+,7}^{(1)} = \begin{pmatrix}
\frac{404}{3} + \frac{130\widetilde{a}_1}{3} \\
\frac{172}{3} + \frac{32\widetilde{a}_1}{3} \\
-\frac{1720}{3} - \frac{88a_1}{3} + \frac{32\widetilde{a}_1}{3} \\
-\frac{584}{3} - \frac{80a_1}{3} + \frac{28\widetilde{a}_1}{3} \\
\frac{1576}{3} + \frac{80a_1}{3} - \frac{32\widetilde{a}_1}{3} + \frac{8a_2}{3} \\
\frac{1664}{3} + \frac{28a_1}{3} - \frac{28\widetilde{a}_1}{3} + \frac{52a_2}{3}
\end{pmatrix},$$

$$\gamma_{-,7}^{(1)} = \begin{pmatrix}
-\frac{52}{3} - \frac{110\widetilde{a}_1}{3} \\
-60 + 4\widetilde{a}_1 \\
\frac{1592}{3} + \frac{8a_1}{3} - \frac{16\widetilde{a}_1}{3} \\
-88 + 8a_1 + 4\widetilde{a}_1 \\
-\frac{1160}{3} - \frac{16a_1}{3} + \frac{16\widetilde{a}_1}{3} + \frac{8a_2}{3} \\
-128 - 4a_1 - 4\widetilde{a}_1 - 4a_2
\end{pmatrix}. \tag{6.15}$$

The dependence on $\widetilde{b}_1$ cancels from (6.15), although it is present in the individual contributions to the first two components of $\gamma^{(1)}_{\pm,7}$. Yet we discover a dependence on the a_i's and $\widetilde{a}_1$ as stated in (4.43) and (4.44).
For the numerical analysis we will use

$$a_1 \;=\; -8, \qquad a_2 \;=\; -16, \qquad \widetilde{a}_1 \;=\; -8. \tag{6.16}$$

The first two choices have to made to comply with [44], from which we have taken the $|\Delta S|=1$ anomalous dimension matrix and the initial condition for the $|\Delta S|=1$ coefficient vector.

6.5. η_3

We describe the initial condition and the RG evolution for the formalism of sect. 5.4.1 using $\vec{D}$ according to (5.36) and (5.38). All formulas refer to the NLO. The LO expressions can be simply obtained from them by only keeping the leading terms and using the LO running α.

6.5.1. Initial Condition

The initial condition for the $|\Delta S|=1$ coefficient vector can be taken from [44]:

$$\vec{C}(\mu_W) \;=\; \begin{pmatrix} 0\\1\\0\\0\\0\\0 \end{pmatrix} + \frac{\alpha(\mu_W)}{4\pi} \left[\begin{pmatrix} \gamma^{(0)}_{21}\\ \gamma^{(0)}_{22}\\ \gamma^{(0)}_{23}\\ \gamma^{(0)}_{24}\\ \gamma^{(0)}_{25}\\ \gamma^{(0)}_{26} \end{pmatrix} \ln\frac{\mu_W}{M_W} + \begin{pmatrix} B_1\\ B_2\\ -\widetilde{E}(x_t(\mu_W))/(2N)\\ \widetilde{E}(x_t(\mu_W))/2\\ -\widetilde{E}(x_t(\mu_W))/(2N)\\ \widetilde{E}(x_t(\mu_W))/2 \end{pmatrix} \right], \tag{6.17}$$

with

$$\begin{aligned} B_1 \;&=\; \frac{11}{2} \qquad B_2 \;=\; -\frac{11}{2N}\\ \widetilde{E}(x) \;&=\; -\frac{2}{3}\ln x + \frac{x^2(15-16x+4x^2)}{6(1-x)^4}\ln x + \frac{x(18-11x-x^2)}{12(1-x)^3} - \frac{2}{3} \end{aligned}$$

In (6.17) we have introduced a term involving the second row of the LO $|\Delta S|=1$ anomalous dimension matrix $\gamma^{(0)}$ to allow for the choice $\mu_W \neq M_W$.
Further $\vec{D}$ in (5.36) involves the initial coefficients of the operators Q_+ and Q_-:

$$C_+(\mu_W) \;=\; B_1 + B_2 + \gamma^{(0)}_+ \ln\frac{\mu_W}{M_W}, \qquad C_-(\mu_W) \;=\; -B_1 + B_2 + \gamma^{(0)}_- \ln\frac{\mu_W}{M_W}. \tag{6.18}$$

For the initial coefficient of $\widetilde{C}_7$ we have to perform the matching calculation with the diagrams of fig. 5.1 and fig. 5.4. If the evanescent operator of $\widetilde{Q}_7$ is defined as in (6.13), one easily finds:

$$\begin{aligned}\widetilde{C}_7(\mu_W) &= \left[-8\ln\frac{\mu_W}{M_W} + 4F(x_t(\mu_W)) - (6+\widetilde{a}_1)\right] \\ &= \widetilde{C}_7^+(\mu_W) + \widetilde{C}_7^-(\mu_W),\end{aligned} \tag{6.19}$$

where $F(x_t)$ is the top–dependent part of $S(x_c, x_t)$:

$$S(x_c, x_t) = -x_c \ln x_c + x_c F(x_t).$$

6.5.2. RG Evolution between μ_W and μ_c

The 8×8 anomalous dimension matrix $\overline{\gamma}$ has been introduced in (5.38):

$$\overline{\gamma} = \begin{pmatrix} \gamma & 0 & 0 \\ \gamma_{+,7}^T & \widetilde{\gamma} - \gamma_+ & 0 \\ \gamma_{-,7}^T & 0 & \widetilde{\gamma} - \gamma_- \end{pmatrix}. \tag{6.20}$$

While the $|\Delta S|=1$ mixing matrix γ can be taken from [44] and $\gamma_\pm$ and $\gamma_{\pm,7}^T$ have been given in (5.19), (6.1) and (6.15), we still have to list the anomalous dimension $\widetilde{\gamma}$ of $\widetilde{Q}_7$. Here one has to take into account the running of the mass and coupling in its definition:

$$\widetilde{\gamma} = \gamma_+ + 2\gamma_m - 2\beta_0. \tag{6.21}$$

The anomalous dimension γ_m of the mass has been given in (3.11).
Now one can build the matrices $\overline{U}^{(0)}$ and $\overline{J}^{(f)}$ as described in (3.40) and (3.43). The NLO evolution matrix (3.42) from μ_W down to μ_c reads:

$$\begin{aligned}\vec{D}(\mu_c) = &\left[1 + \frac{\alpha(\mu_c)}{4\pi}\overline{J}^{(4)}\right] \overline{U}^{(0)}(\mu_c, \mu_b) \left[1 + \frac{\alpha(\mu_b)}{4\pi}\left(\overline{J}^{(5)} - \overline{J}^{(4)} + \overline{r}^{T\,(5)} - \overline{r}^{T\,(4)}\right)\right] \\ &\overline{U}^{(0)}(\mu_b, \mu_W) \left[1 - \frac{\alpha(\mu_W)}{4\pi}\overline{J}^{(5)}\right] \vec{D}(\mu_W).\end{aligned} \tag{6.22}$$

Here the matching correction at the b–threshold has been taken into account, $\overline{r}^{(f)}$ coincides in the upper left 6×6 submatrix with the result of [44]. The 7th and 8th row and column are zero, because there is no b–quark involved in the diagrams of fig. 5.5 and fig. 5.13.
Now after obtaining $D_{7/8}(\mu_c)$ in (6.22) we can find the coefficient $\widetilde{C}_7(\mu_c)$:

$$\widetilde{C}_7(\mu_c) = C_+(\mu_c) D_7(\mu_c) + C_-(\mu_c) D_8(\mu_c). \tag{6.23}$$

6.5.3. Matching at μ_c

The matching condition at μ_c has been given in (5.44). Now both the diagrams of fig. 5.4 and those of fig. 5.12 have to be calculated. One finds for the quantities $r_{ij,S2}$ defined in (5.43):

$$r_{ij,S2}(\mu_c) = \begin{cases} [-4\ln(m_c/\mu_c) + (3+\widetilde{a}_1/2)]\,\tau_{ij} & \text{for } j \le 2 \\ [-8\ln(m_c/\mu_c) - 4]\,\tau_{ij} & \text{for } 3 \le j \le 4 \\ [8\ln(m_c/\mu_c) + 4]\,\tau_{ij} & \text{for } 5 \le j \le 6 \end{cases} \tag{6.24}$$

with the colour factors

$$\begin{aligned} \tau_{\pm 1} = \tau_{\pm 3} = \tau_{\pm 5} &= \frac{1}{2}(1 \pm N), \\ \tau_{+j} = 1 \quad \text{and} \quad \tau_{-j} &= 0 \quad \text{for } j \text{ even}. \end{aligned} \tag{6.25}$$

Finally with (5.46) we write down the NLO result for η_3:

$$\begin{aligned} \eta_3 = \frac{x_c(\mu_c)}{S\left(x_c(\mu_c), x_t(\mu_W)\right)} \left[\alpha(\mu_c)\right]^{d_+^{(3)}} \Bigg[& \frac{1}{4}\frac{4\pi}{\alpha(\mu_c)} \left(1 - \frac{\alpha(\mu_c)}{4\pi} J_+^{(3)}\right) \widetilde{C}_7(\mu_c) \\ & + \frac{1}{2} \sum_{i=+,-} \sum_{j=1}^{6} r_{ij,S2} C_i(\mu_c) C_j(\mu_c) \Bigg] \cdot \left(1 + O(\alpha^2)\right). \end{aligned} \tag{6.26}$$

Order α terms should be consistently removed here.
In most cases it is more useful to define η_3 such that it multiplies $S(x_c^*, x_t^*)$ in the hamiltonian, where $x_c^* = x_c(m_c)$ and $x_t^* = x_t(m_t)$. We then mark η_3 with a star:

$$\begin{aligned} \eta_3^* = \frac{x_c(\mu_c)}{S\left(x_c^*, x_t^*\right)} \left[\alpha(\mu_c)\right]^{d_+^{(3)}} \Bigg[& \frac{1}{4}\frac{4\pi}{\alpha(\mu_c)} \left(1 - \frac{\alpha(\mu_c)}{4\pi} J_+^{(3)}\right) \widetilde{C}_7(\mu_c) \\ & + \frac{1}{2} \sum_{i=+,-} \sum_{j=1}^{6} r_{ij,S2} C_i(\mu_c) C_j(\mu_c) \Bigg] \cdot \left(1 + O(\alpha^2)\right). \end{aligned} \tag{6.27}$$

I.e. one has

$$\eta_3 S\left(x_c(\mu_c), x_t(\mu_W)\right) = \eta_3^* S\left(x_c^*, x_t^*\right).$$

(6.26) has been checked by expanding all evolution matrices to the first order in α to verify that the leading logarithm in $S(x_c, x_t)$ is correctly reproduced. Indeed it has been found that $\eta_3 b(\mu) = 1 + O(\alpha)$, when the RG improvement is switched off in this way. Further η_3^* has been expanded around $\mu_c = m_c$ to check whether the logarithm in (6.24) cancels the dependence of the LO term on μ_c in the calculated order. This is also the case.

6.6. η_1

As discussed in sect. 5.4.1 the RG factors in η_1 only involve the known RG evolution of C_+ and C_-. The only complicated task is the matching at the scale μ_c shown in (5.41), which requires the finite parts of the diagrams of fig. 5.5 and fig. 5.6. We will be sketchy here, for more details on the calculation we refer to [17] and [61].
The LO matrix element of $\mathcal{O}_{ij}$ reads

$$\langle \mathcal{O}_{ij}(\mu)\rangle^{(0)} \;=\; \tau_{ij}\frac{m_c^2(\mu)}{8\pi^2}\langle \widetilde{Q}_{S2}\rangle^{(0)} \tag{6.28}$$

with the colour factors

$$\tau_{++} \;=\; \frac{N+3}{4}, \quad \tau_{+-} \;=\; \tau_{-+} \;=\; \frac{-N+1}{4}, \quad \tau_{--} \;=\; \frac{N-1}{4}.$$

In the NLO one obtains:

$$\langle \mathcal{O}_{ij}\,(\mu)\rangle^{(1)} \;=\; \frac{m_c^2(\mu)}{8\pi^2}\left[\langle \widetilde{Q}_{S2}\rangle^{(0)} a_7^{(ij)}(\mu) + \langle \hat{T}\rangle^{(0)}\tau_{ij}h_T + \langle \hat{U}\rangle^{(0)}\tau_{ij}h_U\right]. \tag{6.29}$$

The coefficients multiplying the unphysical matrix elements are of course the same as those of the Standard Model amplitude given in (5.13). We split $a_7^{(ij)}$ in (6.29) into its physical part $c_7^{(ij)}$ and those parts which depend on the infrared regulators or involve the gauge parameter:

$$\begin{aligned} a_7^{(ij)}(\mu) \;=\; & c_7^{(ij)}(\mu) + \tau_{ij}\left\{\frac{N-1}{2N}3\log\frac{m_d^2 m_s^2}{\mu^4}\right. \\ & + \xi\left[\left(C_F+\frac{N-1}{2N}\right)\left(2-2\frac{m_s^2\log(m_s^2/\mu^2)-m_d^2\log(m_d^2/\mu^2)}{m_s^2-m_d^2}\right)\right. \\ & \left.\left. + \frac{N-1}{2N}\log\frac{m_d^2 m_s^2}{\mu^4}\right]\right\}. \end{aligned} \tag{6.30}$$

The desired physical parts in (6.30) are found as

$$\begin{aligned} c_7^{(++)}(\mu) \;=\; & \tau_{++}\,3(1-N)\log\frac{m_c^2(\mu)}{\mu^2} \\ & + \frac{102-73N-32N^2+3N^3}{8N} + \pi^2\frac{-6+6N+N^2-N^3}{12N}, \\ c_7^{(+-)}(\mu) \;=\; c_7^{(-+)}(\mu) \;=\; & \tau_{+-}\,3(-1-N)\log\frac{m_c^2(\mu)}{\mu^2} \\ & + \frac{34-39N+8N^2-3N^3}{8N} + \pi^2\frac{-2+4N-3N^2+N^3}{12N}, \\ c_7^{(--)}(\mu) \;=\; & \tau_{--}\,3(-3-N)\log\frac{m_c^2(\mu)}{\mu^2} \\ & + \frac{-34+19N+12N^2+3N^3}{8N} + \pi^2\frac{2-6N+5N^2-N^3}{12N} \end{aligned} \tag{6.31}$$

The matrix element of $\widetilde{Q}_{S2}$ can be found in [15, 43]. Writing

$$\langle \widetilde{Q}_{S2}(\mu)\rangle = \langle \widetilde{Q}_{S2}(\mu)\rangle^{(0)} + \frac{\alpha(\mu)}{4\pi}\left[\langle \widetilde{Q}_{S2}\rangle^{(0)} a(\mu) + \langle \hat{T}\rangle^{(0)} h_T + \langle \hat{U}\rangle^{(0)} h_U\right] \quad (6.32)$$

the coefficient $a(\mu)$ reads

$$\begin{aligned} a(\mu) &= c + \left\{ \frac{N-1}{2N} 3 \log\frac{m_d^2 m_s^2}{\mu^4} \right. \\ &\quad + \xi\left[\left(C_F + \frac{N-1}{2N}\right)\left(2 - 2\frac{m_s^2\log(m_s^2/\mu^2) - m_d^2\log(m_d^2/\mu^2)}{m_s^2 - m_d^2}\right)\right. \\ &\quad \left.\left. + \frac{N-1}{2N}\log\frac{m_d^2 m_s^2}{\mu^4}\right]\right\}, \\ c &= -3\,C_F - 5\,\frac{N-1}{2N}. \end{aligned} \quad (6.33)$$

Now we can solve the matching condition (5.41) for $\widetilde{C}_{S2}^{(c)}(\mu_c)$:

$$\widetilde{C}_{S2}^{(c)}(\mu_c) = m_c^2(\mu_c) \sum_{i,j=+,-} C_i(\mu_c) C_j(\mu_c)\left[\tau_{ij} + \frac{\alpha(\mu_c)}{4\pi} r_{ij}(\mu_c)\right]. \quad (6.34)$$

with

$$r_{ij}(\mu_c) = c_7^{ij}(\mu_c) - \tau_{ij} c. \quad (6.35)$$

Again the unphysical terms have canceled from the Wilson coefficient.
Hence (5.46) gives for η_1:

$$\eta_1 = (\alpha(\mu_c))^{d_+^{(3)}} \sum_{i,j=+,-} C_i(\mu_c) C_j(\mu_c)\left[\tau_{ij} + \frac{\alpha(\mu_c)}{4\pi}\left(r_{ij}(\mu_c) - \tau_{ij} J_+^{(3)}\right)\right]. \quad (6.36)$$

η_1^* is simply given by

$$\eta_1^* = \frac{m_c^2(\mu_c)}{m_c^{*2}}\,\eta_1. \quad (6.37)$$

We close the section on η_1 by looking back to the matching at the scale μ_W as displayed in (5.30) to analyze the findings of [39] and sect. 5.4.1:
Consider first the diagrams D_1 and D_3. They can only be divided into their $|\Delta S|=1$ substructures by a three-particle cut. This cut separates two $|\Delta S|=1$ subdiagrams with four external (anti–) quarks and one external gluon. The cut is flown through by two integration momenta, but both refer to loop integrals which are finite after using the GIM mechanism, which reduces the UV behaviour of the integral involving the internal up–type quark propagators. Hence these diagrams match their counterparts in fig. 5.2 with the tree–level Wilson coefficients $C_i^{(0)} C_j^{(0)}$. The same reasoning applies to the self–energy

insertion in diagram D_5. Now the remaining diagrams can be divided by a two–particle cut into their $|\Delta S|=1$ substructures. Again the divergences of the loop integration associated with the momentum flowing through the cut are canceled by the GIM mechanism. But now the cut separates a tree–level $|\Delta S|=1$ vertex from a dressed one, which involves an UV–divergent loop. These UV divergences are responsible for the $O(\alpha)$ corrections to the $|\Delta S|=1$ coefficients $C_\pm(\mu_W)$. In fact the colour singlet diagram D_6 does not contribute to the $|\Delta S|=1$ Wilson coefficient. We have verified that only D_2, D_4 and D_7 contain terms requiring $C^{(1)}(\mu_W)$ to match their Standard Model counterparts. Finally only D_7 gives a term involving $\ln \mu_W/M_W$, which appears in the NLO matching to compensate the LO scale ambiguity. This can be traced back to the fact that D_7 involves diagram (3) of fig. 4.1 as a subdiagram, which is the only source of the LO anomalous dimension of the $|\Delta S|=1$ operators.

7. Numerical Results and Phenomenology

7.1. η_3

At first we will investigate the dependence of η_3 and η_3^* on the various physical parameters and on the scales at which particles are integrated out.
Recall the relevant part of the effective low–energy hamiltonian from (5.40):

$$\begin{aligned} H^{ct}(\mu) &= \frac{G_F^2}{16\pi^2} M_W^2 2\lambda_c\lambda_t\eta_3 S(x_c(\mu_c), x_t(\mu_W)) b(\mu)\widetilde{Q}_{S2}(\mu) \\ &= \frac{G_F^2}{16\pi^2} M_W^2 2\lambda_c\lambda_t\eta_3^* S(x_c^*, x_t^*) b(\mu)\widetilde{Q}_{S2}(\mu). \end{aligned} \tag{7.1}$$

We will start with the discussion of the scale dependence: η_3 and η_3^* depend on the initial scale μ_W and on $\mu_c \approx m_c$, at which the c–quark is removed from the theory. There is also a dependence on the scale $\mu_b \approx m_b$, at which we pass from a five–quark theory to a four–quark theory. But μ_b only appears in the running α and the dependence is so small that one could even set $\mu_b = \mu_c$. Now η_3 in (7.1) multiplies $S(x_c(\mu_c), x_t(\mu_W))$, which also depends on the scales, and ideally the product is scale independent. Clearly for the discussion of this issue the notion of η_3^* is more useful, because it multiplies a scale independent function and should therefore also be independent of μ_W and μ_c. In sect. 6.5 we have mentioned that the LO scale dependences of η_3^* are analytically canceled by the NLO terms within the calculated order. Hence we can use the remaining scale dependence as a measure of the accuracy of the calculation. Since W–boson and top–quark are simultaneously integrated out at $\mu = \mu_W$, the range for μ_W is

$$M_W \lesssim \mu_W \lesssim m_t.$$

We expect the dependence of η_3^* on $\mu_c \approx m_c$ to be larger than the one on μ_W because of the larger coupling constant involved.
Next consider the dependence on the QCD scale parameter $\Lambda_{\rm QCD}$: In the following $\Lambda_{\rm QCD}$ is understood to be defined with respect to four active flavours, the corresponding quantities in the three– and five–flavour theory are obtained by imposing continuity on the coupling at μ_b and μ_c. The world average for $\alpha(M_Z) = 0.117$ [11] correspond to $\Lambda_{\overline{\rm MS}} = 310$MeV for $\mu_b = 4.6\,$GeV and $\Lambda_{\overline{\rm MS}} = 315$MeV for $\mu_b = 5.0\,$GeV. The leading order $\Lambda_{\rm QCD}$, however, differs from $\Lambda_{\overline{\rm MS}}$ by an overall μ–dependent factor, see (3.15). If one equates the LO coupling and the NLO $\overline{\rm MS}$–coupling constant at the scale $\mu = M_Z = 91\,$GeV, one finds that $\Lambda_{\overline{\rm MS}} = 315$MeV corresponds to $\Lambda_{\rm QCD}^{\rm LO} = 110$MeV. If the relation is imposed at the low scale

$\mu = 1.3\,\mathrm{GeV}$, one finds $\Lambda^{\mathrm{LO}}_{\mathrm{QCD}} = 180\mathrm{MeV}$. This shows one contribution to the error bar in LO calculations. It is, however, more pronounced in η_1 than in η_3.
Let us therefore pick the following set of parameters:

$$\begin{array}{ll} \Lambda_{\overline{\mathrm{MS}}} = 0.31\,\mathrm{GeV}, & \Lambda^{\mathrm{LO}}_{\mathrm{QCD}} = 0.15\,\mathrm{GeV}, \\ m_c = \mu_c = 1.3\,\mathrm{GeV}, & \mu_b = 4.8\,\mathrm{GeV}, \\ M_W = 80\,\mathrm{GeV}, & m_t(m_t) = 170\,\mathrm{GeV}, \quad \mu_W = 130\,\mathrm{GeV}. \end{array} \tag{7.2}$$

The value for η_3^* corresponding to this set reads:

$$\eta_3^{*\mathrm{LO}} \;=\; 0.365, \quad \eta_3^{*\mathrm{NLO}} \;=\; 0.468. \tag{7.3}$$

Hence the NLO calculation has enhanced η_3^* by 27%. From the difference of 0.103 between the two values in (7.3) 0.019 originates in the change from the LO to the NLO running α. The smallness of this contribution is of course caused by the adjustment of $\Lambda^{\mathrm{LO}}_{\mathrm{QCD}}$ to fit the NLO running coupling as described in the previous paragraph. The explicit $O(\alpha)$–corrections from the NLO mixing and matching contribute 0.084. Let us list the dominant sources of the enhancement: At the initial scale μ_W the coefficients C_2, C_+ and C_- have a size of the order 1, while all other coefficients are almost negligible. The RG evolution from μ_W to μ_c enhances the coefficient C_- by roughly 75 % because of the negative sign of the anomalous dimension of Q_-, while the coefficient C_+ is damped by 25%. Now the penguin coefficients C_3 to C_6 are still negligible at $\mu = \mu_c$, only $C_1(\mu_c), C_2(\mu_c)$ and $\widetilde{C}_7(\mu_c)$ are important. In the matching at μ_c the contribution of $C_+(\mu_c)C_1(\mu_c)$ numerically cancels the one of $C_-(\mu_c)C_1(\mu_c)$, because the RG damping of the former is compensated by a larger colour factor $\tau_{+1} = 2$ having the opposite sign of $\tau_{-1} = -1$. Finally $\widetilde{C}_7(\mu_c) \approx 0.7$ has become large due to the RG admixtures from C_2. Hence only $C_-(\mu_c)C_2(\mu_c)$, $C_+(\mu_c)C_2(\mu_c)$ and $\widetilde{C}_7(\mu_c)$ are important. In LO only $\widetilde{C}_7(\mu_c)$ enters η_3. Keeping only $C_7(\mu_c)$ in the NLO expression, however, overestimates the NLO enhancement by a factor of roughly 1.5, because $C_2(\mu_C)$ contributes with a negative sign to η_3 (for the standard definition of the evanescents: $\widetilde{a}_1 = -8$), see (6.26).
Next we will display the dependence of η_3 and η_3^* on the various parameters. In all plots we take the fixed quantities from the standard data set (7.2). First consider the dependence of η_3^* on the initial scale μ_W as depicted in fig. 7.1. We find a sizeable scale dependence of 14% in the LO result. It is almost totally removed in the NLO, where we find less than 3% change in η_3^*, when μ_W is varied between 70 GeV and 190 GeV. The situation is not so

Figure 7.1: Dependence of η_3^* on the scale μ_W, at which the initial condition is defined.

nice in the case of the dependence on μ_c. To show the large effects related to the running c–quark mass in (7.1) we first display the running of η_3 with μ_c. In (7.1) it multiplies $S(x_c(\mu_c), x_t(\mu_W))$, which grows with increasing x_c and therefore falls off with increasing μ_c. Hence η_3 has to grow with increasing μ_c. From fig. 7.2 one realizes that the LO result for η_3 worsens the effect of the running mass in $S(x_c(\mu_c), x_t(\mu_W))$, while the NLO η_3 correctly grows with increasing μ_c.

Figure 7.2: Dependence of η_3 on the scale μ_c, at which the charm quark is integrated out. η_3 has to compensate the large running of the charm quark mass. See also fig. 7.3.

Figure 7.3: Dependence of η_3^* on the scale μ_c. For the scales below 1 GeV one recognizes the breakdown of perturbation theory. For a realistic estimate of the scale ambiguity take $1.1\,\text{GeV} \lesssim \mu_c \lesssim 1.6\,\text{GeV}$.

The corresponding plot for η_3^* is shown in fig. 7.3. We have intentionally extended the range for μ_c to the unphysically low value of $\mu_c \approx 0.7\,\text{GeV}$ to visualize the breakdown of perturbation theory. Varying μ_c within the range $1.1\,\text{GeV} \leq \mu_c \leq 1.6\,\text{GeV}$ yields the following estimate of the scale uncertainty:

$$0.33 \leq \eta_3^{*\,\text{LO}} \leq 0.40, \qquad 0.43 \leq \eta_3^{*\,\text{NLO}} \leq 0.50. \tag{7.4}$$

This corresponds to a reduction of the scale uncertainty from 19% to 15%. One reason for the poor improvement is the fact that the NLO running of the mass is stronger than the LO one. One realizes from (7.4) that the scale ambiguity alone is not always a good measure of the accuracy of the calculation, because the central value for $\eta_3^{*\,\text{NLO}}$ is not in the range quoted for $\eta_3^{*\,\text{LO}}$. Yet in the NLO order one may also judge the contribution of the uncalculated $O(\alpha^2)$–terms by squaring the calculated $O(\alpha)$ corrections. By this one is lead to the same interval as in (7.4), so that we may consider (7.4) as a realistic estimate for $\eta_3^{*\,\text{NLO}}$.
Let us now look at the dependence of η_3^* on the physical parameters. From the smallness of the initial coefficient $\widetilde{C}_7$ we expect the QCD correction to be almost independent of $m_t^* = m_t(m_t)$. The relevant quantity to be discussed is the product $\eta_3^* S(x_c^*, x_t^*)$ which enters (7.1) and physical observables. It is shown in fig. 7.4. Clearly the LO curve is flat.

Figure 7.4: Dependence of $\eta_3^* S(x_c^*, x_t^*)$ on $m_t^* = m_t(m_t)$. There is no dependence on m_t in the leading log approximation.

We also display the dependence of η_3^* alone on m_t, see fig. 7.5. One cannot get much physical insight from this plot, it only serves to verify that we can treat η_3^* as a constant function of m_t in phenomenological analyses.
On the other hand there is a sizeable dependence of $\eta_3^* S(x_c^*, x_t^*)$ on $m_c^* = m_c(m_c)$ as shown in fig. 7.6. In η_3^* alone, however, the LO dependence on m_c^* happens to be washed out in the NLO as can be seen in fig. 7.7. We close this section with a plot of the dependence of η_3^* on Λ_{QCD}. fig. 7.8 reveals a very moderate dependence on the QCD scale parameter. Recall that the actual measurements of $\alpha(M_Z)$ corresponds to LO values for Λ_{QCD} close to the left edge of the plot, while the NLO scale parameter $\Lambda_{\overline{\text{MS}}}$ is close to the highest values displayed.
Now we can easily summarize the result: The largest uncertainty of our estimate of η_3 is

Figure 7.5: Dependence of η_3^* on m_t^*.

Figure 7.6: Dependence of $\eta_3^* S(x_c^*, x_t^*)$ on m_c^*.

due to the the scale ambiguity stemming from μ_c and we obtain:

$$\eta_3^{*\,\mathrm{NLO}} = 0.47\ ^{+0.03}_{-0.04} \tag{7.5}$$

Figure 7.7: Dependence of η_3^* on m_c^*.

Figure 7.8: Dependence of η_3^* on $\Lambda_{\rm QCD}$. The NLO curve corresponds to $\Lambda_{\rm QCD} = \Lambda_{\overline{\rm MS}}$. Realistic values are 300MeV $\lesssim \Lambda_{\overline{\rm MS}} \lesssim$ 330MeV and 100MeV $\lesssim \Lambda_{\rm QCD}^{\rm LO} \lesssim$ 200MeV.

7.2. η_1

Again we only sketch the NLO result for η_1 and refer to [17,61] for more details. The part of the effective hamiltonian involving η_1 has been found to be

$$\begin{aligned} H^c(\mu) &= \frac{G_F^2}{16\pi^2}\lambda_c^2\eta_1 m_c^2(\mu_c) b(\mu)\widetilde{Q}_{S2}(\mu) \\ &= \frac{G_F^2}{16\pi^2}\lambda_c^2\eta_1^* m_c^{*\,2} b(\mu)\widetilde{Q}_{S2}(\mu). \end{aligned} \tag{7.6}$$

For the set of parameters given in (7.2) one finds:

$$\eta_1^{*\,\rm LO} = 0.80\ {}^{+0.20}_{-0.16}\ , \quad \eta_1^{*\,\rm NLO} = 1.32\ {}^{+0.21}_{-0.23}\ . \tag{7.7}$$

For $m_c^* = 1.4\,\text{GeV}$ one likewise finds

$$\eta_1^{*\,\rm LO} = 0.78\ {}^{+0.17}_{-0.14}\ , \quad \eta_1^{*\,\rm NLO} = 1.22\ {}^{+0.16}_{-0.18}\ . \tag{7.8}$$

Here the the dominant source of the error is again the dependence on μ_c, which has also been varied between 1.1 GeV and 1.6 GeV in (7.7) and between 1.2 GeV and 1.7 GeV in (7.8). Now the dependence on $\Lambda_{\rm QCD}$ is more pronounced than in the case of η_3^*. Therefore we have included the variation with $\Lambda_{\rm QCD}^{\rm LO}$ for 110MeV $\leq \Lambda_{\rm QCD}^{\rm LO} \leq$ 180MeV in the error bar for the LO result. The dependence on $\Lambda_{\rm QCD}$ is displayed in fig. 7.9. The NLO calculation has therefore yielded a reduction of the theoretical error from 45% to 33% for $m_c^* = 1.3\,\text{GeV}$ and from 40% to 26% for $m_c^* = 1.4\,\text{GeV}$.

Figure 7.9: The dependence of η_1^* on $\Lambda_{\rm QCD}^{\rm LO}, \Lambda_{\overline{\rm MS}}$. The choice $m_c^* = 1.4\,\text{GeV}$ has been made. All other fixed parameters are as in (7.2).

(7.7) reveals a much larger scale dependence for η_1^* than we have found for η_3^*in (7.5). Let us therefore investigate the origin of this uncertainty: There are three different contributions to η_1^* in (6.36) stemming from the products $C_+(\mu_c)C_+(\mu_c)$, $C_+(\mu_c)C_-(\mu_c)$ and $C_-(\mu_c)C_-(\mu_c)$. The last one is clearly the largest, because of the negative anomalous dimension of Q_-. These different sources are displayed in fig. 7.10: One can easily see, that the NLO curves related to C_+C_+ and C_+C_- are almost flat as they should be, but they contribute with opposite sign to η_1^* and therefore almost cancel in the sum. On the other hand the part

Figure 7.10: The dependence of the individual contributions to η_1^* on μ_c for $\Lambda^{\rm LO}_{\rm QCD}, \Lambda_{\overline{\rm MS}} = 300$MeV. $m_c^* = 1.4\,$GeV has been chosen. The line labeled by *(all)* refers to η_1^*.

stemming from C_-C_- contains a large residual scale dependence and is identified as the source of the large theoretical error in (7.7).
We have already noticed in (7.7) and (7.8) that η_1^* exhibits a sizeable dependence on m_c^*. We therefore plot η_1^* as a function of m_c^* in fig. 7.11. Physical quantities involve $m_c^{*\,2}\eta_1^*$, which is shown in fig. 7.12.

Figure 7.11: The dependence of η_1^* on m_c^*. For very low values $m_c^* \approx 1.1\,$GeV as favoured by some sum rule analyses our perturbative calculation of η_1^* is not very reliable.

Figure 7.12: The dependence of $\eta_1^* m_c^{*\,2}$, which enters the hamiltonian (7.6), on m_c^*. The (dominant) contribution of η_1^* to the short distance contribution to the $\rm K_L - K_S$–mass difference is obtained by multiplying the displayed value for $\eta_1^* m_c^{*\,2}$ by $1.371 \cdot 10^{-15}\,\text{GeV}^{-1} \cdot B_K$, where B_K is defined in (5.49)

7.3. Indirect CP–Violation in $\rm K^0 - \overline{K^0}$–Mixing

Here we briefly describe the indirect CP–violation in the neutral Kaon system (cf. e.g. [62]). The immediate consequence of $\rm K^0 - \overline{K^0}$–mixing is that the weak interaction eigenstates $|K^0\rangle$ and $|\overline{K^0}\rangle$ do not coincide with the mass eigenstates. Yet if the CP symmetry were conserved, the latter would be identical to the CP eigenstates $|K_1\rangle$ and $|K_2\rangle$:

$$\begin{aligned} |K_1\rangle &= \frac{1}{\sqrt{2}}\left(|K^0\rangle + |\overline{K^0}\rangle\right) \qquad \text{(CP=+1)}, \\ |K_2\rangle &= \frac{1}{\sqrt{2}}\left(|K^0\rangle - |\overline{K^0}\rangle\right) \qquad \text{(CP=–1)}. \end{aligned}$$

Now the mass eigenstates $|K_L\rangle$ and $|K_S\rangle$ differ from $|K_1\rangle$ and $|K_2\rangle$ by small admixtures of the other CP eigenstate:

$$|K_L\rangle = \frac{|K_2\rangle + \overline{\varepsilon}|K_1\rangle}{\sqrt{1+|\overline{\varepsilon}|^2}}, \quad |K_S\rangle = \frac{|K_1\rangle + \overline{\varepsilon}|K_2\rangle}{\sqrt{1+|\overline{\varepsilon}|^2}}.$$

The decay of K_L into the CP–even two–pion state may proceed via a CP–conserving decay of the small admixture of $|K_1\rangle$ or via a CP–violating decay of the dominant contribution of $|K_2\rangle$. These possibilities are termed *indirect* and *direct* CP–violation and are compactly

explained by the following picture:

$$|K_L\rangle = \frac{1}{\sqrt{2(1+|\overline{\varepsilon}|^2)}} \Big[\overbrace{\underbrace{|K^0\rangle - |\overline{K^0}\rangle}}^{\text{CP=–1}} + \overline{\varepsilon} \Big(\overbrace{\underbrace{|K^0\rangle + |\overline{K^0}\rangle}}^{\text{CP=+1}} \Big) \Big]$$

Decay: $\pi^0\pi^0$ (CP=+1)

A measure of the indirect CP–violation which is independent of phase conventions is given by the ratio of the amplitudes

$$\varepsilon_K \;=\; \frac{\mathcal{A}\left(K_L \to (\pi\pi)_{I=0}\right)}{\mathcal{A}\left(K_S \to (\pi\pi)_{I=0}\right)}. \tag{7.9}$$

In terms of the off–diagonal element of the mass matrix

$$M_{12} \;=\; \langle K^0 | H^{\Delta S=2} | \overline{K^0} \rangle \tag{7.10}$$

ε_K reads

$$\varepsilon_K \;=\; \frac{e^{i\pi/4}}{\sqrt{2}\Delta m}\left(\mathrm{Im}\, M_{12} + 2\xi \mathrm{Re}\, M_{12}\right),$$

where ξ is a small quantity involving the amplitude of $\Delta I = 1/2$ transitions and Δm is the $\mathrm{K_L}-\mathrm{K_S}$–mass difference. Experimentally ε_K is very well measured [11]:

$$\varepsilon_K \;=\; (2.266 \pm 0.023) \cdot 10^{-3} e^{i\pi/4}. \tag{7.11}$$

7.3.1. Parametrization of the CKM–Matrix

Since one may redefine the quark mass eigenstates by an arbitrary phase factor, there are many physically equivalent forms of the CKM–matrix. We adopt the standard convention, in which V_{ud}, V_{us}, V_{cb} and V_{tb} are real and positive. It is further advantageous to have a simple parametrization of the CKM–matrix. Here we use the improved Wolfenstein parametrization, which is used in [8]. It reads

$$V_{CKM} \;=\; \begin{pmatrix} 1-\frac{\lambda^2}{2} & \lambda & A\lambda^3(\rho - i\eta) \\ -\lambda - iA^2\lambda^5\eta & 1-\frac{\lambda^2}{2} & A\lambda^2 \\ A\lambda^3(1-\overline{\rho}-i\overline{\eta}) & -A\lambda^2 - iA\lambda^4\eta & 1 \end{pmatrix} \tag{7.12}$$

with

$$\overline{\rho} \;=\; \rho\left(1-\frac{\lambda^2}{2}\right), \qquad \overline{\eta} \;=\; \eta\left(1-\frac{\lambda^2}{2}\right).$$

(7.12) is an expansion in the parameter $\lambda = |V_{us}| + O(\lambda^6)$. (7.12) is exact to order λ^3 and contains the phenomenologically important terms up to the order λ^5. One of the relations provided by the unitarity of V_{CKM} is

$$V_{ud}V_{ub}^* + V_{cd}V_{cb}^* + V_{td}V_{tb}^* \;=\; 0.$$

When expressed in terms of the parameters introduced above, this relation corresponds to a *unitarity triangle* in the $(\overline{\rho}, \overline{\eta})$–plane with edges $(0,0), (1,0)$ and $(\overline{\rho}, \overline{\eta})$.
One finds to an accuracy of 0.2% [8] for $\lambda_j = V_{jd}V_{js}^*$:

$$\mathrm{Im}\, \lambda_t \;=\; -\mathrm{Im}\, \lambda_c \;=\; \eta A^2 \lambda^5. \tag{7.13}$$

CP–violation occurs for $\eta \neq 0$. Because of (7.13) we may use $\mathrm{Im}\, \lambda_t$ to parametrize all CP–violating quantities in the Standard Model.

7.3.2. $\varepsilon_{\mathbf{K}}$–Phenomenology[1]

Inserting (5.40), (5.48) and (7.11) into (7.9) yields the following relation between $\overline{\rho}$ and $\overline{\eta}$ [8]:

$$\overline{\eta}\left[(1-\overline{\rho})A^2\eta_2 S(x_t) + P_0\right] A^2 B_K \;=\; 0.223. \tag{7.14}$$

with

$$P_0 \;=\; \left[\eta_3 S(x_c, x_t) - \eta_1 x_c\right] \frac{1}{\lambda^4}.$$

When A is fixed, (7.14) defines a hyperbola in the $(\overline{\rho}, \overline{\eta})$–plane.
Now from (7.12) we notice that A is simply related to V_{cb} via $A = |V_{cb}|/\lambda^2$. We remark here that much progress has been made in the recent past to determine $|V_{cb}|$. Exclusive tree–level $b \to c$ decays allow the extraction from the endpoint of the spectrum, where heavy quark symmetry reduces the problem to the determination of a single form factor. Here typically values in the range $0.036 \leq |V_{cb}| \leq 0.050$ are stated [63]. The theoretical predictions for inclusive analyses still suffer from large scheme and scale dependences, because they are proportional to the fifth power of the bottom quark mass [64]. The latter can be determined from Υ spectroscopy [63] or by the use of heavy quark symmetry from inclusive D–decays [64,65]. The different lifetimes of the charmed hadrons, however, make the use of heavy quark symmetry troublesome here. Inclusive analyses give lower central values for $|V_{cb}|$ than the exclusive method.
To fix the third edge $(\overline{\rho}, \overline{\eta})$ of the unitarity triangle, we need a further input. It is straightforward to verify that the knowledge of $|V_{ub}/V_{cb}|$ fixes a circle in the $(\overline{\rho}, \overline{\eta})$–plane:

$$\overline{\rho}^2 + \overline{\eta}^2 \;=\; \left(1 - \frac{\lambda^2}{2}\right)^2 \frac{1}{\lambda^2} \frac{|V_{ub}|^2}{|V_{cb}|^2}. \tag{7.15}$$

If the phase δ in the CKM–matrix is the only source of indirect CP–violation in the K^0–system, the equations (7.14) and (7.15) must have a common solution $(\overline{\rho}, \overline{\eta})$. In general the hyperbola will intersect the circle in two points to give two solutions. Yet there is a critical set $\{(m_t, V_{cb}, |V_{ub}/V_{cb}|, B_K)\}$, for which the hyperbola only touches the circle. This set encodes a lower bound on any of the four quantities as a function of the other parameters [8,66].
Fig. 7.13 shows the hyperbola for the LO and the NLO result for η_3. One can see that the hyperbola has moved downwards. Therefore the NLO value for η_3 allows for a wider range of $m_t, V_{cb}, |V_{ub}/V_{cb}|$ and B_K than the older imprecise LO result. In this sense the Standard Model mechanism for CP–violation has been vindicated. For example a future determination $(m_t, V_{cb}, |V_{ub}/V_{cb}|, B_K) = (170\,\mathrm{GeV}, 0.040, 0.08, 0.7)$ would have been interpreted as a signal of new physics, if the LO values $\eta_1 = 0.78$, $\eta_3 = 0.37$ had been used. With the NLO results $\eta_1 = 1.32$, $\eta_3 = 0.47$, however, the hyperbola (7.14) intersects the circle (7.15) and there is no conflict with the CKM mechanism of CP–violation.

[1] for more details see [67]

Figure 7.13: ε_K: The hyperbolas in the $(\overline{\rho},\overline{\eta})$–plane for $\eta_3^{*\,LO} = 0.37$ and $\eta_3^{*\,NLO} = 0.47$. The other parameters are $\eta_1^* = 1.32$, $\eta_2^* = 0.57$, $m_t = 165\,\text{GeV}$, $|V_{cb}| = 0.041$, $m_c = 1.3\,\text{GeV}$ and $B_K = 0.7$. The circle corresponds to $|V_{ub}/V_{cb}| = 0.08$. The NLO value for η_3 permits two solutions for $(\overline{\rho},\overline{\eta})$ in this example.

The effect of the NLO calculation for η_3^* on the bounds on m_t and B_K is shown in fig. 7.14 and fig. 7.15.

Figure 7.14: Lower bound on m_t from ε_K for $|V_{ub}/V_{cb}| = 0.08$, $B_K = 0.5$, 0.7 and 0.9, $\eta_1^* = 1.32$, $\eta_2^* = 0.57$, $\eta_3^{*\,\text{NLO}} = 0.47$ and $\eta_3^{*\,\text{LO}} = 0.37$.

Figure 7.15: Lower bound on B_K from ε_K for $m_t = 165\,\text{GeV}$, $|V_{ub}/V_{cb}| = 0.06$, 0.08 and 0.10, $\eta_1^* = 1.32$, $\eta_2^* = 0.57$, $\eta_3^{*\,\text{NLO}} = 0.47$ and $\eta_3^{*\,\text{LO}} = 0.37$.

Table of $\mathbf{Im\,\lambda_t}$

Since $\text{Im}\,\lambda_t$ enters all CP–violating quantities, we now give a table of the two solutions for this quantity for various values of $m_t, V_{cb}, |V_{ub}/V_{cb}|$ and B_K. The fixed quantities are as in (7.2). The corresponding η_j's are

$$\eta_1 \;=\; 1.32, \qquad \eta_2 \;=\; 0.57 \quad \text{and} \qquad \eta_3 \;=\; 0.47.$$

Both solutions are listed, the entries have to be multiplied by 10^{-4}. *n.s.* means that there is no solution.

$B_K = 0.5$ and $m_t = 160$ GeV:

$\lvert V_{cb}\rvert =$	0.034	0.036	0.038	0.04	0.042	0.044
$\frac{\lvert V_{ub}\rvert}{\lvert V_{cb}\rvert} = 0.06$	*n.s.*	*n.s.*	*n.s.*	*n.s.*	*n.s.*	*n.s.*
$\frac{\lvert V_{ub}\rvert}{\lvert V_{cb}\rvert} = 0.08$	*n.s.*	*n.s.*	*n.s.*	*n.s.*	*n.s.*	*n.s.*
$\frac{\lvert V_{ub}\rvert}{\lvert V_{cb}\rvert} = 0.1$	*n.s.*	*n.s.*	*n.s.*	*n.s.*	1.61 1.75	1.37 1.87

$B_K = 0.5$ and $m_t = 170$ GeV:

$\lvert V_{cb}\rvert =$	0.034	0.036	0.038	0.04	0.042	0.044
$\frac{\lvert V_{ub}\rvert}{\lvert V_{cb}\rvert} = 0.06$	*n.s.*	*n.s.*	*n.s.*	*n.s.*	*n.s.*	*n.s.*
$\frac{\lvert V_{ub}\rvert}{\lvert V_{cb}\rvert} = 0.08$	*n.s.*	*n.s.*	*n.s.*	*n.s.*	*n.s.*	1.43 1.54
$\frac{\lvert V_{ub}\rvert}{\lvert V_{cb}\rvert} = 0.1$	*n.s.*	*n.s.*	*n.s.*	*n.s.*	1.41 1.76	1.25 1.81

$B_K = 0.5$ and $m_t = 190$ GeV:

$\lvert V_{cb}\rvert =$	0.034	0.036	0.038	0.04	0.042	0.044
$\frac{\lvert V_{ub}\rvert}{\lvert V_{cb}\rvert} = 0.06$	*n.s.*	*n.s.*	*n.s.*	*n.s.*	*n.s.*	*n.s.*
$\frac{\lvert V_{ub}\rvert}{\lvert V_{cb}\rvert} = 0.08$	*n.s.*	*n.s.*	*n.s.*	*n.s.*	*n.s.*	1.15 1.49
$\frac{\lvert V_{ub}\rvert}{\lvert V_{cb}\rvert} = 0.1$	*n.s.*	*n.s.*	*n.s.*	1.35 1.6	1.17 1.67	1.06 1.68

$B_K = 0.7$ and $m_t = 160$ GeV:

$\lvert V_{cb}\rvert =$	0.034	0.036	0.038	0.04	0.042	0.044
$\frac{\lvert V_{ub}\rvert}{\lvert V_{cb}\rvert} = 0.06$	*n.s.*	*n.s.*	*n.s.*	*n.s.*	*n.s.*	*n.s.*
$\frac{\lvert V_{ub}\rvert}{\lvert V_{cb}\rvert} = 0.08$	*n.s.*	*n.s.*	*n.s.*	*n.s.*	1.13 1.38	1.01 1.39
$\frac{\lvert V_{ub}\rvert}{\lvert V_{cb}\rvert} = 0.1$	*n.s.*	*n.s.*	*n.s.*	1.14 1.54	1.03 1.55	0.94 1.54

$B_K = 0.7$ and $m_t = 170$ GeV:

$\lvert V_{cb}\rvert =$	0.034	0.036	0.038	0.04	0.042	0.044
$\frac{\lvert V_{ub}\rvert}{\lvert V_{cb}\rvert} = 0.06$	*n.s.*	*n.s.*	*n.s.*	*n.s.*	*n.s.*	1.03 1.16
$\frac{\lvert V_{ub}\rvert}{\lvert V_{cb}\rvert} = 0.08$	*n.s.*	*n.s.*	*n.s.*	1.19 1.27	1.02 1.33	0.92 1.32
$\frac{\lvert V_{ub}\rvert}{\lvert V_{cb}\rvert} = 0.1$	*n.s.*	*n.s.*	1.19 1.44	1.04 1.49	0.94 1.49	0.86 1.46

$B_K = 0.7$ and $m_t = 190$ GeV:

$\lvert V_{cb}\rvert =$	0.034	0.036	0.038	0.04	0.042	0.044
$\frac{\lvert V_{ub}\rvert}{\lvert V_{cb}\rvert} = 0.06$	*n.s.*	*n.s.*	*n.s.*	*n.s.*	0.98 1.06	0.86 1.07
$\frac{\lvert V_{ub}\rvert}{\lvert V_{cb}\rvert} = 0.08$	*n.s.*	*n.s.*	*n.s.*	0.97 1.23	0.87 1.23	0.79 1.2
$\frac{\lvert V_{ub}\rvert}{\lvert V_{cb}\rvert} = 0.1$	*n.s.*	1.18 1.28	0.99 1.38	0.89 1.38	0.81 1.36	0.74 1.33

$B_K = 0.9$ and $m_t = 160$ GeV:

$\lvert V_{cb}\rvert =$	0.034	0.036	0.038	0.04	0.042	0.044
$\frac{\lvert V_{ub}\rvert}{\lvert V_{cb}\rvert} = 0.06$	*n.s.*	*n.s.*	*n.s.*	*n.s.*	0.93 1.05	0.83 1.04
$\frac{\lvert V_{ub}\rvert}{\lvert V_{cb}\rvert} = 0.08$	*n.s.*	*n.s.*	1.08 1.15	0.93 1.2	0.84 1.19	0.76 1.16
$\frac{\lvert V_{ub}\rvert}{\lvert V_{cb}\rvert} = 0.1$	*n.s.*	1.09 1.29	0.95 1.34	0.86 1.33	0.78 1.31	0.72 1.28

$B_K = 0.9$ and $m_t = 170$ GeV:

$\lvert V_{cb}\rvert =$	0.034	0.036	0.038	0.04	0.042	0.044
$\frac{\lvert V_{ub}\rvert}{\lvert V_{cb}\rvert} = 0.06$	*n.s.*	*n.s.*	*n.s.*	*n.s.*	0.84 1.01	0.76 0.99
$\frac{\lvert V_{ub}\rvert}{\lvert V_{cb}\rvert} = 0.08$	*n.s.*	*n.s.*	0.96 1.14	0.85 1.15	0.77 1.13	0.7 1.09
$\frac{\lvert V_{ub}\rvert}{\lvert V_{cb}\rvert} = 0.1$	*n.s.*	0.99 1.27	0.87 1.29	0.79 1.27	0.72 1.25	0.66 1.21

$B_K = 0.9$ and $m_t = 190$ GeV:

$\lvert V_{cb}\rvert =$	0.034	0.036	0.038	0.04	0.042	0.044
$\frac{\lvert V_{ub}\rvert}{\lvert V_{cb}\rvert} = 0.06$	*n.s.*	*n.s.*	*n.s.*	0.8 0.93	0.71 0.92	0.65 0.89
$\frac{\lvert V_{ub}\rvert}{\lvert V_{cb}\rvert} = 0.08$	*n.s.*	0.94 1.04	0.81 1.07	0.72 1.05	0.66 1.02	0.6 0.98
$\frac{\lvert V_{ub}\rvert}{\lvert V_{cb}\rvert} = 0.1$	0.97 1.15	0.83 1.2	0.75 1.19	0.68 1.16	0.62 1.13	0.57 1.09

7.4. $\mathrm{K_L}-\mathrm{K_S}$–mass difference

We will now discuss the short distance contribution to the $\mathrm{K_L}-\mathrm{K_S}$–mass difference: Neglecting the small imaginary parts of the CKM elements, one finds

$$\begin{aligned}(\Delta m)_{SD} &= \frac{G_F^2}{6\pi^2} m_K f_K^2 B_K \Big[(\mathrm{Re}\,\lambda_c)^2 m_c^{*\,2} \eta_1^* + 2(\mathrm{Re}\,\lambda_t)(\mathrm{Re}\,\lambda_c) M_W^2 S(x_c^*, x_t^*)\eta_3^* \\ &\qquad + (\mathrm{Re}\,\lambda_t)^2 M_W^2 S(x_t^*)\eta_2^*.\Big] \end{aligned} \tag{7.16}$$

Here the relative size of the three terms in the brackets is roughly $100 : 10 : 1$. Hence the $\mathrm{K_L}-\mathrm{K_S}$–mass difference is dominated by η_1. This contribution has already been tabulated

in [17,61], so that we comment on the corrections stemming from the second term involving η_3 here: Since

$$\mathrm{Re}\,\lambda_t \;=\; -\left(1-\frac{\lambda^2}{2}\right)A^2\lambda^5(1-\overline{\rho}) \tag{7.17}$$

to an accuracy of 2%, the term with η_3 depends on $|V_{cb}|$ and $\overline{\rho}$. Its average contribution to $(\Delta m)_{SD}/((\Delta m)_{exp})$ is about 0.06. Hence one can obtain the full $(\Delta m)_{SD}$ from the tabulated values for the first term in (7.16) in [17, 61] by multiplying with 1.1. With the central value for η_1^{NLO} listed in (7.8) our short distance calculation therefore reproduces 68% of the observed mass difference for $m_c = 1.3$ and 73% of $(\Delta m)_{exp})$ for $m_c = 1.4$, if the $1/N$–result $B_K = 0.7$ is used. Taking into account the large theoretical error in (7.8) the short distance contribution from (7.16) is between 52% and 95%.
In most textbooks the $K_L - K_S$ –mass difference is termed to be dominated by poorly calculable long–distance effects. Indeed, with the old LO result for η_1 and with the old smaller values for $\Lambda_{\mathrm{QCD}}^{\mathrm{LO}}$ the short distance part of Δm is less than 50%. Long distance effects come from the operators with only light quarks in (5.28), which are also present below the charm threshold and may generate meson poles in the low–energy matrix elements. But a long distance dominance is clearly a puzzle, because by power counting these contributions are suppressed with $\Lambda_{\mathrm{QCD}}^2/m_c^2$ with respect to the short distance part, because the coefficient of the leading dimension–six operator in (5.40) is proportional to m_c^2 (for a discussion see e.g. [68]). This fact has even stimulated speculations about new physics contributing to the $K_L - K_S$ –mass difference (e.g. in [69]). With the new NLO result for η_1 the short distance part is well above potential long distance contributions. Keeping in mind the large uncertainties in the problem it appears to be hopeless to find evidence of new physics in the $K_L - K_S$ –mass difference.

Bibliography

[1] W. E. Lamb and R. C. Retherford, Phys. Rev. 72 (1947) 241.

[2] J. Schwinger (ed.), *Quantum Electrodynamics*, Dover, New York 1958, and references therein.

[3] M. Gell–Mann, Phys. Lett. 8 (1964) 214.
G. Zweig, CERN reports TH–401 and TH–412 (1964).
M. Gell–Mann, A. Phys. Austr. Suppl. 9 (1972) 733.
D. J. Gross and F. Wilczek, Phys. Rev. Lett., 30 (1973) 1343.
H. D. Politzer, Phys. Rev. 30 (1973) 1346.

[4] S. L. Glashow, Nucl. Phys. 22 (1961) 579.
S. Weinberg, Phys. Rev. Lett. 19 (1967) 1264.
A. Salam in *Elementary Particle Physics (Nobel Symp. 8)*, ed. N. Svartholm, Almquist and Wilsell, Stockholm, 1968.

[5] P. W. Higgs, Phys. Rev. Lett. 12 (1964) 132.
P. W. Higgs, Phys. Rev. 145 (1966) 1156.

[6] N. Cabibbo, Phys. Rev. Lett. 10 (1963) 531.
M. Kobayashi and T. Maskawa, Progr. Theor. Phys. 49 (1973) 652.

[7] The CDF Collaboration (F. Abe et al.), Phys. Rev. Lett. 73 (1994) 225.

[8] A. J. Buras, M. E. Lautenbacher, G. Ostermaier, Phys. Rev. D50 (1994) 3433.

[9] S. Herrlich and U. Nierste, New bounds on standard model parameters from next–to–leading order corrections to $K^0-\overline{K^0}$–mixing,
in preparation.

[10] J. H. Christenson, J. W. Cronin, V. L. Fitch and R. Turlay,
Phys. Rev. Lett. 13 (1964) 138.
J. H. Christenson, J. W. Cronin, V. L. Fitch and R. Turlay,
Phys. Rev. 140B (1965) 74.

[11] Particle Data Group, Phys. Rev. D50 (1994) 1173.

[12] S. L. Glashow, J. Iliopoulos and L. Maiani, Phys. Rev. D2 (1970) 1285.

[13] M. K. Gaillard and B. W. Lee, Phys. Rev. D10 (1974) 897.

[14] T. Inami and C. S. Lim, Progr. Theor. Phys. 65 (1981) 297 [Erratum: 65 (1981) 1772].

[15] A. J. Buras, M. Jamin and P. H. Weisz, Nucl. Phys. B347 (1990) 491.

[16] S. Herrlich and U. Nierste, The complete $\Delta S = 2$–hamiltonian in next–to–leading order, in preparation.

[17] S. Herrlich and U. Nierste, Nucl. Phys. B419 (1994) 292.

[18] J.-M. Frère, W. A. Kaufman and Y.-P. Yao, Phys. Rev. D36 (1987) 809.

[19] S. Herrlich and U. Nierste, Evanescent operators, scheme dependences and double insertions, preprint TUM–T31–66/94, hep-ph/9412375, Nucl. Phys. B, in press.

[20] T.D. Lee and C.N. Yang, Phys. Rev. 104 (1956) 254.

[21] G. Lüders, Dan. Mat. Phys. Medd. 28 (1954) 5.
W. Pauli in *Niels Bohr and the Development of Physics*, ed. W. Pauli, L. Rosenfeld and V. Weisskopf, McGraw–Hill, New York, and Pergamon Press, London, 1955.
G. Lüders, Ann. Phys. 2 (1957).

[22] P. W. Higgs, Phys. Lett. 12 (1964) 132.
P. W. Higgs, Phys. Rev. Lett. 13 (1964) 508.
P. W. Higgs, Phys. Rev. 145 (1966) 1156.
F. Englert and R. Brout, Phys. Rev. Lett. 13 (1964) 321.
T. W. Kibble, Phys. Rev. 155 (1967) 1554.

[23] H. Lehmann, K. Symanzik and W. Zimmermann, Nuovo Cim. Ser. 10, 1 (1955) 205.

[24] L. D. Faddeev and V. N. Popov, Phys. Lett. 25B (1967) 29.

[25] K. Wilson, Phys. Rev. 179 (1969) 1699.

[26] C. Becchi, A. Rouet and R. Stora, Comm. Math. Phys. 42 (1975) 127.

[27] W. Zimmermann, Comm. Math. Phys. 15 (1969) 208.

[28] J. C. Ward, Phys. Rev. 78 (1950) 182.
Y. Takahashi, Nuovo Cim. 6 (1957) 371.

[29] A. A. Slavnov, Teor. Mat. Fiz. 10 (1972) 153.
J. C. Taylor, Nucl. Phys. B33 (1971) 436.

[30] G. 't Hooft, Nucl. Phys. B33 (1971) 173.

[31] G. 't Hooft, Nucl. Phys. B61 (1973) 455.

[32] S. Weinberg, Phys. Rev. 118 (1960) 838.

[33] J. Collins, *Renormalization*, Cambridge Univ. Press, Cambridge, 1984.

[34] W. A. Bardeen, A. J. Buras, D. W. Duke and T. Muta, Phys. Rev. D18 (1978) 3998.

[35] E. C. G. Stückelberg and A. Petermann, Acta Phys. Helv. 26 (1953) 499.

[36] T. Muta, *Foundations of Quantum Chromodynamics*, World Scientific, Sinagapore, 1987.

[37] A. J. Buras, E. G. Floratos, D. A. Ross and C. Sachrajda, Nucl. Phys. B131 (1977) 308.

[38] W. Zimmermann, Ann. Phys. 77, 536.

[39] E. Witten, Nucl. Phys. B122 (1977) 109.

[40] T. Appelquist and J. Carrazone, Phys. Rev. D11 (1975) 2856.

[41] G. Buchalla and A. J. Buras, Nucl. Phys. B412 (1994)106.

[42] G. 't Hooft and M. Veltman, Nucl. Phys. B44 (1972) 189.

[43] A. J. Buras and P. H. Weisz, Nucl. Phys. B333 (1990) 66.

[44] A. J. Buras, M. Jamin, M. E. Lautenbacher and P. H. Weisz, Nucl. Phys. B370 (1992) 69.

[45] F. J. Gilman and M. B. Wise, Phys. Rev. D27 (1983) 1128.

[46] A. J. Buras, M. Jamin, M. E. Lautenbacher and P. H. Weisz, Nucl. Phys. B400 (1993) 37.

[47] D. Kreimer, preprint UTAS-PHYS-94-01, hep-ph/9401354.

[48] M. J. Dugan and B. Grinstein, Phys. Lett. B256 (1991)239.

[49] A. J. Buras, M. E. Lautenbacher, M. Misiak, M. Münz, Nucl. Phys. B423 (1994)349.

[50] S. Joglekar and B.W. Lee, Ann. of Physics 97 (1976) 160.
S. Joglekar, Ann. of Physics 108 (1977) 233.

[51] H. D. Politzer, Nucl. Phys. B172 (1980) 349.

[52] J. Collins, Nucl. Phys. B92 (1975) 477.

[53] C. Arzt, preprint UM-TH-92-28, hep-ph/9304230.

[54] H. Simma, Z. Phys. C61 (1994) 67.

[55] A. I. Vaĭnsteĭn, V. I. Zakharov, V. A. Novikov and M. A. Shifman, Sov. J. Nucl. Phys. 23 (1976) 540.
M. I. Vysotskiĭ, Sov. J. Nucl. Phys. 31 (1980) 797.

[56] J. M. Flynn, Mod. Phys. Lett. A5 (1990) 877.

[57] A. Datta, J. Fröhlich and E. A. Paschos, Z. Phys. C46 (1990) 63.

[58] M. Jamin and M. E. Lautenbacher, Comp. Phys. Comm. 74 (1993) 265.

[59] J. van der Bij and M. Veltman, Nucl. Phys. B231 (1984) 205.
A. Davydychev and B. Tausk, Nucl. Phys. B397 (1993) 123.

[60] A. Davydychev, Phys. Lett. B263 (1991) 107.

[61] S. Herrlich, *QCD Korrekturen höherer Ordnung zur* $\mathrm{K}^0-\overline{\mathrm{K}^0}$ *Mischung (in German)*, PhD thesis, TU Munich, 1994.

[62] A. J. Buras and M. K. Harlander, *A Top–Quark Story: Quark Mixing, CP–Violation and Rare Decays in the Standard Model*, in *Heavy Flavours*, ed. A. J. Buras and M. Lindner, World Scientific, Singapore, 1993.

[63] M. Shifman, N.G. Uraltsev and A. Vainshtein, Phys. Rev. D51 (1995) 2217, erratum: D52 (1995) 3149.

[64] P. Ball and U. Nierste, Phys. Rev. D50 (1994) 5841.
U. Nierste, *Conference talk at QCD 1994, Montpellier*, hep-ph/9408401, Nucl. Phys. Proc. Suppl. 39B, C(1995), 393

[65] M. Luke and M. Savage, Phys. Lett. B321 (1994) 88.

[66] A. J. Buras, Phys. Lett. B317 (1993) 449.

[67] S. Herrlich and U. Nierste, preprint TUM-T31-81/95, hep-ph/9507262, Phys. Rev. D, in press.

[68] M. A. Shifman, Int. J. of Mod. Phys. A12 (1988) 2769.

[69] B. A. Campbell, J. Ellis, K. Enquist, M. K. Gaillard and D. V. Nanopoulos, Int. J. of Mod. Phys. A2 (1987) 831.

Acknowledgements

In the first place I would like to thank my advisor, Andrzej Buras, for guiding my way into the exciting field of QCD corrections to weak processes. I am grateful for the suggestion of the topic and the permanent encouragement during my work. In my future places I will certainly miss the stimulating and creative atmosphere of his *Munich next–to–leading order club*.
Next I would like to thank Stefan Herrlich for exploring the field of $K^0-\overline{K^0}$–mixing and the associated field theoretic subtleties together with me. The collaboration with him has been very pleasant and certainly very fruitful. I also owe most of my knowledge on computers to him.
I do not want to miss the numerous stimulating talks with Patricia Ball, Gerhard Buchalla, Matthias Jamin, Markus Lautenbacher, Mikołaj Misiak and Manfred Münz. I would like to thank Patricia for her patience in our collaboration on inclusive semileptonic decays. I owe a large part of my knowledge about tree–level decays of heavy hadrons to her. I am grateful for Gaby Ostermaier's help with figs. 7.14 and 7.15 and for Stefan's preparation of some of the figures, which have been used in our common publications. Hubert Simma's thorough explanation of the role of the unphysical operators described in sect. 3.10 is gratefully acknowledged.
I have enjoyed many discussions on other fields of particle physics with many members of the TUM Elementary Particle Physics Division, especially with Manfred Lindner, Kurt Rießelmann and Erhard Schnapka. I have also learned a lot from friends outside the department, in particular from Dirk Kreimer and David Broadhurst. This thesis would not have been completed in time, if Stephan Stieberger had not provided me with many lifts from Garching to Munich after the departure of the last bus. I am grateful to Andrzej Buras, Stefan Herrlich and Manfred Münz for proofreading the manuscript.
Finally I would like to thank everybody in the group for creating an extraordinary pleasant social environment.

Financial support of *Studienstiftung des deutschen Volkes*, *Bundesministerium für Forschung und Technologie* and *Freistaat Bayern* is gratefully acknowledged.